Charles University in Prague

Faculty of Science

Doctoral study program: Molecular and Cellular Biology, Genetics and Virology

Anna Malinová

The role of pre-mRNA splicing in human hereditary diseases

Role sestřihu pre-mRNA při rozvoji lidských dědičných onemocněních

Doctoral Thesis

Supervisor: doc. Mgr. David Staněk, Ph.D.

Department of RNA biology

Institute of Molecular Genetics AS CR

Prague, 2017

PROHLÁŠENÍ

Prohlašuji, že jsem závěrečnou práci zpracovala samostatně a že jsem uvedla všechny použité informační zdroje a literaturu. Tato práce ani její podstatná část nebyla předložena k získání jiného nebo stejného akademického titulu.

Praha, 29.5. 2017

Podpis:

Anna Malinová

ACKNOWLEDGEMENT

I would like to thank my supervisor, David Staněk, for his valuable guidance throughout my Ph.D. studies. Many thanks belong to my colleagues for creating friendly atmosphere and for being always willing to help me. I would also like to thank my parents for their constant support, Honza for his patience and care, our dogs for their boundless love and Real Madrid for being the best.

ABSTRACT

U5 small ribonucleoprotein particle (U5 snRNP) is a crucial component of the spliceosome, the complex responsible for pre-mRNA splicing. Despite the importance of U5 snRNP, not much is known about its biogenesis. When we depleted one of the core U5 components, protein PRPF8, the other U5-specific proteins do not associate with U5 snRNA and the incomplete U5 was accumulated in nuclear structures known as Cajal bodies. To further clarify the role of PRPF8 in U5 snRNP assembly, we studied PRPF8 mutations that cause an autosomal dominant retinal disorder, retinitis pigmentosa (RP). We prepared eight different PRPF8 variants carrying RP-associated mutations and expressed them stably in human cell culture. We showed that most mutations interfere with the assembly of snRNPs which consequently leads to reduced efficiency of splicing. The mutant PRPF8 together with EFTUD2 are stalled in the cytoplasm in a form of U5 snRNP assembly intermediate. Strikingly, we identified several chaperons including the HSP90/R2TP complex and ZNHIT2 as new PRPF8's interactors and potential U5 snRNP assembly factors. Our results further imply that these chaperons preferentially bind the unassembled U5 complexes and that HSP90 is required for stability of U5 proteins PRPF8 and SNRNP200. Finally, we provide evidence that the R2TP complex is important for proper maturation of U5 snRNPs and it is responsible for retention of mutated PRPF8 in the cytoplasm. We propose that the HSP90/R2TP chaperone system both promotes and controls the assembly U5 snRNP particles.

ABSTRAKT

Malá jaderná ribonukleoproteinová částice U5 (U5 snRNP) je jednou z hlavních komponent spliceozomu, komplexu který katalyzuje sestřih pre-mRNA. U5 snRNP je tvořena molekulou RNA a několika proteiny, nicméně o tom jak jsou jednotlivé díly postupně skládány v maturovanou částici, se mnoho neví. Ukázali jsme, že po depleci proteinu PRPF8, jedné z klíčových složek U5 snRNP, se částice správně neskládají a akumulují se v jaderných strukturách zvaných Cajalova tělíska. K objasnění role PRPF8 v biogenezi U5 snRNP jsme se dále rozhodli využít mutace tohoto proteinu, které byly identifikovány u pacientů s degenerativním onemocněním oční sítnice, retinitis pigmentosa (RP). Vytvořili jsme stabilní buněčné linie exprimující mutantní varianty proteinu PRPF8 a ukázali jsme, že RP mutace narušují skládání U5 snRNP, což následně vede ke snížení efektivity sestřihu pre-mRNA v buňkách. Mutantní PRPF8 se spolu s proteinem EFTUD2 hromadí v cytoplazmě a vytvoření tohoto komplexu je zdá se prvním krokem skládání U5 snRNP. Dále jsme s využitím proteomických metod identifikovali řadu nových faktorů včetně komlexu HSP90/R2TP a proteinu ZNHIT2, které se váží na U5 snRNP. Naše výsledky ukazují, že tyto faktory preferenčně interagují s nehotovými U5 snRNP včetně komplexů s mutantními PRPF8 proteiny. Prokázali jsme, že chaperon HSP90 se podílí na udržení stability některých proteinů specifických pro U5 snRNP částici, konkrétně proteinů PRPF8 a SNRNP200. V neposlední řadě ukazujeme, že komplex R2TP je nezbytný pro správné formování U5 snRNP a je zodpovědný za zadržování mutantních proteinů PRPF8 v cytoplazmě. Z našich výsledků vyplývá, že komplex HSP90/R2TP se nejen přímo podílí na skládání U5 snRNP částic, ale také dohlíží na správný průběh tohoto procesu.

TABLE OF CONTENT

PROHLÁŠENÍ 2
ACKNOWLEDGEMENT 3
ABSTRACT 4
ABSTRAKT 5
TABLE OF CONTENT 6
ABBREVIATIONS 9
INTRODUCTION 12
AIMS 14
LITERARY REVIEW 15
1 Splicing of pre-mRNA 15
1.1 Spliceosome 15
1.2 Splicing decisions 15
1.3 Splicing reaction 16
2 Composition of the spliceosome 17
2.1 Uridine-rich snRNAs 17
2.2 Sm and LSm ring 18
2.3 SnRNP specific proteins 19
3 U5 snRNP 20
3.1 SNRNP200 20
3.2 PRPF8 21
3.3 EFTUD2 23
3.4 PRPF6 23
4 Biogenesis of snRNPs 24
4.1 Transcription of snRNAs and their export 24
4.2 Cytoplasmic assembly of core snRNPs 25
4.3 Nuclear import and final maturation of snRNPs 25
4.4 Biogenesis of U6 snRNP 26
4.5 Addition of snRNP-specific proteins 27
5 Factors involved in snRNP biogenesis 29
5.1 AAR2 29
5.2 HSP90/R2TP complex 29
5.2.1 HSP90 29
5.2.2 R2TP complex 30

5.2.3 HSP90/R2TP complex function 31
6 Cajal bodies 32
6.1 Nature of Cajal bodies 32
6.2 Function of Cajal bodies 33
6.3 Role of Cajal bodies in snRNP biogenesis 34
6.4 Coilin - the scaffold protein of Cajal bodies 35
7 Splicing and disease 37
7.1 Cis-acting mutations 37
7.2 Trans-acting mutations 37
7.3 Spinal muscular atrophy (SMA) 39
7.4 Retinitis pigmentosa (RP) 40
7.4.1 RP mutations in spliceosomal proteins 42
PRPF3 44
PRPF4 44
PRPF6 45
PRPF8 45
PRPF31 46
SNRNP200 47
RP9/PAP1 47
DHX38 48
MATERIALS AND METHODS 49
1 Cell culture 49
2 Preparation of PRPF8-LAP stable cell lines 50
3 Red/ET recombeneering 50
4 RNA interference 51
5 Transfection of plasmids 51
6 Immunofluorescence (IF) – sample preparation 52
7 Fluorescence *in situ* hybridization (FISH) – sample preparation 53
8 Microscopy 54
9 Immunoprecipitation (IP) 55
10 SDS-PAGE and Western blot (WB) 56
11 Antibodies 58
12 Total RNA isolation and cDNA synthesis 59
13 RT-PCR, RT-qPCR and colony PCR 60
14 SILAC-IP and proteomic analysis 62

RESULTS 63
1 Cell lines expressing PRPF8-LAP variants were prepared 64
2 RP mutations affect PRPF8 localization and stability 65
3 PRPF8-LAP gets stabilized after depletion of the endogenous protein 68
4 RP mutations reduce the efficiency of splicing 69
5 RP mutations compromise U5 snRNP and tri-snRNP formation 73
6 Incomplete snRNPs accumulate in Cajal bodies 76
7 RP mutants are stalled in a complex with AAR2 79
8 AAR2 is important for U5 snRNP assembly 81
9 PRPF8 interacts with ZNHIT2 and ECD proteins and the R2TP complex 82
10 HSP90 is involved in maturation of U5 proteins 84
11 RUVBL proteins are required for proper U5 snRNP maturation 85
12 The HSP90/R2TP complex and ZNHIT2 associate preferentially with mutated PRPF8 88
13 The R2TP complex sequesters mutated PRPF8 in the cytoplasm 90
DISCUSSION 92
1 RP-associated PRPF8 mutations disrupt splicing 92
2 U5 snRNP step-wise assembly 96
3 Factores involved in U5 snRNP assembly 98
SUMMARY 103
REFERENCES 105

ABBREVIATIONS

3'ss - 3' splice site

5'ss - 5' splice site

adRP - autosomal dominant retinitis pigmentosa

APS - ammonium persulfate

arRP - autosomal recessive retinitis pigmentosa

ASCR - Academy of Sciences of the Czech Republic

BAC - bacterial artificial chromosome

BMKS - Burn-McKeown syndrome

BP - branch point

BSA - bovine serum albumine

CB - Cajal body

CBC - cap binding complex

CCMS - cerebrocostomandibular syndrome

cDNA - complementary DNA

CHX - cycloheximide

Cy5 - cyanine dye number 5

DAPI - 4',6-diamidino-2-phenylindole

DMEM - Dulbecco's Modified Eagle Medium

DMSO - dimethyl sulfoxide

dNTP - deoxynucleoside triphosphate

DTT - Dithiothreitol

EF-G - elongation factor G

EGTA - triethylene glycol diamine tetraacetic acid

En domain - endonuclease-like

FACS - fluorescence-activated cell sorting

FCS - fetal calf serum

FISH - fluorescence *in situ* hybridization

FRAP - fluorescence recovery after photobleaching

FSCN2 - fascin actin-bundling protein 2

GA - geldanamycin

GAPDH - glyceraldehyde 3-phosphate dehydrogenase

GFP - green fluorescent protein

HLB body - histone locus body

HR - homologous recombination

HRP - horseradish peroxidase

iCLIP - individual-nucleotide resolution UV crosslinking and immunoprecipitation

IF - immunofluorescence/ impact factor

IMG - Institute of Molecular Genetics

IP - immunoprecipitation

Jab1 domain - c-Jun activation domain binding protein1-like domain

kDa - kiloDalton

m^7G-cap - 7-methylguanosine cap

MFDGA syndrome - mandibulofacial dysostosis of Guion-Almeida type syndrome

MPG - monomethyl-phosphate-guanosine

mRNA - messenger ribonucleic acid

NC - negative control

NLS - nuclear localization signal

NS - Nager syndrome

NTD - N-terminal domain

PAGE - polyacrylamide gel electrophoresis

PBS - phosphate buffered saline

PBST - phosphate buffered saline with Tween

PcG body - Polycomb body

PCR - polymerase chain reaction

PDB - protein data bank

PFA - paraformaldehyde

PIPES - piperazine-N,N'-bis(2-ethanesulfonic acid)

PML body - promyelocytic leukemia oncoprotein body

pre-mRNA - precursor messenger ribonucleic acid

PTC - premature termination codon

RG - arginine-glycin

RH domain - RNase H-like domain

RHO - rhodopsin

RNAi - RNA interference

RNP - nuclear ribonucleoprotein particle

ROM1 - retinal outer segment membrane protein 1

RP - retinitis pigmentosa

RT - reverse transcriptase

RT-qPC - real-time quantitative PCR

scaRNA - small Cajal body-specific ribonucleoprotein particle

SDS - sodium dodecyl sulfate

SDS-PAGE - polyacrylamide gel electrophoresis in sodium dodecyl sulfate running buffer

SEM - standard error of the mean

SILAC - stable isotope labeling in cell culture

siRNA - small interfering RNA

snoRNP - small nucleolar ribonucleoprotein particle

snRNA - small nuclear ribonucleic acid

snRNA - small nucleolar ribonucleic acid

snRNP - small nuclear ribonucleoprotein particle

SSC - saline sodium citrate

SSD - saline sodium citrate

TEMED - tetramethylethylenediamine

TMG - trimethylguanosine

TPR - tetratricopeptide repeats

UV - ultraviolet light

v/v - volume/volume

w/v - weight/volume

WB - Western blot

WT - wild-type

xRP - X-linked retinitis pigmentosa

Y2H - yeast two-hybrid

INTRODUCTION

The instruction manual for life is written in molecules of DNA. All known organisms use DNA to encode and store their genetic information. An essential part of the information stored in DNA is represented by protein-coding genes, segments of DNA describing which proteins should be made. During gene expression, cells read the gene information encoded in the sequence of nucleotides, basic building blocks of DNA, and translate it into the amino-acid sequence of a protein. However, the process is not straightforward and messenger RNA (mRNA) serves as a mediator that transfers the information from DNA to the proteosyntetic machinery. While prokaryotes make mRNA that is ready for translation into protein, eukaryotic genes are more complex and are first transcribed into precursor mRNA (pre-mRNA), which needs to be further modified. One of the key processing steps is pre-mRNA splicing. Pre-mRNA contains not only sequences coding for a protein but also large intervening sequences. During splicing, the non-coding sequences (introns) are removed from the pre-mRNA and coding sequences (exons) are joined to form the final mRNA. Splicing is catalyzed by a huge molecular machinery, spliceosome. The major building blocks of the spliceosome are five small nuclear ribonucleoprotein particles (snRNPs), formed from small nuclear RNAs (snRNAs) and a large number of different proteins.

The unifying element of my work is the U5 snRNP, a crucial component of the splicing machinery. U5 particle occupies a central position in the activated human spliceosome as confirmed by recent structural studies (Bertram *et al.*, 2017). Protein PRPF8 is particularly important in this context as it is the main U5-specific scaffolding protein and its large central cavity forms the catalytic center of the spliceosome (Galej *et al.*, 2013; Yan *et al.*, 2015; Agafonov *et al.*, 2016). PRPF8 attracts a great deal of attention also because mutations in the gene encoding this protein cause an inherited human disease, retinitis pigmentosa (RP). PRPF8 mutation were studied mainly in yeast and brought the first insights not just into the mechanism of these mutations but also into the biogenesis of the U5 particle. However, not much is known about the maturation of the PRPF8 and about the assembly of the human U5 snRNPs. In particular, we have little information regarding the order in which proteins join the U5 snRNA, whether they come alone or as pre-assembled complexes, or which chaperone systems

are involved in human U5 snRNP assembly, if any. We have decided to address these questions and to start by analysis of the RP-associated PRPF8 mutations in human cells.

AIMS

The main goal of this work is to gain a deeper insight into the intricate machinery of the spliceosomal complex. We aim to extend our knowledge about the formation of this machinery and we try to address the question using a cellular model of a human hereditary disease, retinitis pigmentosa. We focus on three main goals:

- to decipher molecular mechanisms underlying retinitis pigmentosa mutations in spliceosomal protein PRPF8
- to better characterize the step-wise assembly of the U5 snRNP particle in human cells
- to identify factors involved in the biogenesis of U5 snRNP particles and to outline their possible means of action

LITERARY REVIEW

1 Splicing of pre-mRNA

Splicing of pre-mRNA is a crucial step in eukaryotic gene expression during which intronic sequences are removed from the nascent pre-mRNA and coding sequences (exons) are joined to form the final mRNA.

1.1 Spliceosome

Splicing is catalyzed by the spliceosome, a complex of small nuclear ribonucleoprotein particles (snRNPs). There are two types of spliceosomes in most eukaryotic cells, major and minor. The major spliceosome catalyzes removal of vast majority of introns and contains U1, U2, U4, U5 and U6 snRNPs, whereas the minor spliceosome splices a specific subset of introns and consists of U11, U12, U4atac, U5 and U6atac snRNPs. It worth noticing that the U5 snRNP is the same in both spliceosomal types (reviewed by Patel & Steitz, 2003; Matera & Wang, 2014). Throughout this thesis, I will mainly focus on the major spliceosome as it is dominant in splicing and it is much better characterized. If not mentioned otherwise, I will also describe mainly human spliceosome because it is the subject matter of my work.

1.2 Splicing decisions

An average human gene contains 8 relatively small exons of about 150 nucleotides in length and approximately 10 times longer introns (Lander & et al, 2001). Spliceosome recognizes the exon/intron boundaries mainly by base paring with short consensus sequences at the 5' and 3' splice site of an intron (5' ss and 3' ss) and with so called branch point and polypyrimidine tract. However, additional enhancer or silencer elements on the pre-mRNA can bind regulatory proteins that affect the recruitment of the splicing machinery (reviewed by Will & Lührmann, 2011; Matera & Wang, 2014). On the top of it, splicing occurs mainly co-transcriptionally (Tilgner *et al.*, 2012) and thus chromatin and adjacent proteins can influence the splicing outcome as well (reviewed

by Bentley, 2014). Depending on the interplay of all the regulatory factors, the exons and introns can be either included or excluded from the final mRNA. This phenomenon is called alternative splicing and it gives rise to enormous variety of protein products (reviewed by Kornblihtt *et al.*, 2013).

1.3 Splicing reaction

Pre-mRNA splicing takes place in the nucleus. Introns are excised from pre-mRNA by two subsequent transesterification reactions and the process involves dynamic assembly and rearrangement of the spliceosomal complex (Fig. 1). Although snRNPs are the main players of the splicing reaction, many non-snRNP proteins are also part of the spliceosomal complex and are involved in the reaction (reviewed by Wahl *et al.*, 2009; Matera & Wang, 2014). The energy demands of the two catalytic steps are negligible, however substantial energy amounts are consumed by RNA helicases that are required for remodeling of the spliceosome (reviewed by Cordin *et al.*, 2012). In the first step of splicing, U1 snRNP and U2 snRNP with help of associated factors bind the 5' ss and sequences around the branch point respectively, forming the early complex E. Subsequently, U2 snRNP interacts with the U1 snRNP thereby bringing to close proximity the two splice sites of one intron (complex A). At that point, U4, U5 and U6 snRNPs join the spliceosome as a preassembled tri-snRNP and the complex B is formed, although still inactive. Further rearrangements are needed that lead to release of U1 and U4 snRNPs and to formation of the catalytically active complex B*. When ready, the 2'OH of the branch point adenosine cleaves and binds the pre-mRNA at the 5'ss, generating a lariat structure on the RNA and the spliceosomal complex C. Finally, the 3'OH of the 5'exon attacks the 3'ss, the exons are joint together and the intron with remaining snRNPs is excised and released. For the next round of splicing, individual snRNPs are recycled (Fig. 1) (reviewed by Wahl *et al.*, 2009; Matera & Wang, 2014).

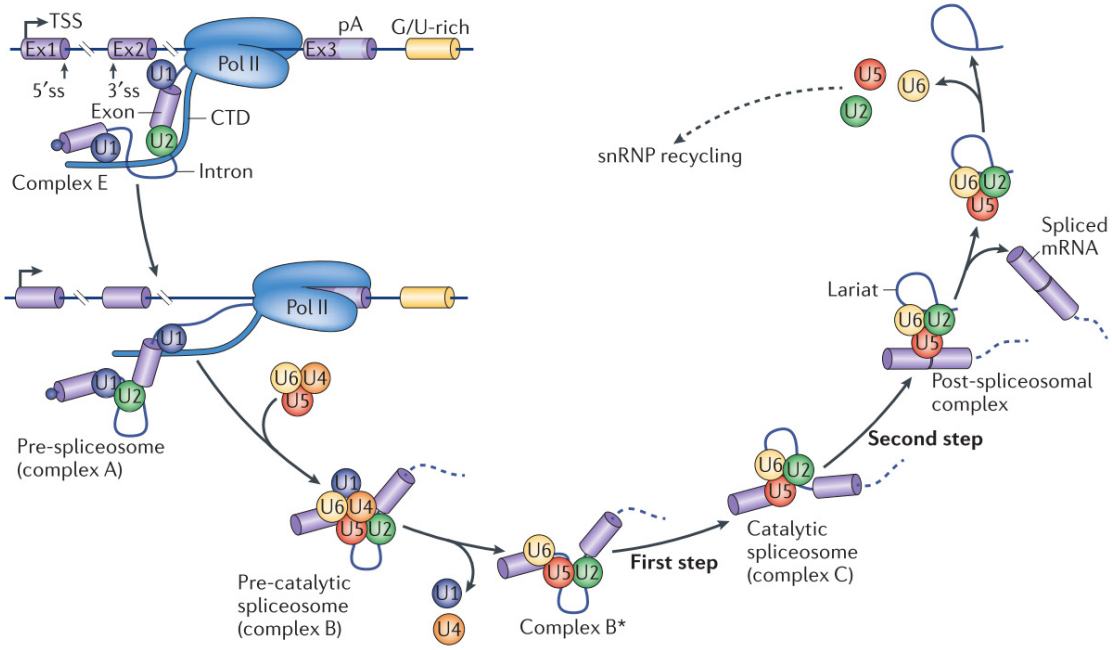

Fig. 1: The splicing of pre-mRNA
The spliceosome is assembled on the pre-mRNA in a step-wise manner. In two subsequents catalytic steps the introns are removed and the spliced mRNA is formed. The scheme is adapted from Matera & Wang (2014).

2 Composition of the spliceosome

The major subunits of the spliceosome are 5 small nuclear ribonucleoprotein particles (snRNPs) which each consists of a core and a set of specific proteins. The core snRNP is formed of uridine-rich small nuclear RNA (U1, U2, U4, U5 or U6 snRNA) and Sm or LSm ring (Fig. 2).

2.1 Uridine-rich snRNAs

The key component of each snRNP is non-coding RNA rich in uridines, U snRNA (Weinberg & Penman, 1968). These RNAs are about 100-200 nucleotides long and are rather abundant. In human cells, there are many copies of each snRNA gene (e.g. up to 30 copies in case of the U1 snRNA gene) and they are expressed in many different isoforms (Dahlberg & Lund, 1988; Sontheimer & Steitz, 1992). Based on the structure, sequence specifics and interacting partners, we distinguish two types of snRNAs and consequently snRNPs. Sm-type snRNAs (U1, U2, U4 and U5) have a 2,2,7-trimethyl-guanosine cap (TMG) at the 5'end, a site for binding of the Sm ring (Sm site) and a 3'stem

loop (Fig. 2A). LSm-type snRNAs (U6) are characterized by a 5' monomethyl-phosphate cap (MPG) and 3' uridines that form the binding site for LSm ring (Fig. 2B) (reviewed by Wahl *et al.*, 2009; Matera & Wang, 2014). The differences between Sm and LSm-type snRNA processing and snRNP biogenesis will be discussed later in Chapter 4.

2.2 Sm and LSm ring

Sm-type snRNPs contain a ring of proteins SNRNP B/B', D1, D2, D3, E, F and G (also known as Sm proteins) formed around each snRNA (Fig. 2A). LSm-type snRNPs have a very similar ring which is formed of like-Sm proteins, LSM2-8 (Fig. 2B) (reviewed by Wahl *et al.*, 2009; Matera & Wang, 2014). Both Sm and LSm proteins belong to the same family which is defined by the Sm motif. This motif is characterized by two conserved Sm domains (Sm1 and Sm2) separated by a linker region. The Sm domains were shown to be important for interactions between Sm proteins and thus enable formation of the heptameric ring (Hermann *et al.*, 1995). In case of the Sm ring, its formation is facilitated by the SMN complex which binds symmetrically dimethylated arginines in the C-terminal arginine-glycine (RG) repeats of human proteins SNRNPD1 a D3 (Brahms *et al.*, 2000; Friesen *et al.*, 2001). Despite the structural similarity of Sm and LSm ring, the location and the mechanism of the assembly differs substantially, as will be discussed later Chapter 4).

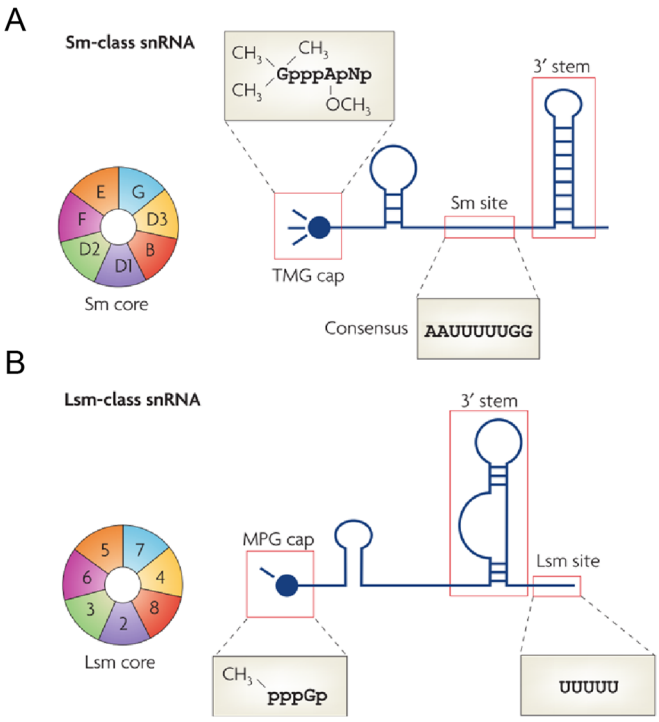

Fig. 2: The core Sm/LSm-typ snRNPs
A schematic structure and main features of Sm-type (A) and LSm-type (B) snRNA together with a diagram of the Sm and LSm ring are shown (adapted from Matera *et al.* 2007).

2.3 SnRNP specific proteins

Apart from the Sm and LSm proteins, the spliceosome has many other protein components specific for each snRNP. However, the snRNP composition is not fixed and many specific proteins join or leave snRNPs in the course of the splicing reaction. An overview of the proteins specific for the mature snRNPs just before the catalytic activation of the spliceosome (complex B) is shown in Fig. 3. One of the main topics of my work is the U5 snRNP and U5 specific protein PRPF8. On that account, I will describe the composition of U5 snRNP to more detail in the next chapter.

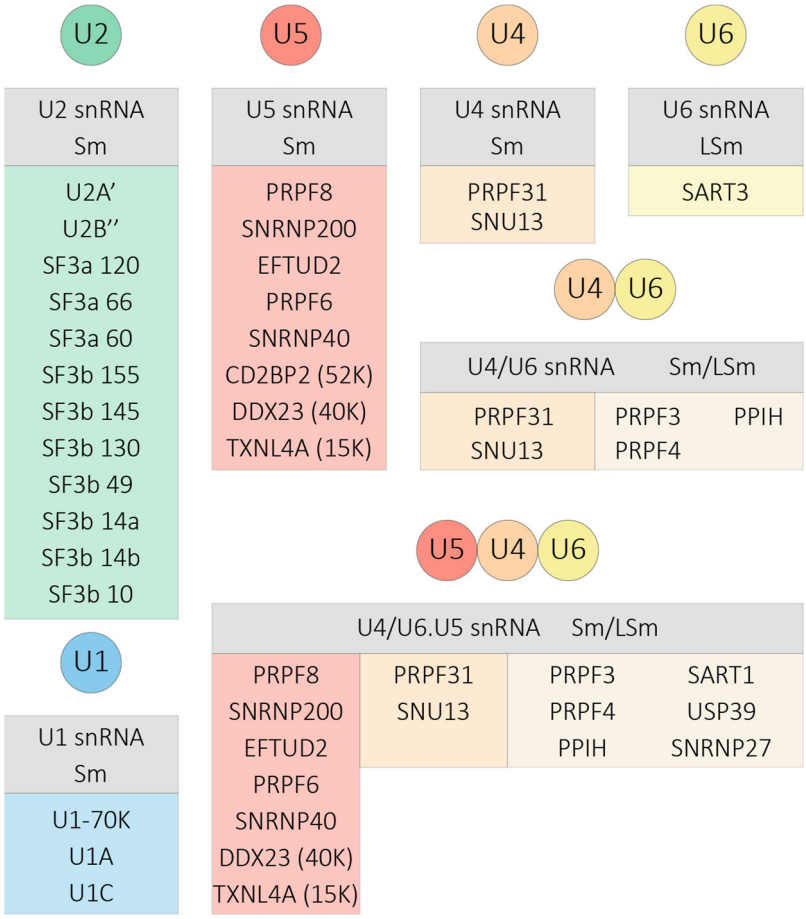

Fig. 3: Composition of major spliceosomal snRNPs in human
Each snRNP consists of a core snRNP (in grey) and a set of specific proteins (in colors). The ring of seven Sm proteins (SNRNP B/B', D1, D2, D3, E, F and G) or LSm proteins (LSM2-8) is simplified as "Sm" or "LSm".

3 U5 snRNP

Several forms of U5 snRNP with different protein composition have been described and are termed according to their sedimentation coefficient. Apart from the core U5 snRNP, the stable components of the particle are proteins PRPF8 (220K), SNRNP200 (200K), EFTUD2 (116K) and a smaller protein SNRNP40 (40K). When the mature U5 particle is formed, it is called 20S U5 snRNP and it contains additional proteins, specifically CD2BP2 (52K), DDX23 (100K), PRPF6 (102K) and TXNL4A (Dib1 or 15K) (Bach *et al.*, 1989). Later on, the U5 snRNP joins the U4/U6 di-snRNP, giving rise to the 25S particle. At this point, the protein CD2BP2 (52K) leaves U5 snRNP and is thus the only 20S U5-specific protein that is not part of the U4/U6.U5 tri-snRNP (Laggerbauer *et al.*, 2005). Major rearrangements of the U5 snRNP occur during the catalytic activation of the spliceosome. U5 snRNP specific proteins DDX23 (100K) and TXNL4A (Dib1 or 15K) dissociate and other non-snRNP splicing factors (including PRPF19 complex and SKIP protein) are recruited to the spliceosomal complex B* (45S). Finally, U5 snRNP with many splicing factors still attached is released from the post-splicing complex in a form of the 35S particle (Makarov *et al.*, 2002). The 35S U5 snRNP is then recycled, however the mechanism is still not very well understood.

3.1 SNRNP200

The protein SNRNP200 (also known as Brr2) is a member of the family of Ski2-like helicases (Noble & Guthrie, 1996) but has an unusual architecture. Unlike typical helicases, it has two tandem helicase cassettes. The N-terminal cassette possesses ATPase and RNA unwinding activities and is indispensable for splicing. The C-terminal cassette is catalytically inactive but it stimulates the activity of the N-terminal cassette (Hahn *et al.*, 2012; Santos *et al.*, 2012).

SNRNP200 is the key player for the catalytic activation of the spliceosome. It unwinds the U4/U6 snRNAs duplex, displacing U4 snRNP from the spliceosome and enabling U6 snRNA to base pair with U2 snRNA and to form the catalytically active complex B* (Laggerbauer *et al.*, 1998; Raghunathan & Guthrie, 1998). Furthermore, SNRNP200 is needed for rearrangements between the first and the second step of splicing (Hahn *et al.*, 2012), as well as for the spliceosome disassembly (Small *et al.*,

2006). Given the complexity of the SNRNP200 function in the spliceosome, it needs to be strictly regulated to guarantee precise timing of the process. Two U5 snRNP-specific proteins, PRPF8 and EFTUD2, are known to modulate the activity of SNRNP200 (see chapter 3.23.2 and 3.3).

3.2 PRPF8

PRPF8 (also known as hPrp8) is the largest of spliceosomal proteins (>220 kDa) and it is highly conserved from yeast to human (61% sequence identity) (Hoddges *et al.*, 1995). Despite being conserved, PRPF8 has no obvious homology to other proteins and only distant similarities with known protein domains were found. Based on them, the following names were assigned to individual PRPF8 regions (from N to C terminus): NTD1 and 2 (N-terminal domain 1 and 2), RT (reverse transcriptase-like)/En (endonuclease-like) domain, RH (RNase H-like) domain and Jab1 (c-Jun activation domain binding protein1-like) domain (Agafonov *et al.*, 2016). A consensus nuclear localization signal (NLS) was found in the NTD1 of PRPF8 (Grainger & Beggs, 2005).

As the main scaffolding protein of the U5 snRNP, PRPF8 lies in the catalytic center of the spliceosome and is involved in multiple interactions. UV-crosslinking experiments revealed that PRPF8 or its yeast orthologue interact with the 5' and 3' ss (Wyatt *et al.*, 1992; Teigelkamp *et al.*, 1995), the branch point of the pre-mRNA (MacMillan *et al.*, 1994) and U5 and U6 snRNAs (Dix *et al.*, 1998; Vidal *et al.*, 1999). Apart from RNA, PRPF8 binds U5 snRNP-specific proteins PRPF6, EFTUD2 and SNRNP200 (Achsel *et al.*, 1998; Liu *et al.*, 2006) and the recently identified assembly factor AAR2 (Santos, *et al.*, 2015).

The interaction of PRPF8 with the RNA helicase SNRNP2000 is particularly important for the purpose of this thesis, therefor I will describe it in more detail (Fig. 4). PRPF8 regulates both positively and negatively the helicase activity of SNRNP200 and thus controls its precise timing and prevents premature dissociation of U4/U6 snRNA (reviewed in Mozaffari-Jovin *et al.*, 2014). The first level of regulation takes place before the catalytic activation of the spliceosome, when the PRPF8 RH domain outcompetes SNRNP200 in binding of U4 snRNA and prevents U4/U6 duplex unwinding in tri-snRNP and complex B (Mozaffari-Jovin *et al.*, 2012). At the same time, the Jab1 domain binds the N-terminal cassette of SNRNP200. While the globular part and the C-terminal tail of

the Jab1 domain can stimulate SNRNP200 activity, the final 15 residues of the tail are inserted to the RNA binding tunnel and block it (Mozaffari-Jovin *et al.*, 2013). For catalytic activation, the SNRNP200 blocks need to be removed, but the information about the mechanism is still rather fragmentary. The whole process is most likely triggered by an exchange of U1 snRNA on 5'ss for U6 snRNA and RH domain of PRPF8, which leaves U4 snRNA free for SNRNP200 binding. Subsequently, a conformational change of SNRNP200 decreases the affinity for the distal part of Jab1 tail and releases the inhibition. What induces the conformational change of SNRNP200, is not clear. Free of blocks, SNRNP200 is stimulated by its own C-terminal cassette and by the rest of Jab1 domain, and the unwinding of U4/U6 snRNA can begin. The Jab1 domain stays with SNRNP200 and can influence also later steps of splicing (reviewed in Mozaffari-Jovin *et al.*, 2014).

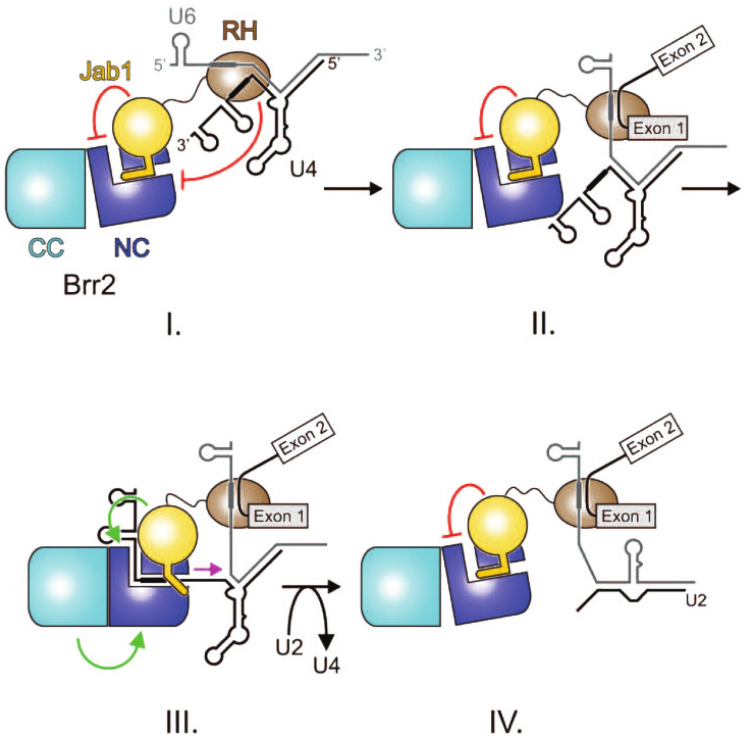

Fig. 4: Model for the regulation of SNRNP200 by PRP8
The model shows how are Jab1 and RH domains of PRPF8 involved in regulation of SNRNP200's U4/U6 duplex unwinding activity. Red lines mark inhibitory effects; green arrows stimulatory effects; magenta arrow indicates movement of SNRNP200 on U4 snRNA. The scheme is adapted from (Mozaffari-Jovin *et al.*, 2014).

3.3 EFTUD2

EFTUD2 (also known as Snu114) is a GTPase that is highly homologous to the translation elongation factor G (EF-G) (Fabrizio *et al.*, 1997). It directly interact with both PRPF8 and SNRNP200 (Liu *et al.*, 2006). It was proposed that GTP hydrolysis leads to conformational changes of EFTUD2 which are communicated through PRPF8, SNRNP200 or other factors, and regulate both spliceosome activation and disassembly (Brenner & Guthrie, 2006; Small *et al.*, 2006).

3.4 PRPF6

PRPF6 (also known as hPrp6) contains 19 tetratricopeptide repeats (TPRs) and thus belongs to the TPR protein family (Makarov *et al.*, 2000). Proteins from the family are usually involved in multiple protein-protein interactions and consistently, PRPF6 is bridging the U5 snRNP to U4/U6 di-snRNP through association with several proteins from both sides, including PRPF8 and SNRNP200 from U5 and PRPF31 from U4 snRNP (Makarov *et al.*, 2000; Liu *et al.*, 2006; Agafonov *et al.*, 2016).

4 Biogenesis of snRNPs

The biogenesis of each snRNPs is a complicated process and in case of the Sm-type snRNPs involves both cytoplasmic and nuclear phase (Fig. 5). The spatial separation of the mature and immature forms is common in a biogenesis of compound particles and its role is to prevent contact of partially assembled complexes with their substrates. The maturation pathway of U6 snRNP is rather exceptional and will be discussed in detail at the end of this chapter.

4.1 Transcription of snRNAs and their export

The biogenesis of Sm-type snRNPs starts in the nucleus with transcription of pre-snRNA (Fig. 5). Similarly to protein-coding genes, snRNAs are transcribed by RNA polymerase II (Chandrasekharappa *et al.*, 1983), however they have different promoters and require additional transcription factors (reviewed by Egloff *et al.*, 2008). The nascent snRNA acquires co-transcriptionally a 7-methylguanosin (m^7G) cap but it does not have a polyadenylation signal at the 3' end. Instead, the transcription of Sm-type snRNA genes terminates downstream of the 3' box element, a processing signal recognized by a large complex called Integrator. The Integrator then endonucleolytically cleaves the nascent RNA and releases it from the site of transcription (Baillat *et al.*, 2005). The m^7G cap on the RNA serves as a signal for an export from the nucleus. It is recognized by a cap binding complex (CBC) which recruits other factors including ARS2 and the export adaptor PHAX (Izaurralde *et al.*, 1995; Ohno *et al.*, 2000). The hyperphosphorylated PHAX is bound by the export receptor CRM1 (also known as exportin 1) and the GTPase RAN and the whole complex is then exported to the cytoplasm through a nuclear pore (Fig. 5) (Fornerod *et al.*, 1997; Ohno *et al.*, 2000). As will be discussed later (chapter 6.2), there are indications that on the way from the nucleus, the pre-snRNA travels through nuclear structures known as Cajal bodies (CBs) where the assembly of the export complex seems to be facilitated (Fig. 5).

4.2 Cytoplasmic assembly of core snRNPs

Outside of the nucleus, PHAX is dephosphorylated, GTP on RAN is hydrolyzed and the whole export complex disintegrates (Fig. 5) (Kitao *et al.*, 2008). The control over the newly exported snRNA is taken by the SMN complex, which consists of SMN (survival motor neuron), GEMINs 2-8 and UNRIP proteins. The complex helps the stepwise assembly of the Sm ring around a sequence termed the Sm site and thus stabilizes the snRNA (Fig. 5). Although the Sm ring is able to self-assemble on RNA *in vitro*, the SMN complex is controlling the specificity and it is facilitating the Sm ring assembly *in vivo* (reviewed by Raimer *et al.*, 2016). It also recruits the methyltransferase TGS1 which transforms the m^7G cap to the TMG (Fig. 5) (Mattaj, 1986; Mouaikel *et al.*, 2003). Finally, the snRNA is trimmed at its 3'end (Dahlberg *et al.*, 1990) and the newly established „core snRNP" is re-imported to the nucleus (Fig. 5). The Sm ring together with the TMG cap both serve as nuclear localization signals, the ring is indispensable for nuclear transport whereas the cap importance depends on the type of snRNP and cell line (Fischer *et al.*, 1993).

In case of the TMG cap-dependent import pathway, the cap is bound by SNUPN, snurportin1, which subsequently serves as an adaptor for KPNB1, importin-β (Fig. 5) (Palacios *et al.*, 1997; Huber *et al.*, 1998). The Sm ring-dependent pathway is not well established and it can work either independently or synergically with the first one.

4.3 Nuclear import and final maturation of snRNPs

The assembled core snRNPs are re-imported to the nucleus where the final stages of snRNP biogenesis take place. In most mammalian cells, the final maturation of snRNPs is believed to occur in CBs and includes snRNA modifications and addition of the snRNP-specific proteins (Fig. 5) (Sleeman & Lamond, 1999; Darzacq *et al.*, 2002; Nesic *et al.*, 2004). At the end, the mature snRNPs form higher complexes like di-snRNP (U4/U6 snRNP) and tri-snRNP (U4/U6·U5 snRNP) and leave CBs (Staněk *et al.*, 2003; Staněk & Neugebauer, 2004; Schaffert *et al.*, 2004). The assembled particles are stored within compartments called nuclear speckles and are prepared to join the splicing reaction which occurs at the border of speckles and adjacent chromatin (reviewed in Spector &

Lamond, 2011). For more details about the addition of snRNP-specific proteins and the role of CBs, see Introduction, chapters 4.5 and 6.3 respectively.

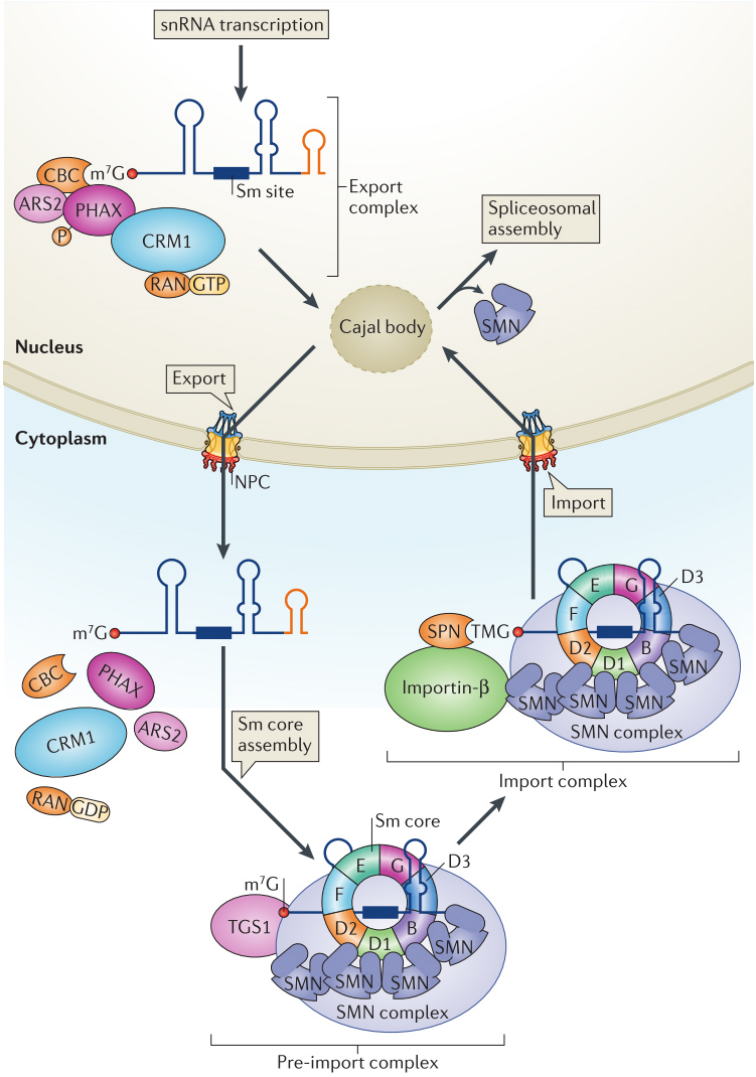

Fig. 5: Maturation pathway of Sm-type snRNPs
The biogenesis of Sm-type snRNPs involves both cytoplasmic and nuclear phase. Cajal bodies were suggested to play role in early steps befor the export of the snRNA to the cytoplasm as well as after the nuclear import of the core snRNP. The scheme is adapted from Matera & Wang (2014).

4.4 Biogenesis of U6 snRNP

The maturation pathway of U6 snRNP differs from that of other U snRNPs. First of all, the U6 snRNA is transcribed by RNA polymerase III (Reddy *et al.*, 1987). During transcription, the snRNA acquires a 5'-triphosphate cap and a 3'-polyuridine tract and similarly to other RNA polymerase III transcripts, it is recognized and bound by La protein (Terns *et al.*, 1992). This association protects U6 snRNA against degradation and it

targets the RNA to nucleolus where it undergoes further modifications. In nucleoli, the cap is methylated to a γ-monomethyl-phosphate cap (Singh & Reddy, 1989), the 3' end of the U6 snRNA is adjusted and a terminal cyclic 2',3'-phosphate is formed (Lund & Dahlberg, 1992). Subsequently, La protein leaves the snRNA and a preformed heteroheptameric ring of like-Sm (LSm proteins) associates with the modified 3' end forming the core U6 snRNP (Achsel *et al.*, 1999). Finally, small nucleolar RNAs (snoRNAs) modify the U6 snRNA by 2'O-ribose-methylation and pseudouridynilation (Ganot *et al.*, 1999). Then, the core U6 snRNP leaves the nucleolus and is escorted by SART3 to CBs, where the mature U6 snRNP is assembled and joins other snRNPs (Staněk *et al.*, 2003).

4.5 Addition of snRNP-specific proteins

Taken together, the pathway of snRNA to the mature snRNP is well described. However, it still remains unclear how the specific proteins are assembled on the particle. Specifically, in which order do the proteins join the snRNP and whether they come alone or form pre-complexes.

Several pieces of evidence indicate that most snRNP-specific proteins are added to the core snRNP in the nucleus. Many of them contain a NLS and were shown to travel to the nucleus independently (U1-70K) or in groups (U2A+U2B, U2-SF3A heterotrimer) (Kambach & Mattaj, 1994; Romac *et al.*, 1994; Nesic *et al.*, 2004). Also a pre-assembled complex of PRPF3/PRPF4/PPIH proteins associates with di-snRNP after U4/U6 snRNA annealing, an event that was shown to occur in the nucleus and specifically in CBs (Nottrott *et al.*, 2002). Moreover, some snRNAs are able to get to the nucleus and accumulate in CBs even after depletion of key snRNP-specific proteins – SF3A for U2 and PRPF31 for U4 snRNA (Schaffert *et al.*, 2004; Tanackovic & Kramer, 2005). Together with the localization of many snRNP-specific proteins in CBs, these findings support the role of CBs in the final snRNP assembly. However, there are at least some exceptions. For example SART3, the only U6 snRNP-specific protein, associates with the core U6 snRNP already in the nucleoplasm and is responsible for its targeting to CBs (Staněk *et al.*, 2003). The biogenesis of U1 snRNP seems to be entirely independent of CBs as it does not accumulate in these structures like other snRNPs, but instead its components were found in nuclear bodies called "gems" (Stejskalová & Staněk, 2014).

The assembly pathway of the human U5 snRNP is poorly characterized. The only piece of information comes from budding yeast. Gottschalk *et al.* (2001) identified yeast intermediate complex containing the core U5 snRNP together with yPrp8 and ySnu114, orthologues of the human proteins PRPF8 and EFTUD2. According to the model proposed later on (Fig. 6), the intermediate is formed in the cytoplasm and remaining U5 snRNP-specific proteins join the complex in nucleus. The nuclear import is dependent on the NLS of yPrp8 (Boon *et al.*, 2007).

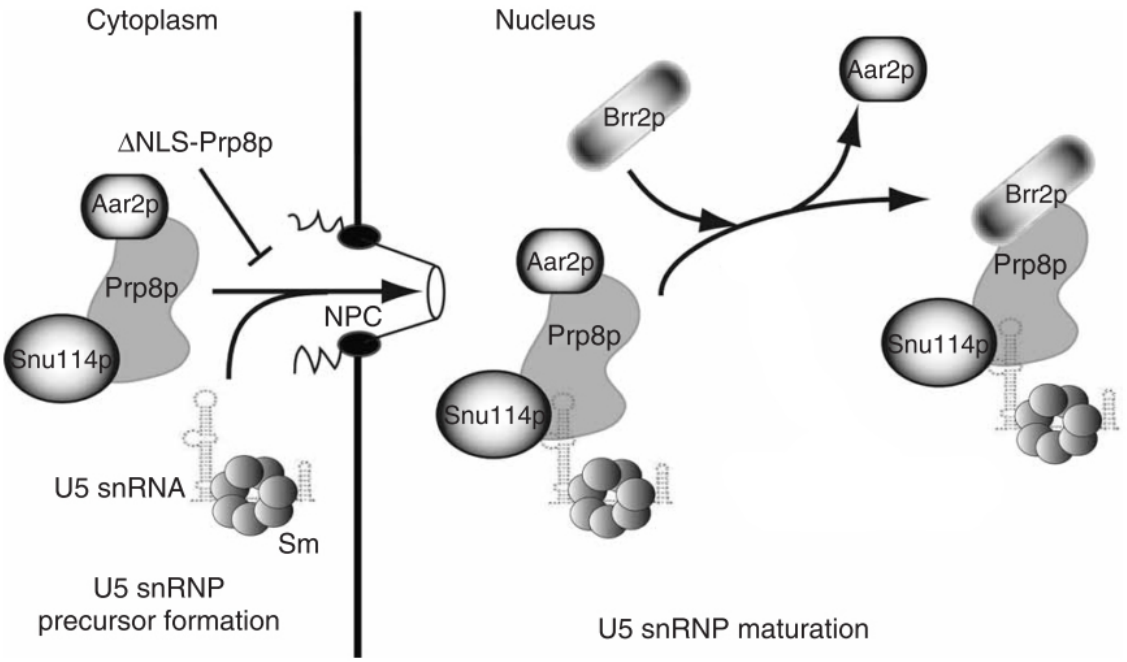

Fig. 6: U5 snRNP biogenesis in budding yeast
The cartoon shows a model of U5 snRNP biogenesis in yeast (adapted from Boon *et al.* (2007)). NPC stands for nuclear pore complex.

5 Factors involved in snRNP biogenesis

The biogenesis of complex particles, such as snRNPs, is an intricate and multistep process. Therefore, assembly factors are often required to assist during folding of individual components and during assembly and remodeling of intermediate complexes. Yet, not much is known about such factors involved in maturation of snRNPs. Protein yAar2 was suggested to play a role in the biogenesis of U5 snRNP in yeast (Gottschalk *et al.* 2001). Only recently, a role of the HSP90/R2TP chaperon system in the biogenesis of the human U4 snRNP was shown (Bizarro *et al.*, 2015).

5.1 AAR2

The orthologue of human AAR2 (yAar2) was first noticed in *Saccharomyces cerevisiae.* Mutation in the gene gave rise to splicing defects of mating-type protein pre-mRNA (Nakazawa *et al.*, 1991). A decade later, the protein yAar2 was found to be associated with the cytoplasmic U5 snRNP assembly intermediate and was suggested to be a factor important for maturation and recycling of U5 (see Introduction, chapter 4.5 and Gottschalk *et al.* 2001). Crystal structures of the yPrp8/yAar2 complex revealed that the binding of yAar2 to yPrp8 sterically interferes with binding of yBrr2. When the intermediate U5 snRNP complex gets to the nucleus, yAar2 is phosphorylated, its affinity towards yPrp8 decreases and it is replaced by the yBrr2 helicase (SNRNP200 in human). Thus, yAar2 adds another level of Brr2 activity regulation and prevents premature spliceosome activation (Weber *et al.*, 2011; Nguyen *et al.*, 2013; Weber *et al.*, 2013).

5.2 HSP90/R2TP complex

5.2.1 HSP90

Heat shock protein 90 (HSP90) is a highly abundant and conserved molecular chaperon which is essential in eukaryotes (reviewed in Li & Buchner, 2013). The protein forms homodimers which are connected through the C-terminal domains (Nemoto *et al.*, 1995). The N-terminal domain of HSP90 is able to bind ATP and this binding and hydrolysis trigger conformational rearrangements and modulate the activity of the dimer (Prodromou *et al.*, 1997; Panaretou *et al.*, 1998; Obermann *et al.*, 1998).

HSP90 is involved in variety of cellular processes. It participates in protein folding and stabilization, in assembly of complex machineries, as well as in protein degradation (reviewed in Picard, 2002; Boulon *et al.*, 2012; Li & Buchner, 2013) . In contrast to other chaperons, HSP90 selectively targets just a sub-group of proteins and instead of helping with maturation of nascent proteins, it rather facilitates last steps of the client proteins folding. These qualities make it convenient for controlling formation of bigger protein complexes (Jakob *et al.* , 1995; Nathan *et al.*, 1997). HSP90 collaborates with a number of auxiliary factors, called co-chaperons, which can be either single molecules or multisubunit complexes. Their role is to recruit specific client proteins and modulate HSP90 function. Alternatively, co-chaperons might have yet unanticipated role of their own (reviewed in Picard, 2002; Boulon *et al.*, 2012; Li & Buchner, 2013).

5.2.2 R2TP complex

One of the HSP90's co-chaperons is the R2TP complex (Zhao *et al.*, 2005). In human, the complex consists of 4 subunits: RPAP3 (Jeronimo *et al.*, 2007), PIH1D1 (Te *et al.*, 2007) and two ATPases, RUVBL1 and RUVBL2 (Puri *et al.*, 2007).

The protein RPAP3 (Tah1 in yeast) contains two TPR regions that are able to bind both C-terminal conserved MEEVD peptide motifs of HSP90 dimer, and thus serves as a link between HSP90 and R2TP (Pal *et al.*, 2014).

The second R2TP component, PIH1D1 (Pih1 in yeast), serves as an adaptor protein since it binds the other R2TP proteins as well as it recruits specific substrates (Pal *et al.*, 2014). Studies in yeast have shown that yPih1 is rather unstable and less abundant than other R2TP factors and so it is the limiting element. The HSP90 together with yTah1 are able to stabilize it and via this feedback loop modulate R2TP complex activity (Zhao *et al.*, 2008; Paci *et al.*, 2016).

RUVBL1 and RUVBL2 are highly conserved proteins that belong to the family of AAA+ ATPases and are essential in eukaryotes. Together, they assemble into hetero-hexamers and/or double hexameric structures and this ring-like formations synergically increase ATPase and helicase activity of the proteins. Most RUVBL1 and 2 functions are ATP-dependent, however the exact molecular mechanism has not been clarified (Puri *et al.*, 2007; López-Perrote *et al.*, 2012).

5.2.3 HSP90/R2TP complex function

Together, HSP90 and R2TP complex help the assembly of several multi-protein complexes including small nucleolar RNPs (Zhao *et al.*, 2008), the RNA polymerase II complex (Boulon *et al.*, 2010), PIKKs complexes (Hořejší *et al.*, 2010) and for the purpose of this thesis most importantly, also U4 snRNP (Bizarro *et al.*, 2015). Interestingly, RUVBL1 and 2 were found to be associated with many cellular complexes themselves, independently of the R2TP complex. They were suggested to be involved in the biogenesis of chromatin remodeling complex, mitotic spindle or telomerase, and even to participate in regulation of transcription (reviewed in Nano & Houry, 2013). An alternative hypothesis is that these complexes are actually HSP90/R2TP clients and that the main role of the complex in this case is to load RUVBL1 and 2, which would explain the absence of remaining R2TP components. Subsequently, RUVBL1 and 2 might help to stabilize the client complexes and/or to promote the assembly processes (Verheggen *et al.*, 2015).

The above mentioned role of the HSP90/R2TP complex in the assembly of U4 snRNP confirms that the formation of so complex particles as snRNPs requires help of additional factors. What facilitates the assembly of the remaining U snRNPs is not clear. Recently, a phosphate-dependent interaction was described between R2TP-protein PIH1D1 and U5-specific EFTUD2 (Hořejší *et al.*, 2014) suggesting that the R2TP complex might play a role also in the biogenesis of U5 snRNP.

6 Cajal bodies

The cell nucleus is an overcrowded place. In order to guarantee a fluent course of many important ongoing processes, including splicing, it needs to be tightly organized. DNA is packed into chromatin and a substantial part of the interchromatin space is occupied by nuclear bodies. The bodies composed of proteins and RNA molecules are not held together by membranes but rather by a large number of weak interactions. They can exchange their content with the surrounding environment and quickly adapt to the actual needs of the cell. It seems that their main role is to separate different biochemical processes and speed them up by bringing all players to a close proximity. Many different kinds of nuclear bodies exist, for instance nucleoli, histone locus bodies (HLBs), promyelocytic leukemia oncoprotein (PML) bodies, Polycomb (PcG) bodies, speckles, paraspeckles and last but not least, Cajal bodies (Mao *et al.*, 2011; Sleeman & Trinkle-Mulcahy, 2014).

6.1 Nature of Cajal bodies

Cajal bodies (CBs) are nuclear spherical structures (Fig. 7) that were discovered more than a hundred years ago by Spanish neurobiologist Ramón y Cajal (Cajal, 1903). Formerly, they were termed accessory bodies (Cajal, 1903), endobodies (Bier *et al.*, 1967) or coiled bodies (Monneron & Bernhard, 1969) until they were renamed Cajal bodies in honor of the discoverer (Gall *et al.*, 1999).

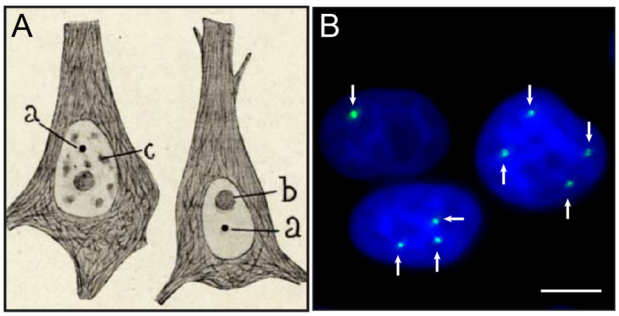

Fig. 7: Cajal bodies
(A) The original drawing of Ramón y Cajal depicting human pyramidal cells with labled CBs by letter „a“ (adapted from Gall (2003)).
(B) HeLa cells with CBs visualized by the marker protien coilin and highlighted by arrowheads. DAPI (blue); coilin (green); scalebar - 10 µm.

CBs are evolutionarily conserved and were found in a wild range of eukaryotic organisms including mammals, amphibians, insect and plants. Usually, there are one to six CBs in a cell and their average size ranges from 0.2 to 1.0 µm (Fig. 7) (reviewed in Cioce & Lamond, 2005). Furthermore, the number and size of CBs is dependent on the

cell cycle; they are maximal at the G1/S phase and disintegrate at M phase (Andrade *et al.*, 1993).

Although their high conservation points out to an important role of CBs, they are not ubiquitous and typically occur just in highly proliferative or metabolically active cells like embryonic cells, tumor cells or neurons (reviewed in Cioce & Lamond, 2005). Indeed, when CBs were compared in experimental models of cell proliferation, the cells with higher levels of gene expression and metabolic activity contained more CBs and of larger size (Andrade *et al.*, 1993)

The composition of CBs is surprisingly complex but they share a common feature – the protein coilin – which is nowadays considered the marker of CBs (Andrade *et al.*, 1991; Raška *et al.*, 1991). Besides coilin, they contain variety of other factors. The snRNAs, snRNP-specific proteins, SMN and factors responsible for snRNA modifications are accumulated in these nuclear compartments (Raška *et al.*, 1991; Liu & Dreyfuss, 1996; Darzacq *et al.*, 2002). Additionally, other elements involved in transcription, DNA damage response and RNA processing localize to CB, e.g. RNA polymerases with transcription factors (Schul *et al.*, 1998), telomeric RNA with telomerase reverse transcriptase (Zhu *et al.*, 2004), DNA repair protein WRAP53 (Tycowski *et al.*, 2009), U7 snRNA involved in histone mRNA processing (Frey & Matera, 1995) or small nucleolar RNAs (snoRNAs) with fibrillarin that guide RNA modification (Andrade *et al.*, 1991; Narayanan *et al.*, 1999).

Interestingly, CBs are very dynamic structures and components stay inside them just temporarily. The exchange rate depends on a molecule type but even coilin remains in CB merely several minutes (Sleeman *et al.*, 2003; Dundr *et al.*, 2004). This suggests that there is an equilibrium between nucleoplasmic and CBs pool of molecules and that higher concentration of interaction partners are the driving force attracting new components to CBs.

6.2 Function of Cajal bodies

Up to now, CBs were implicated in biogenesis of various complexes. The role of CBs in the assembly of spliceosomal snRNPs is well established and explains the abundance of the spliceosomal components in these structures. On the top of it, CBs

seem to be involved also in formation of other RNPs, like snoRNPs or telomerase. Hence, the role of CBs might simply be to increases the efficiency of higher complexes assembly by serving as a meeting place for individual precursors and auxiliary factors (reviewed in Staněk & Neugebauer, 2006). Accordingly, mathematical models and kinetic monitoring of U4/U6.U5 tri-snRNP assembly showed that the process is 10-fold faster in CBs than in the nucleoplasm (Novotný *et al.*, 2011). Higher demands of functional RNPs in metabolically active cells could explain the tissue-specific importance of CBs. This idea is further supported by the fact that the overexpression of snRNP-specific Sm proteins enhances the formation of Cajal bodies while overexpression of coilin does not (Sleeman *et al.*, 2001). Therefore, in this case the excess of snRNP precursors and need for their fast assembly, rather than levels of the building block - coilin, are the key factors launching CBs formation.

Several lines of evidence indicate that CBs are also engaged in transcription and organization of chromatin. They were found specifically associated with genes coding for snRNAs, snoRNAs and histones, and the association is dependent on active transcription of these genes. CBs disruption leads to reorganization of gene clusters and reduced expression of involved genes. Hence, CBs are actively contributing to nuclear architecture and gene expression (Frey & Matera, 1995; Wang *et al.*, 2016).

Other functions of CBs still remain elusive. It is known that they are disrupted upon treatment causing DNA damage. Moreover, several factor involved in DNA damage response localize to CBs and one of them, WRAP53, is essential for CBs integrity. It thus remains to be determined what role CBs have in DNA repair.

6.3 Role of Cajal bodies in snRNP biogenesis

The role of CBs in snRNP life was already outlined in Introduction, chapter 4. The first contact occurs right at the beginning of snRNP biogenesis, as the pre-snRNAs were detected in CBs by *in situ* hybridization (Smith & Lawrence, 2000). This was further confirmed by experiments done in frog oocytes; the pre-snRNAs microinjected to the nucleus accumulated first in CBs before being exported to the cytoplasm (Suzuki *et al.*, 2010). PHAX and CRM1, factors responsible for pre-snRNA export, were also found in

CBs, which supports the hypothesis that CBs are involved in the assembly of the export complex (Frey & Matera, 2001).

After traveling to the cytoplasm and back again to the nucleus, snRNAs visit CBs once more. This time, snRNAs go through modifications that are guided by small Cajal body-specific RNPs (scaRNPs). This special sort of RNPs is very similar to snoRNPs but instead of modifying ribosomal RNAs in the nucleolus, works in CBs on snRNAs. The modifications include 2'-O-methylation of the sugar backbone and a conversion of selected uridines to pseudouridines (Darzacq *et al.*, 2002).

Finally, specific proteins join snRNPs also mainly in CB and the formation of snRNPs is then completed (see also Introduction, chapter 4.3). Subsequently, the annealing of U4 and U6 snRNAs is promoted by the U6-specific protein SART3; an event that preferentially occurs in CBs as well. Next, U5 snRNP is connected with the U4/U6 di-snRNP via a protein bridge and SART3 disassociates as the U4/U6•U5 tri-snRNP complex is formed (Staněk *et al.*, 2003; Staněk & Neugebauer, 2004). Interestingly, depletion of the bridging proteins inhibits tri-snRNP formation and results in di-snRNP accumulation in CBs (Schaffert *et al.*, 2004). Similarly, disruption of the U2 snRNP biogenesis leads to the sequestration of U2 snRNP components in CBs (Tanackovic & Kramer, 2005). Thus, it seems that the role of CBs is not only to enhance spliceosome assembly but also to control the final steps of snRNP maturation and to sequester immature snRNPs.

During splicing reaction, the spliceosome undergoes substantial rearrangements, including changes in the composition of individual snRNPs. In order to make use of the post-splicing snRNPs, they need to be rebuilt and reassembled but the process is not well understood. It was shown that snRNPs repeatedly cycle through CBs and it was therefore proposed that the snRNP reassembly occurs in CBs as well (Staněk *et al.*, 2008).

6.4 Coilin - the scaffold protein of Cajal bodies

Coilin is a protein essential for the proper formation of CBs as its depletion leads to CBs disappearance. The N' and C' termini of the protein are both relatively conserved and are necessary for CBs formation (reviewed in Machyna *et al.*, 2015). The N-terminal domain is able to self-interact and the network of coilins thus serves a scaffold of CBs

(Hebert & Matera, 2000). The C-terminus has a Tudor domain like structure and interacts with Sm proteins that are the core part of snRNPs (Xu *et al.*, 2005; Shanbhag *et al.*, 2010). Interestingly, the ability of coilin to self-interact is modulated by the C-terminal domain which determines the number and size of CBs (Shpargel *et al.*, 2003). Concerning the central region of coilin, it is not conserved and is highly unstructured. It contains two NLS and in case of the human protein also a so called RG box. The arginines of RG box can be symmetrically methylated and in that state are bound by the Tudor domain of the SMN protein (Hebert *et al.*, 2001).

On the top of these interactions, coilin directly interacts with many other CBs proteins (reviewed in Machyna *et al.*, 2015). Even though coilin does not have a canonical RNA binding motive, iCLIP experiments provide evidence that it is also able to bind RNAs *in vivo* (Machyna *et al.*, 2014). Whether coilin has other tasks in CBs apart from being the scaffold, is not clear.

The deficiency of coilin has serious consequence in vertebrates. In mice, knockout of coilin leads to reduced rate of embryonic survival and lower fertility (Walker *et al.*, 2009). In zebrafish, coilin depletion is lethal for the developing embryos but it can be rescued by microinjection of mature snRNPs (Strzelecka *et al.*, 2010). Human cancer cell lines lacking coilin exhibit reduced proliferation and splicing efficiency (Whittom *et al.*, 2008). These observations go in line with higher metabolic demands of affected cells. Surprisingly, in flies and plants coilin is not necessary for the viability. It is worth noticing, however, that coilin in these species differs significantly from other coilin orthologues and it is therefore possible that it has slightly different role or mechanism of function (Collier *et al.*, 2006; Liu *et al.*, 2009).

7 Splicing and disease

Given the importance of splicing, it is not surprising that mutations altering splicing can cause serious problems and give rise to various diseases. The disorders connected to splicing can be caused either by mutations in sequence elements which determine splicing (cis-acting mutations) or by mutations in a splicing machinery component that give rise to general splicing problems (trans-acting mutations).

7.1 Cis-acting mutations

The cis-acting mutations can be found at splice sites, branch point, polypyrimidine tract or other silencer and enhancer regulatory elements, and usually lead to mis-splicing of important genes. Up to now, many hereditary diseases caused by splicing alterations of specific genes have been identified. Additionally, changes in the splicing pattern often serve as a trigger of cancer progression, as some mis-spliced protein isoforms may for example promote cell growth or survivor (reviewed by David & Manley, 2010; Singh & Cooper, 2012; Scotti & Swanson, 2015). The frequency of the cis-acting mutations is hard to predict due to the insufficient knowledge of the splicing code. It was suggested that up to 50-60 % of disease-causing mutations actually alter splicing patterns rather than affect normal function of the proteins (Pagenstecher *et al.*, 2006; López-Bigas *et al.*, 2005).

7.2 Trans-acting mutations

The trans-acting mutations in the spliceosomal components are not particularly common, probably due to the fact that the majority of the components are essential for cell viability. The mutations can potentially work in either loss-of-function or gain-of-function manner. In case of the loss-of-function mutations, there is not enough of the functional protein in the cell due to its decreased or lost ability to fulfil the duties (haploinsufficiency). With the gain-of-function mutations, the mutated protein acquires a new function or alters the current one, which consequently impairs cellular processes. Alternatively, the mutant can even have a dominant toxic effect on cells.

First of all, number of somatic mutations of splicing machinery were identified by comparisons of sequences from cancerous and normal tissues (reviewed in David & Manley, 2010; R. K. Singh & Cooper, 2012; Scotti & Swanson, 2015).

The germline spliceosomal mutations are also found in variety of human disorders. The best studied examples are the mutations causing a human hereditary dystrophy called retinitis pigmentosa (see also Introduction, chapter 7.4). Over the recent years, mutations in several other splicing factors have been identified in a group of relatively rare genetically determined syndromes that have craniofacial malformations as the common feature. Out of these, mandibulofacial dysostosis of Guion-Almeida type (MFDGA) is a syndrome caused by autosomal dominant loss-of-function mutations in U5 snRNP-specific protein, EFTUD2 (Lines *et al.*, 2012). Another U5 protein, TXNL4A, is mutated in case of Burn-McKeown Syndrome (BMKS), the mode of inheritance is autosomal-recessive and the mutations cause loss-of-function of the protein (Wieczorek *et al.*, 2014). Further examples are the Nager syndrome (NS) caused mainly by frameshift mutations in U2-specific *SF3B4* gene (Bernier *et al.*, 2012), and cerebrocostomandibular syndrome (CCMS) induced by mutations in *SNRPB* gene (Lynch *et al.*, 2014). The CCMS is particularly interesting from the perspective of splicing as it is caused by mutations in exonic splicing silencer which promotes inclusion of exon with premature termination codon (PTC). The PTC triggers nonsense-mediated mRNA decay and leads to decreased levels of SNRPB protein (Lynch *et al.*, 2014). Finally, congenital malformances are also connected to disruption of the minor spliceosome; biallelic mutations in U4atac snRNA cause a rare developmental defect, microcephalic osteodysplastic primordial dwarfism type I (Edery *et al.*, 2011; He *et al.*, 2011).

Mutations in spliceosome assembly factors belong to the trans-acting mutations as well. A typical example is a disease called spinal muscular atrophy (SMA) which is caused by mutation in *SMN* gene (see also Introduction, chapter 7.3).

Finally, another class of trans-acting mutations are those found in splicing regulatory factors or regions that influence these factors. Similarly as in previous cases, these mutations can easily lead to cancer development via mis-regulation of alternative splicing (reviewed in David & Manley, 2010; Singh & Cooper, 2012; Scotti & Swanson, 2015). Apart from that, mutations in the splicing regulator FOX1 were found to be associated with autism (Martin *et al.*, 2007). A nice example of mis-regulation of trans-

acting factors is that of myotonic dystrophy (MD). In case of this disease, an introduction of microsatellite expansion mutations leads to the expression of expanded RNAs that accumulate in nuclear foci and sequester muscleblind-like splicing regulators (MBNLs). The consequences of the MBNL insufficiency manifest in a form of MD (reviewed in Ranum & Cooper, 2006).

Given the focus of my thesis, I would like to look closer on disorders disrupting spliceosomal biogenesis and function.

7.3 Spinal muscular atrophy (SMA)

SMA is an autosomal recessive neuromuscular disorder characterized by gradual degeneration of motor neurons and consequent atrophy of skeletal muscles, usually leading to death in early childhood (reviewed in Coady & Lorson, 2011; Markowitz *et al.*, 2012). In human genome, there are two very similar genes, *SMN1* and *SMN2* (Lefebvre *et al.*, 1995). Due to a single point mutation that affects alternative splicing pattern, the genes differ in the expression levels of full-length SMN, which is high for *SMN1* and low for *SMN2* (Lorson *et al.*, 1999). The absence of SMN is embryonically lethal (Schrank *et al.*, 1997). SMA is caused by low levels of SMN when *SMN1* gene is mutated and *SMN2* does not produce enough of the functional protein (Lorson *et al.*, 1999).

The protein SMN has been implicated in several cellular activities. It not only facilitates the assembly of the Sm ring during snRNPs biogenesis but it is was for instance suggested to specifically function in axonal RNA trafficking (reviewed in Coady & Lorson, 2011; Fallini *et al.*, 2012; Raimer *et al.*, 2016). Since SMA is a neurodegenerative disease, speculations have arisen about which function of SMN is crucial in this case. Animal models revealed that snRNP assembly is impaired and snRNP levels are decreased in SMA animals, and that the extent of the defects correlates with disease severity (Gabanella *et al.*, 2007). Remarkably, lack of SMN preferentially affects U11 snRNP levels and some genes associated with axonal function were shown to be enriched for minor introns, implicating gene specific splicing defects (Wu & Krainer, 1999; Gabanella *et al.*, 2007). Other studies oppose that specific reduction in minor snRNAs levels is rather a secondary consequence of developmental arrests caused by SMN loss in *Drosophila* (Praveen *et al.*, 2012; Garcia *et al.*, 2013). In agreement, the previously mentioned

mutations in minor spliceosomal snRNA gene do not display a neuron specific phenotype (Edery *et al.*, 2011; He *et al.*, 2011). On the top of that, splicing defects are detectable only in the later stages of disease development in mouse whereas neuromuscular deficits start sooner (Bäumer *et al.*, 2009). Therefore, it seems that various factors contribute to SMA etiology, but the precise mechanism remains unclear.

7.4 Retinitis pigmentosa (RP)

RP is the most prevalent form of a hereditary retinal disorder affecting 1 out of 4000 people worldwide. It causes gradual damage of photoreceptor cells, rods and cones, as well as disruption of the retinal pigment epithelium (RPE), and eventually leads to blindness. The rods, which are responsible for peripheral and low-light vision, are affected earlier and more severely; the cones are able to detect colors and are degraded later on (reviewed in Hartong *et al.*, 2006; Hamel, 2006; Wright *et al.*, 2010). Upon loss of photoreceptors, the RPE cells migrate away from their original place, invade other retinal layers and accumulate around retinal vessels forming characteristic pigment deposits known as “bone spicules” (Fig. 8) (Li *et al.*, 1995). Due to a huge genetic heterogeneity of the disease, the exact molecular mechanisms underlying its etiology are not known.

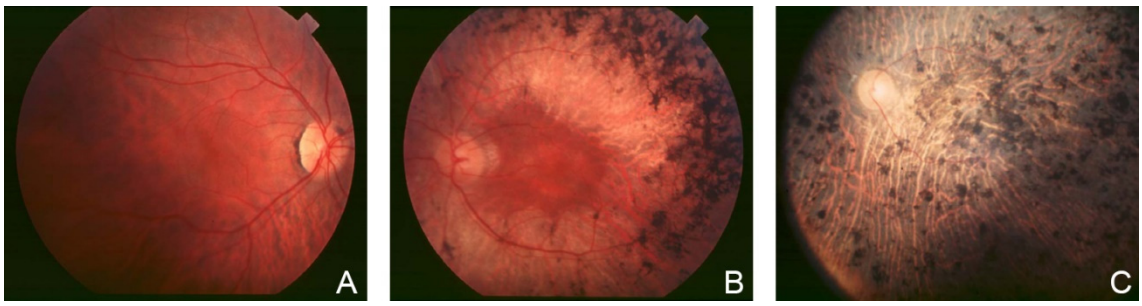

Fig. 8: Retina of RP patients
(A-C) Eye fundus of patients with retinitis pigmentosa in early stage (A), mid stage (B) and late stage (C) is shown. The pigment deposits are acumulated over time, retinal vessels are attenuated and optic disks appear pale. Adapted from Hamel (2006).

The age of onset and pace of progression of RP varies widely among patients. Most patients manifest first symptoms of the disease in adolescence and slowly develop blindness over several decades of life. In accordance with the preferential loss of rods,

RP usually starts with night blindness and excessive light sensitivity, photophobia. As it progresses, patients are losing the peripheral vision until their sight is narrowed to a so called “tunnel vision”. At the end, patients potentially become completely blind, although this is not always the case (reviewed in Hartong *et al.*, 2006; Hamel, 2006; Sahel *et al.*, 2015).

RP is a monogenic disease and can be inherited in autosomal dominant (adRP; 30-40 % of cases), autosomal recessive (arRP; 50-60 % of cases) or X-linked (xRP; 5-15 % of cases) mode (Hartong *et al.*, 2006). More than 80 genes have been associated with RP so far, which explains the heterogeneity of phenotypes. Majority of the causal genes are predominantly or specifically expressed in retina and are involved in processes like phototransduction, retinal cell signaling, vitamin A metabolism or structural organization of photoreceptors (Hartong *et al.*, 2006; Daiger *et al.*, 2013; RetNet database: https://sph.uth.edu/Retnet/disease.htm). Mutations within these genes interfere with physiological ocular pathways and the selective death of retinal cells is thus not particularly surprising. It is interesting in this respect that genes coding ubiquitously expressed pre-mRNA splicing factors also represent a common target of RP mutations (reviewed in Mordes *et al.*, 2006; Růžičková & Staněk, 2016).

Many efforts have been directed to find the cure of RP. Some general treatments can slow down the progress of the disease, but no therapy up to now is able to effectively prevent or reverse the death of retinal cells. Currently, nutritional supplements like vitamin A together with docosahexaenoic acid (DHA) or lutein are already used in clinic as they were found to have beneficial effect on treated RP patients (Berson *et al.*, 1993; Berson *et al.*, 2004; Berson *et al.*, 2010). Other medications in trial including neurotropic factors, neuroprotective valproic acid or calcium channel blockers, prolong the viability of the photoreceptors in animal models and are thus waiting for potential application (reviewed in Sahel *et al.*, 2015). Further therapeutic strategies based on transplantation of cells that replace the damaged photoreceptors or RPE cells are being actively investigated. The transplanted cells are either derived from stem cells or from photoreceptor precursor cells, attempts to implant whole fetal or adult retinal tissue have also been reported (MacLaren *et al.*, 2006; Radtke *et al.*, 2008; Gonzalez-Cordero *et al.*, 2013). Owing to the great technical progress of the recent years, retinal prosthetic devices has become an alternative option to restore sight in patients with

retinal degeneration, yet the quality of the artificial vision still remains rather low (Humayun *et al.*, 2012). Finally, the gene therapy represents probably the most promising therapeutic procedure that could intervene as soon as RP is diagnosed and prevent the disease development. The therapeutic delivery of nucleic acids to particular cell types aims to repair or replace mutated genes with healthy forms, alternatively it can be also used for increasing the expression of affected gene or for silencing of the mutated allele in case of mutations with dominant negative effect. Gene therapy for RP is being tested in various animal models and arouses expectations for future. Nonetheless, understanding of the genetic background and the underlying mechanism of individual RP mutations is essential for the application of the approach (reviewed in Petrs-Silva & Linden, 2013; Sahel *et al.*, 2015).

7.4.1 RP mutations in spliceosomal proteins

RP mutations in 8 genes related to splicing have been identified so far, specifically in 6 genes coding for tri-snRNP specific proteins, PRPF31, PRPF8, PRPF3, PRPF6, SNRNP200 and PRPF4, and in 2 genes encoding non-snRNP spliceosomal components, RP9/PAP1 and DHX38 (Vithana *et al.*, 2001; McKie *et al.*, 2001; Chakarova *et al.*, 2002; Maita *et al.*, 2004; Zhao *et al.*, 2009; Tanackovic *et al.*, 2011a). All these genes are commonly expressed in human body and are needed for pre-mRNA splicing in vast majority of cells. Similarly to SMA (Introduction, chapter 7.3), the tissue-specific phenotype is puzzling. It is also unclear why only tri-snRNP specific proteins are effected whereas no mutations in U1 and U2 proteins have been found.

There are several hypotheses explaining how mutations in ubiquitous proteins could lead to a retina-specific phenotype. The most likely explanation is that retinal cells have higher demands of pre-mRNA splicing than other tissues. Indeed, photoreceptors have one of the most active metabolisms which is reflected in increased number of mitochondria and an extensive oxygen consumption. The energy is needed mainly for maintenance of electrochemical gradients for signal transduction, as well as for constant renewal of photo-damaged structures. Both rods and cones consist of synaptic terminus, cell body with the nucleus, inner segment full of mitochondria and outer segment where the light is absorbed by photo-pigments (Fig. 9). The pigments are anchored within

invaginations of cell membranes that fill the whole space of outer segments. These so called membranous disks are prone to light-induced damage and need to be renewed on a daily basis. Thus, the protein turnover in photoreceptors is extremely high and so is the need for splicing (reviewed in Travis, 1998; Ferrari *et al.*, 2011). This is supported by an observation that in healthy retina, snRNAs levels are up to seven times higher than in other tissues and the amount of processed pre-mRNAs is also the highest. On the top of it, in lymphoblast cell lines derived from RP patients with mutations within spliceosomal PRPF proteins, the snRNP levels and pre-mRNA splicing seem to be altered (Tanackovic *et al.*, 2011b). Therefore, mutations in splicing factors could cause mild but general splicing defects that would be manifested only in retinal cells. Alternatively, RP mutations in splicing factors could preferentially affect splicing of some retina-specific transcripts which are crucial for the function of the eye. Yet another hypothesis is that affected proteins might play some unexpected role in retina outside of the spliceosome.

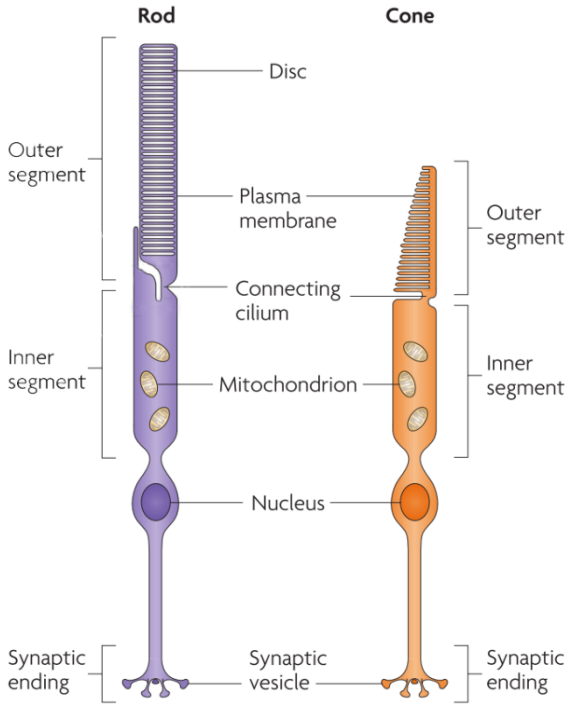

Fig. 9: Photoreceptor cells
Schematic representations of basic anatomic features of photoreceptore cells, rods and cones. The inner segment contains the major metabolic and trafficking machinery. The outer segment contains the phototransduction apparatus. Adapted from Wright *et al.* (2010).

Another unclear aspect of the spliceosome-associated RP mutations is the precise molecular mechanism of their effect. The vast majority of these mutations cause autosomal dominant form of RP and can act in either loss-of-function or gain-of-function manner. In order to treat RP patients effectively, we need to understand the precise mode of action of individual mutations. Unfortunately, it seems that the mechanism

varies substantially among different mutations, even among mutations within the same spliceosomal factor. In the next chapter, I will focus on the known facts about mutations in splicing-associated proteins.

PRPF3

Five missense RP mutations in *PRPF3* gene have been discovered so far but just the first two were studied in more detail (Chakarova *et al.*, 2002; Gamundi *et al.*, 2008; Zhong *et al.*, 2016). These mutants alter the association of several snRNP-specific proteins with the tri-snRNP and consequently result in defects of the spliceosome assembly and of pre-mRNA splicing in cell lines derived from RP patients (Tanackovic *et al.*, 2011b). Gonzalez-Santos *et al.*, 2008 showed that in case of the mutation T494M, problems with phosphorylation might be behind the disrupted spliceosome assembly. Interestingly, the same mutation forms detrimental aggregates specifically in photoreceptors cells which suggest rather a dominant negative effect of the mutations than a haploinsufficiency model (Comitato *et al.*, 2007). Consistently, knockout of one allele of PRPF3 homologues in mice and zebra fish did not reveal any developmental problems nor any signs of retinal degeneration (Graziotto *et al.*, 2008). On the other hand, knockin mouse with RP-associated PRPF3 mutation in one endogenous allele, showed pathological changes of RPE and decreased rod function (Graziotto *et al.*, 2011). These results indicate that one PRPF3 allele is enough to produce sufficient amounts of functional protein and support the hypothesis of toxic effect of studied PRPF3 mutants.

PRPF4

Three missense and one deletion RP mutations have been identified in the gene coding PRPF4, di and tri-snRNP-specific protein (Benaglio *et al.*, 2014; Chen *et al.*, 2014; Linder *et al.*, 2014). Unlike in PRPF3, some RP mutations in PRPF4 seem to be causing loss-of-function and haploinsufficiency. While overexpression of R192H PRPF4 mutant in zebrafish did not interfere with the embryonic development, the PRPF4 depletion led to embryonic lethality which was rescued by wild type (WT) but not by mutated protein. Detailed analysis of the R192H mutation in human cells showed that it disrupts PRPF4 integration into U4/U6 di-snRNP (Linder *et al.*, 2014). On the other hand, overexpression

of other mutant, P315L PRPF4, led to systemic deformations of the larvae which suggests its dominant-negative effect (Chen *et al.*, 2014).

PRPF6

Only one RP mutation has been found in gene encoding PRPF6, U5 and di-snRNP bridging protein. It is an autosomal dominant missense mutation of highly conserved arginine located in the TPR domain of PRPF6. The region around mutated residue is involved in binding of PRPF4 from di-snRNP and thus the mutation could potentially disrupt the interaction and prevent tri-snRNP formation. Interestingly, the mutated protein is accumulated in Cajal bodies (Tanackovic *et al.*, 2011a).

PRPF8

PRPF8 is a large U5-snRNP specific protein from the core of the spliceosome. In the *PRPF8* gene , 21 adRP mutations have been described; most of them result in amino acid substitution (McKie *et al.*, 2001; Martinez-Gimeno *et al.*, 2003; De Erkenez *et al.*, 2002; Kondo *et al.*, 2003; Ziviello *et al.*, 2005; Sullivan *et al.*, 2006; Towns *et al.*, 2010; Audo *et al.*, 2012). All the RP mutations currently known are found at different positions within the C-terminal Jab1 domain, which is crucial for binding and regulation of the helicase SNRNP200 (see Introduction, chapter 3.2). Interestingly, one RP missense mutation results in the stop codon disruption and in 41 amino acids-long extension of the protein (Martinez-Gimeno *et al.*, 2003).

The date concerning behavior of RP PRPF8 in human cells are rather limited. Two PRPF8 mutations, R2310G and Y2334N, were studied in lymphoblast cell lines derived from RP patients. A glycerol gradient sedimentation assay with RP cell extracts suggest that PRPF8 is normally incorporated into U5 snRNP and tri-snRNP. However, the association of U5 snRNP-specific proteins (SNRNP200, EFTUD2 and PRPF6) with the spliceosome was reduced in RP cell lines compared to WT. In accordance, the spliceosome assembly as well as both constitutive and alternative splicing were affected in these cells (Tanackovic *et al.*, 2011b). Similar results were obtained by yeast two-hybrid assay, various RP mutations weaken the interaction of the C-terminal fragment of PRPF8 with SNRNP200 and EFTUD2 (Pena et al, 2007).

The effects of RP mutations on PRPF8 protein function has been mostly studied in yeast, where different mutants exhibited various growth phenotypes (Boon *et al.*, 2007; Maeder *et al.*, 2009; Mozaffari-Jovin *et al.*, 2013). Interestingly, Towns *et al.* (2010) observed a correlation between yeast growth defects and severity of human disease caused by an equivalent mutation. Mozaffari-Jovin *et al.* (2013) divided Jab1 residues affected by RP into three groups. Group I residues within the globular region of Jab1 domain (residues up to 2309) effect mainly the fold stability of the domain. Group II residues in the proximal part of the C-terminal tail of Jab1 domain (residues 2310 – F2314) influence interaction with SNRNP200. Group III residues at the distal part of the C-terminal tail of Jab1 domain (residues 2315 – 2336) regulate SNRNP200 activity. Studies in yeast correlated well with this division and showed that both group I and II mutations inhibit tri-snRNP formation. On the top of that, group I mutations reduced solubility of the protein and group II mutations negatively affected the interaction of PRPF8 with Brr2, yeast SNRNP200 orthologue (Boon *et al.*, 2007; Maeder *et al.*, 2009). On the other hand, one group III mutation, Y2334N in human, did not interfere with tri-snRNP formation but it enhanced Brr2 helicase activity and RNA affinity (Mozaffari-Jovin *et al.*, 2013). Taken together, it seems that the mode of action of individual RP mutations in PRPF8 varies substantially depending on the precise localization of each mutation. Further investigation is needed to map the effects of all known RP mutations and to confirm the similarity between yeast and human mechanisms.

PRPF31

PRPF31 is U4 snRNP-specific protein that interacts with U5 snRNP-specific PRPF6 and this bond is required for the formation of the tri-snRNP particle (Makarova *et al.*, 2002). With more than 100 causative mutations, PRPF31 is one of the most frequent targets of adRP (The Human Gene Mutation Database: http://www.hgmd.cf.ac.uk; Hartong *et al.*, 2006). The mutations found within *PRPF31* gene include substitutions, insertions, deletions or splice-site mutations, and lead to production of non-functional or quickly-degraded protein, to altered gene transcription or even to absence of one copy of the entire gene. Most of these mutations result in decreased concentration of functional protein and hence haploinsufficiency (reviewed in Audo *et al.*, 2010; Rose & Bhattacharya, 2016; Růžičková & Staněk, 2016). Interestingly, majority of families with

PRPF31 mutations show phenotypic non-penetrance, a special phenomenon where autosomal dominant mutation is not always sufficient for disease manifestation. This is probably a consequence of many diverse alleles occurring in the population with different expression rates. The disease is manifested when the amount of PRPF31 drops to critical level, but a functional high-expressivity allele can avert the danger (Rose & Bhattacharya, 2016). The missense mutation A216P was studied in more detail. It was shown to alter the PRPF31 incorporation into di-snRNP and to cause protein instability. However, PRPF31 deficiency itself is not able to explain the slower proliferation of cells expressing A216P mutant. Moreover, the growth defects can be rescued by overexpression of PRFP6. It was therefore suggested, that the mutant actually sequesters PRPF6 and prevents tri-snRNP assembly. Thus, an additional dominant-negative effect probably plays a role in case of the A216P PRPF31 mutation (Huranová *et al.*, 2009).

SNRNP200

At least eleven mutations causing adRP have been described in SNRNP200 up to now and they are all situated in the enzymatically active N-terminal cassette of this U5-specific helicase (Zhao *et al.*, 2009; Li *et al.*, 2010; Benaglio *et al.*, 2011; Liu *et al.*, 2012; Bowne *et al.*, 2013; Xu *et al.*, 2014). Two mutations located in the ratchet helix of Brr2's RNA binding channel, S1087L and R1090L, were subjected to further studies. Unlike most RP mutations in other snRNP-specific proteins, these mutations seem not to interfere with spliceosome assembly. On the other hand, the S1087L and R1090L mutations affect the selection of 5' ss and reduce SNRNP200 unwinding activity, hence influencing the fidelity of splicing (Zhao *et al.*, 2009; Cvačková *et al.*, 2014). Recently, it was shown that the mutations impair ATPase and helicase activity of SNRNP200 (Ledoux & Guthrie, 2016).

RP9/PAP1

The exact role of protein RP9/PAP1 is not clear but it is presumably involved in splicing as it localizes to nuclear speckles, interacts directly with splicing factor U2AF35 and its activity affects outcome of pre-mRNA splicing (Maita *et al.*, 2004). Two missense mutations of RP9/PAP1 causing adRP have been characterized (Keen *et al.*, 2002), but

only one of them, D170G, induced splicing defects when tested by *in vivo* splicing assay (Maita *et al.*, 2004).

DHX38

DHX38 is the human homolog of yPrp16 helicase which transiently interacts with spliceosome and promotes structural rearrangements during spliceosomal activation (Schwer & Guthrie, 1991; Tseng *et al.*, 2011; Hogg *et al.*, 2014). A missense mutation was identified in a family with arRP, which is the first example of recessive RP mutation found in splicing factor (Ajmal *et al.*, 2014).

MATERIALS AND METHODS

1 Cell culture

All the experiments were performed with HeLa cells, human cervical cancer cell line. For selected experiments, stable HeLa cell lines expressing tagged protein variants were used. These include cell lines that express exogenous PRPF8-LAP (for details, see Materials and Methods, chapter 3) or GFP-AAR2, GFP-EFTUD2 and GFP-ZNHIT2 (prepared in the cooperating laboratory of Edouard Bertrand, Montpellier). The cells were cultured at 37°C, 5% CO_2 in Dulbecco's Modified Eagle Medium (DMEM) containing 4.5 g/l of glucose (Sigma-Aldrich) supplemented with 10% fetal calf serum (FCS; Biochrom) and 1% Penicillin/Streptomycin (Gibco). In case of the cell lines expressing GFP-tagged proteins, Hygromycine B at final concentration 40 ng/ml was added to the media (Sigma-Aldrich).

1xPBS buffer:

137 mM NaCl (Sigma-Aldrich)

2.7 mM KCl (Serva)

10 mM Na_2HPO_4 (Sigma-Aldrich)

1.8 mM KH_2PO_4 (Sigma-Aldrich)

fill in with dH_2O

pH 7.4 adjusted with HCl (Penta)

For long-term storage, cells were resuspended in DMEM supplemented with 8% dimethyl sulfoxide (DMSO; Sigma-Aldrich) and 10% FCS and stored at -80°C or in liquid nitrogen.

For HSP90 inhibition, cells were treated with 2 µM Geldanamycin (provided by E. Bertrand lab) for 16 h. For proteosynthesis inhibition, Cycloheximide (Sigma-Aldrich) was added to the cultivation medium at final concentration 30 µg/ml.

2 Preparation of PRPF8-LAP stable cell lines

For preparation of PRPF8-GFP stable cell lines, HeLa cells were transfected with an isolated bacterial artificial chromosome (BAC) carrying *PRPF8* gene with C-terminal LAP tag containing GFP (obtained from Ina Poser; Poser *et al.*, 2008). BAC DNA was isolated using NucleoBond BAC 100 Kit (Macherey-Nagel) and the transformation was done with X-tremeGENE high-performance DNA transfection reagent (Roche), in both cases the manufacturer's guidelines were followed. After transfection, the cells were cultivated in the medium supplemented with G418 selective antibiotic (Sigma-Aldrich) at final concentration of 2 mg/ml. After 10 days, the GFP-positive cells were selected by fluorescence-activated cell sorting (FACS) in the flow cytometry facility at the Institute of Molecular Genetics ASCR (IMG ASCR).

3 Red/ET recombeneering

To introduce retinitis pigmentosa-related mutations into *PRPF8* gene, we applied Red/RT recombineering. We used the Counter-Selection BAC Modification Kit (Gene Bridges) and followed the manufacturer's guidelines. In principle, the Counter-Selection BAC Modification Kit is based on homologous recombination (HR) in *E. coli*, when a counter-selection cassette is first introduced at the target location and is subsequently replaced by DNA fragment with the desired mutation. Eight cell lines were prepared with different RP point mutations in the *PRPF8* gene: S2118F, H2309R, R2310K, R2310G, F2314L (prepared by Zuzana Cvačková and Daniel Matějů) and P2301T, H2309P, Y2334N (prepared by Anna Malinová, the author of the thesis).

More specifically, we first transformed Streptomycin-resistant strain of *E. coli* (DH5) by electroporation with the plasmid pRedET. The plasmid encodes phage-derived proteins, which are able to catalyze the HR. After inducing the expression of these proteins by L-arabinose and temperature shift, the rpsL-neo counter-selection cassette with homology arms was electroporated into the bacteria. The homology arms target a specific sequence in the *PRPF8* gene on the BAC, which enables HR to take place. The cassette also contains genes for Streptomycine sensitivity and Neomycine/Kanamycine resistance and thus only the colonies with the incorporated cassette survived the

selection on Kanamycine-containing plates. These colonies were electroporated again, this time with a DNA fragment with the same homology arms as previously and with *PRPF8* gene fragment carrying desired point mutation. Just the colonies that lost the counter-selection cassette, lost also the Streptomycine sensitivity and grew on Streptomycine-containing plates. The success of the two-step HR was controlled by the colony PCR (see Materials and Methods, chapter 15). The BAC DNA from selected colonies was isolated and the mutations were verified by sequencing.

4 RNA interference

For RNA interference experiments, 30-50% confluent cells were transfected with siRNA using Oligofectamine transfection reagent (Invitrogen) according to the manufacturer's guidelines. The cells were incubated with 20 nM siRNA for 48-92 hours. Knock-down efficiency was assessed by western blotting (for details, see Materials and Methods, chapter 11).

To knock down only the endogenous PRPF8, the siRNA was designed against the sequence around the STOP codon. The PRPF8-LAP used in BAC cell lines contains the LAP tag in this region and thus cannot be targeted by the siRNA.

The following siRNAs and incubation times were used:

- PRPF8: 5'-CCUGUAUGCCUGACCGUUUtt-3' 48 h
- PIH1D1: 5'-GAAUGGAAAUGUAGUCUUAtt-3' 2x48 h
- RUVBL1: 5'-CCUUGAAGCUGAAGAGUAUtt-3' 72 h
- RUVBL2: 5'-AGGAAGAAGAUGUGGAGAUtt-3' 72 h

As a control, we used negative control no.5 siRNA (Thermo Fisher Scientific).

5 Transfection of plasmids

Plasmid DNA was transfected into cells using X-tremeGENE high-performance DNA transfection reagent (Roche) according to the manufacturer's guidelines. The cells were

analyzed 24 hours after transfection. Following plasmids were used for the splicing efficiency experiments:

We used β-globin splicing reporter derived from the E3 vector containing β-globin gene which we obtained as a gift from Yaron Shav-Tal from Bar-Ilan University in Israel (used in Darzacq *et al.*, 2006). Viola Hausnerová modified the E3 plasmid by replacing tetracycline-responsible promoter with a classical CMV promoter from pcDNA3 vector using NruI and HindIII restriction sites and deleted second β-globin intron (nucleotides 496 – 1536). Changes were confirmed by sequencing.

We also used retina specific reporters, RHO, ROM1 and FSCN2 (Mordes *et al.*, 2007; Yuan, 2005) kindly provided by Jane Wu (Northwestern University, Chicago, IL).

6 Immunofluorescence (IF) – sample preparation

IF was used for visualization of specific proteins on a fluorescent microscope. The samples were prepared from the cells grown on glass coverslips. The sample preparation was carried on at room temperature (RT) and individual steps were interspersed by washing in PBS. The cells were grown on cover glasses (Marienfeld Superior) which were previously rinsed in 1M HCl (Penta) overnight, washed in distilled water and stored in 100% ethanol (Merck Milliopore). First, the cells on cover glasses were fixed by 4% (w/v) PFA/PIPES for 10 minutes. Next, the cell membrane was permeabilized by 0,5% (v/v) TRITON X-100 (Serva)/PBS for 10 minutes and the samples were blocked in 5% (v/v) Normal Goat Serum (Jackson ImmunoResearch Laboratories) for 15 minutes. Consequently, the samples were incubated with appropriate primary and secondary antibodies diluted in PBS, 1 hour each step. For appropriate dilutions, see the list of antibodies in Materials and Methods, chapter 13. Finally, the coverslips were washed in water and mounted to microscope slides by Fluoromount G (Southern Biotech) containing 4,6-diamidino-2-phenylindole (DAPI; Southern Biotech) for DNA staining.

4% paraformaldehyde (PFA) in PIPES:

4% (w/v) PFA (Sigma-Aldrich)

0.1 M PIPES pH 6.9 (Sigma-Aldrich)

2 mM $MgCl_2$ (Sigma-Aldrich)

1 mM EGTA pH 8 (Sigma-Aldrich)

fill in with dH_2O

7 Fluorescence *in situ* hybridization (FISH) – sample preparation

FISH was used for visualization of specific snRNAs on a fluorescent microscope. The FISH staining directly followed the secondary antibody step from IF staining (Materials and Methods, chapter 8). The cells were fixed again by 4% (w/v) paraformaldehyde/PIPES for 5 minutes and incubated for 10 min in 0.1M glycine/0.2M Tris (pH 7.4) in order to block aldehydic groups that were left unreacted after the fixation. Next, the coverslips were transferred on drops of 4xSSC, of 2xSSC/50% PFA and finally on a mixture containing the FISH probe (snRNA targeting DNA oligonucleotide labeled by Cy3 at the 5´end; EastPort). After 1 hour, the probe was washed successively in 2xSSC/50% PFA (20 min; 37°C), 2xSSC (20 min; 37°C), 1xSSC (20 min; RT) and 4xSSC (10 min; RT). Finally, the coverslips were mounted to microscope slides by Fluoromount G containing DAPI for DNA staining.

Tris buffer:

Trizma base (Sigma Aldrich)

fill in with dH_2O

pH adjusted with HCl (Penta)

20x SSC (saline sodium citrate) buffer:

3 M NaCl (Sigma-Aldrich)

300 mM sodium citrate (Sigma-Aldrich)

fill in with dH_2O

pH 7.0 adjusted with HCl (Penta)

FISH probe mixture (per 1 coverslip):

DNA probe (100 pmol/µl; EastPort) 0.3 µl

formamide (Sigma-Aldrich) 10 µl

50% dextran sulphate (Sigma-Aldrich) 4 µl

5% BSA (bovine serum albumin) 4 µl (Sigma-Aldrich)

20x SSC buffer 2 µl

yeast tRNA (10 mg/ml; Ambion) 0.75 µl

Sequences of the snRNA-specific probes:

U4: 5'-TCACGGCGGGGTATTGGGAAAAGTTTTCAATTAGCAATAATCGCGCCT-3'

U5: 5'-CTCTCCACGGAAATCTTTAGTAAAAGGCGAAAGATTTATACGATTTGAAGAG-3'

U6: 5'-CACGAATTTGCGTGTCATCCTTGCGCAGGGGCCATGCTAATC-3'

8 Microscopy

The fixed IF or FISH samples were imaged using wide-field fluorescence microscope - Olympus IX70 coupled with DeltaVision system (Applied Precision). We used an oil immersion 60x objective with numerical aperture 1.42 and with plan apochromat correction for optical aberrations. For each image, 20 Z-sections with 0.2 µm Z-steps were taken and subjected to mathematical deconvolution in softWoRx software (Applied Precision). The maximal projection of the pictures is presented. The image processing was done in Photoshop (Adobe). In case the nuclear/cytoplasmic fluorescence intensity measurements, we used the ImageJ software and analyzed 52- 125 cells from each sample.

For live cell measurements, the same microscopic system was used and it was equipped with an environmental chamber controlling CO_2 levels (5%) and temperature (37°C). The cells were grown in glass-bottom 3.5 cm dishes (MatTek). To measure the PRPF8-LAP protein degradation rate, we added cycloheximide (Calbiochem) to the cells (final concentration 30 µg/ml) to inhibit the protheosynthesis. For each cell line, we were taking pictures of 10 different areas at 15 min intervals over a period of 8 hours. From these images, we selected 7-10 cells and analyzed the decrease of GFP fluorescence using the ImageJ software. Specifically, the mean intensity of each cell was

measured, the mean intensity of the background was subtracted and the values were normalized to the first time point. An average of 3 independent experiments was calculated.

For high-content microscopy, the fixed samples were scanned using Scan^R microscope (Olympus) with fully automated image acquisition. An oil immersion 60x objective with numerical aperture 1.35 was used. Each sample was screened at 225 positions and each image was reconstructed from 10 Z-sections with 0.3 µm Z-steps by Analysis Scan^R Software (Olympus). The software was also used to automatically quantify the relative enrichment of the FISH probe fluorescence in CBs over the fluorescence in the nucleoplasm according to the following formula:

$$R = \frac{\frac{\sum total\ IF_{CB\ pre\ nucleus}}{\sum area_{CB\ per\ nucelus}}}{\frac{total\ IF_{nucleus} - \sum total\ IF_{CB\ per\ nucleus}}{area_{nucleus} - \sum area_{CB\ per\ nucleus}}}$$

The cellular compartments (nuclei and CBs) were identified automatically based on the DAPI (nucleus) and anti-coilin IF staining (CBs). An average of the relative enrichment in all the analyzed cells was determined and the standard error of the mean (SEM) was calculated from 3 independent experiments.

9 Immunoprecipitation (IP)

Cell lysate was prepared from cells grown in 10 cm Petri dish. The cells were washed with PBS, harvested into 1 ml of ice-cold PBS and spinned at 1 000 g for 10 min at 4°C. The pellet was resuspended in 1 ml of ice-cold NET2 buffer supplemented with protease inhibitor cocktail (Roche). In order to lysate the cell membranes, the sample was sonicated on ice by thirty 0.5 s pulses at 40% of maximal energy. The residual cell membranes were spinned down at 20 000 g for 10 min at 4°C and the supernatant (cell lysate) was further used for IP. 30 µl of the purified cell lysate were taken as an input sample.

Protein-G Sepharose beads (GE Healthcare) were washed 3 times in NET-2 buffer and the antibodies were bound. For one IP sample, 30 µl of beads were incubated with 0.5 ml of NET-2 buffer with 0.3 µl of the goat anti-GFP antibody (15 mg/ml) for 1 h. After proper washing of the beads, the cell lysate was added and immunoprecipitated overnight at 4°C. The following day, the IP was washed five times with NET-2 buffer and the beads with immunoprecipitated proteins were resuspended in 30 µl of 2x sample buffer, the same was done with inputs. Finally, the incubation at 95°C for 5 min released the proteins from any binding and denaturated them.

NET-2 buffer:

50mM Tris-HCl pH 7.5

150mM NaCl (Sigma-Aldrich)

0.05% Nonidet P-40 (Sigma-Aldrich)

fill in with dH_2O

2x sample buffer:

4% SDS (sodium dodecyl sulfate; Sigma-Aldrich)

10% 2-mercaptoethanol (Sigma-Aldrich)

20% glycerol (Lechner)

0.004% bromphenol blue (Sigma-Aldrich)

125 mM Tris-Cl (pH 6.8)

fill in with dH_2O

10 SDS-PAGE and Western blot (WB)

Proteins samples in a form of either cell lysates or IP samples, were separated by polyacrylamide gel electrophoresis in sodium dodecyl sulfate running buffer (SDS-PAGE). For simple cell lysates, cells were harvested from 12-well plates into 40-60 µl 2x sample buffer, denaturated at 95°C for 5 min and sonicated (10 pulses, 0,5 s each, 40% of maximal energy).

For SDS-PAGE, the 10% separating and stacking gels were poured, the aperture (BioRad) with SDS running buffer was assembled and the samples (20 µl) together with the load marker Page Ruler Presteined Plus (5 µl; Thermo Fisher Scientific) were loaded into the wells. The electrophoresis run first at 60 V for 40 min and then at 120 V for 75 min.

The proteins were transferred from the gel to a nitrocellulose membrane (Protran) using wet WB. For that, the gel together with filter papers, sponges and the membrane were assembled to a so called 'transfer sandwich' which was placed to the wet WB aperture filled with WB transfer buffer. WB was run at 350 mA for 1 h.

The membrane was cut to smaller parts and blocked with 10% (w/v) non-fat milk in PBST for 0.5 h. After washing in PBST, the membrane was incubated for 1 h with a primary antibody diluted in 1% non-fat milk (w/v) in PBST supplemented with 0.1% sodium azide (Sigma-Aldrich). The membrane was then washed again and incubated for 1 h with a secondary antibody conjugated with horseradish peroxidase (HRP) diluted 1:10 000 in 1% non-fat milk (w/v) in PBST. After proper washing, the SuperSignal™ West Femto Maximum Sensitivity Substrate (Thermo Scientific) was poured over the membrane and the chemiluminescence was detected by LAS-3000 Imager (Fujifilm). The intensity of individual bands was determined using ImageJ software.

10% separating gel (5 ml):

2.5 ml dH2O

1.2 ml Acrylamide:N,N'-Methylenebisacrylamide 37.5:1; 40% (Sigma-Aldrich)

1.3 ml 1.5 M Tris (pH 8.8)

50 µl 10% SDS (Sigma-Aldrich)

50 µl 10% APS (ammonium persulfate; Sigma-Aldrich)

4 µl TEMED (Tetramethylethylenediamine; Applichem)

SDS running gel (2 ml):

2.5 ml dH2O

1.2 ml Acrylamide:N,N'-Methylenebisacrylamide 37.5:1; 40% (Sigma-Aldrich)

1.3 ml 1.5 M Tris (pH 8.8)

50 µl 10% SDS (Sigma-Aldrich)

50 µl 10% APS (Sigma-Aldrich)

4 µl TEMED (Applichem)

10x SDS-PAGE running buffer:

30.3 g Trizma base (Sigma-Aldrich)

144 g glycine (Sigma-Aldrich)

10 g SDS (Sigma-Aldrich)

fill with H_2O up to 1 l

10x WB transfer buffer:

30.3 g Trizma base (Sigma-Aldrich)

144 g glycine (Sigma-Aldrich)

fill with H_2O up to 1 l

1x WB transfer buffer:

10% 10x WB transfer buffer

20% methanol (Sigma-Aldrich)

70% dH_2O

PBST:

PBS

0.05% Tween 20 (Sigma Aldrich)

11 Antibodies

The following primary antibodies were used for immunofluorescence, immunoprecipitation and Western blotting:

- rabbit anti-PRPF8 (Santa Cruz)
- rabbit anti-SNRNP200 (Sigma-Aldrich)
- rabbit anti-PRPF6 (Santa Cruz)

- rabbit anti-EFTUD2 provided by R. Lührmann (MPI, Göttingen, Germany)
- rabbit anti-PRPF31 provided by R. Lührmann (MPI, Göttingen, Germany)
- rabbit anti-C20orf4 35-50 (AAR2 splicing factor homolog, Sigma-Aldrich)
- mouse anti-RUVBL1 (Abcam) provided by Z. Hořejší (BCI, London, UK)
- rabbit anti-RUVBL2 (GeneTex) provided by Z. Hořejší (BCI, London, UK)
- mouse anti-PIH1D1 (Abcam) provided by Z. Hořejší (BCI, London, UK)
- rabbit anti-RPAP3 (Abcam)
- rabbit anti-ZNHIT2 (Abcam)
- mouse anti-GFP (Santa Cruz)
- goat anti-GFP provided by D. Drechsler (MPI-CBG, Dresden, Germany)
- rabbit anti-GAPDH (Abcam)
- mouse anti-tubulin provided by P. Draber (IMG, Prague, Czech Republic)
- mouse anti-Sm antibody Y12 produced from a hybridoma cell line (a gift from Karla Neugebauer, Yale University, New Haven, CT) at the antibody facility, Institute of Molecular Genetics ASCR

The following secondary antibodies were used for immunofluorescence:

- goat anti-mouse or anti-rabbit secondary antibody conjugated with DyLight488, 549 or Cy5 (Jackson ImmunoResearch Laboratories)

The following secondary antibodies were used for Western blotting:

- goat anti-mouse or anti-rabbit secondary antibody conjugated with horseradish peroxidase (Jackson ImmunoResearch Laboratories)

12 Total RNA isolation and cDNA synthesis

Total RNA was isolated using TRIZOL reagent (Invitrogen). First, cells from 12-well plate were washed with PBS, harvested into 200 µl of TRIZOL, 40 µl of chloroform (Sigma-Aldrich) was added, and after 3 min, the sample was spinned down at 20 000 g

for 10 min at 4°C. Next, isopropanol (100 µl; Sigma-Aldrich) was added to the colorless upper aqueous phase, the mixture was incubated for 10 min at RT and spinned down at 20 000 g for 10 min at 4°C. The supernatant was removed, the RNA pellet was washed with 70% ethanol (Merck Milliopore) 2 times and resuspended in RNase-free water. The potential DNA contamination was removed using TURBO DNase kit (Thermo Fisher Scientific) according the manufacturer's guidelines.

cDNA was synthesized using SuperScript III Reverse Transcriptase (Invitrogen). First, a mixture of 2 µg of total RNA, 1 µl of random hexamers, 1 µl of 10 mM dNTP and RNase-free water (up to 13 µl) was heated to 65°C for 5 min. Then, 4 µl of First Strand Buffer, 1 µl of 0,1 M DTT and 0,5 µl of SuperScriptTM III reverse transcriptase (200 U/µl) were added, the whole mixture was incubated at 25°C for 5 min and 50°C for 60 min. To inactivate the enzymes and stop the reaction, the sample was put to 70°C for 15 min.

13 RT-PCR, RT-qPCR and colony PCR

Real-time quantitative PCR (RT-qPCR) was performed using LightCycler 480 (Roche) and the LightCycler® 480 SYBR Green I Master mix (Roche). The master mix contains FastStart Taq DNA Polymerase and SYBR Green I dye for detection of DNA double-strand product. Each reaction was prepared from 2.5 µl of the master mix, 0.5 µl of primers (5 µM each) and 2 µl of the cDNA diluted 1:10. The following PCR program was used: 95°C 7 min; 40 cycles of 95°C 20 s, 61°C 20 s and 72°C 35 s. Splicing efficiency was calculated as a ratio of mRNA and pre-mRNA ($2^{[Ct(pre\text{-}mRNA)-Ct(mRNA)]}$). The following primers were used for RT-qPCR:

preLDHA_F: 5'-CCTTTCAACTCTCTTTTGGCAACC-3'
preLDHA_R: 5'-AATCTTATTCTGGGGGGTCTGTTC-3'
mLDHA_F: 5'-AGAACACCAAAGATTGTCTCTGGC-3'
mLDHA_R: 5'-TTTCCCCCATTAGGTAACGG-3'

Reverse transcription PCR (RT-PCR) was run in a PCR cycler from BIO-RAD with the use of Taq polymerase (Thermo Scientific). The PCR reaction with β globin primers

contained: 6 µl of cDNA, 2 µl of Taq pol. buffer, 1 µl of $MgCl_2$, 0.5 µl of dNTPs, 0.5 µl of Taq pol., 0.5 µl of primers (5 µM each) and 9.5 µl of H_2O. The PCR reaction with retina specific genes-detecting primers contained: 2 µl of cDNA, 2 µl of Taq pol. buffer, 1 µl of $MgCl_2$, 0.5 µl of dNTPs, 0.2 µl of Taq pol., 0.5 µl of primers (5 µM each) and 13.8 µl of H_2O. The following PCR program was used: 95°C 4 min; 27 cycles of 95°C 2 min, 55°C 1 min and 72°C 1 min; 95°C 2 min; 55°C 5 min; 72°C 5.5 min. PCR products were separated on 2% agarose gel. The intensity of individual bands was determined using ImageJ software. Splicing efficiency was calculated as a ratio of mRNA and pre-mRNA bands intensity. The experiments showing the splicing efficiency of retina-specific genes were performed in collaboration with Zuzana Cvačková. The following primers were used for RT-PCR:

β globin_F: 5'-CAAGGTGAACGTGGA-3'
β globin_R: 5'-GGACAGATCCCCAAAGGACT-3'
RHO_F: 5'-CGGAGGTCAACAACGAGTCT-3'
RHO_R: 5'-TCTCTGCCTTCTGTGTGGTG-3'
FSCN2_F: 5'-TGCCAACACCATGTTTGAGA-3'
FSCN2_R: 5'-GCTTGAGGGTGAACTCTTCG-3'
ROM1_F: 5'-CAACCCAACCAAAACCTCTG-3'
ROM1_R: 5'-ATAGCCCTGGGTCTCTCCTC-3'

Colony PCR was run in a PCR cycler from BIO-RAD with the use of Taq polymerase (Thermo Scientific). The PCR reaction contained: 2.5 µl of Taq pol. buffer, 1.5 µl of $MgCl_2$, 0.5 µl of dNTPs, 0.2 µl of Taq pol., 2 µl of primers (10 µM each) and 18.3 µl of H_2O. Instead of purified DNA, a small amount of bacteria was added to the reaction on a sterile micropipette tip. The following PCR program was used: 94°C 2 min; 25 cycles of 94°C 1 min, 55°C 1 min and 72°C 1 min; 72°C 7 min. PCR products were separated on 1% agarose gel. The following primers were used for RT-PCR:

PRPF8_colonyPCR_F: 5'-ATGAGCTACAGCTGGCGAAC-3'
PRPF8_colonyPCR_F: 5'-TTAGCAGCAGCGGTTTCTTT-3'

14 SILAC-IP and proteomic analysis

The experiments with stable isotope labeling in cell culture conjugated with immunoprecipitation (SILAC-IP) were performed by our collaborators from the laboratory of Edouard Bertrand (Montpellier, France). The procedure of SILAC-IP experiments was previously described by Boulon *et al.* (2010) and is outlined in the following paragraph.

To achieve an incorporation of isotopic amino acids into proteins, cells were grown for 15 days in either light media with L-arginine and L-lysine (Sigma-Aldrich), or in heavy media with L-arginine $^{13}C/^{15}N$ and L-lysine $^{13}C/^{15}N$ (Cambridge Isotope Laboratory). Cells expressing GFP-phusion proteins were used, parental Hela cells served as a control. Cells from 15 cm-diameter Petri dish were washed with PBS, trypsinized and the cell membranes were disrupted by cryogrinding in SILAC buffer. The extracts were incubated 20 min at 4°C and spinned down at 20 000g for 10 min. The extracts were first precleared by incubation on protein G-sepharose beads (GE healthcare) at 4°C for 1 h and then incubated with GFP-Trap beads (ChromoTek) at 4°C for 75 min. After the affinity purification step, beads were washed five times with the SILAC buffer and the beads with "light" and "heavy" extracts were pooled.

Bound proteins were eluted by 1% SDS and boiled for 10 min. Samples were then reduced with 10 mM DTT (BDH Chemicals) and alkylated with 50 mM iodoacetamide (Sigma-Aldrich). The proteomic analysis was performed as described in detail by Bizarro *et al.* (2014). Briefly, proteins were separated by SDS-PAGE, cut from the gel and trypsinized. Peptides were analyzed on a mass spectrometer (Orbitrap Elite Hybrid Ion Trap; Thermo Fisher Scientific) coupled to a nanoflow liquid chromatography system (UltiMate U3000; Thermo Fisher Scientific). SILAC light/heavy ratios were normalized to the control.

SILAC buffer:

20 mM HEPES pH 7.4 (Sigma-Aldrich)

150 mM NaCl (Sigma-Aldrich)

0.5% TRITON X-100 (Serva)

protease inhibitor cocktail (Roche)

fill in with dH_2O

RESULTS

For the purpose of this thesis, I composed data that have already been published and some unpublished data. If not stated otherwise in the MATERIALS AND METHODS section, I performed the described experiments myself. I have contributed with my data into this two articles:

- The first article, "**SART3-Dependent Accumulation of Incomplete Spliceosomal snRNPs in Cajal Bodies**", was published in the Cell reports journal (IF 2015: 7.87) in 2015. I was a co-author of this article and I contributed to the experiments showing changes of the distribution of snRNAs after depletion of PRPF8, PRPF6 and LSM8.

  Novotný, I., Malinová, A., Stejskalová, E., Matějů, D., Klimešová, K., Roithová, A., Švéda, M., Knejzlík, Z., Staněk, D. (2015). SART3-Dependent Accumulation of Incomplete Spliceosomal snRNPs in Cajal Bodies. Cell Reports, 10(3), 429–440.

- The second article, "**Assembly of the U5 snRNP component PRPF8 is controlled by the HSP90/R2TP chaperones**", was accepted for publication in The Journal of Cell Biology (IF 2015/16: 8.72) in 2017. I was the first author of this article and I performed all the experiments showing RP PRPF8 mutants, the Western blots after PIH1D1 siRNA and GA treatment, and the FISH experiment after RUVBL1 and RUVBL2 KD. I also prepared the figures for this article and I participated on the manuscript writing.

  Malinová, A., Cvačková, Z., Matějů, D., Hořejší, Z., C., Vandermoere, F., Bertrand, E., Staněk, D., Verheggen, C. (2017). Assembly of the PRPF8 module of U5 snRNP is controlled by the HSP90/R2TP chaperone system. J. Cell Biol. 216(5).

1 Cell lines expressing PRPF8-LAP variants were prepared

We prepared cell lines expressing PRPF8-LAP RP variants and tried to determine how RP-linked mutations influence the function of the PRPF8 protein. Up to now, 21 adRP mutations in the *PRPF8* gene have been identified (see Introduction, chapter 7.4.1). For our study, we selected eight mutations that result in single amino acid changes, including the most common substitutions H2309P, H2309R and R2310K. We further chose S2118F, which is the first mutation found outside of exon 42, and mutations P2301T, R2310G, F2314L and Y2334N, which are found at different positions within the Jab1/MPN domain (Fig. 10A and B).

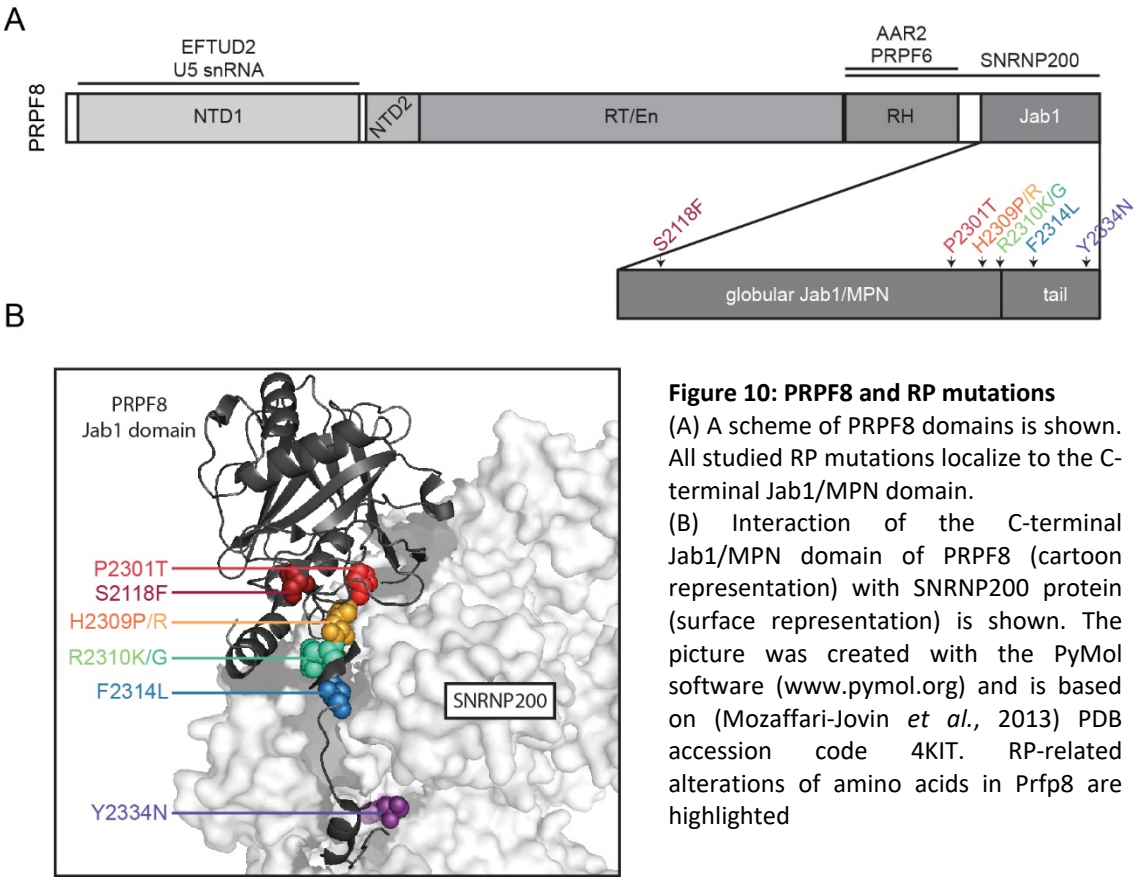

Figure 10: PRPF8 and RP mutations
(A) A scheme of PRPF8 domains is shown. All studied RP mutations localize to the C-terminal Jab1/MPN domain.
(B) Interaction of the C-terminal Jab1/MPN domain of PRPF8 (cartoon representation) with SNRNP200 protein (surface representation) is shown. The picture was created with the PyMol software (www.pymol.org) and is based on (Mozaffari-Jovin *et al.*, 2013) PDB accession code 4KIT. RP-related alterations of amino acids in Prfp8 are highlighted

We introduced mutations into the human *PRPF8* gene that was tagged at the protein C-terminus with a LAP tag (containing GFP) and was located on a bacterial artificial chromosome (BAC). BAC constructs are able to accommodate large inserts,

which brings the advantage of preserving the exon-intron structure of the inserted gene, as well as the promotor region and most other regulatory sequences. This method thus allows for protein expression at levels comparable to that of the endogenous gene. Using a two-step scar-less mutagenesis (Poser *et al.*, 2008), various RP mutations were introduced into the BAC carrying the wild-type (WT) PRPF8-LAP that we obtained from Ina Poser (Poser *et al.*, 2008). All LAP-tagged proteins were stably expressed in human tissue culture of HeLa cells (Fig. 11A).

We chose a C-terminal tag of PRPF8 because the N-terminal FLAG-tag was previously shown to prevent nuclear localization of Prp8 in *Drosophila melanogaster* (Claudius *et al.*, 2014). It should be noted however that a point mutation, which alters the stop codon and causes extension of the PRPF8 C-terminus by 41 amino acids, gives rise to adRP (Martinez-Gimeno *et al.*, 2003). Similarly, the extension of the yPrp8 C´ by C-terminal 3xHA tag was shown to exacerbate yeast growth (Boon *et al.*, 2007). Nevertheless, we did not notice any defects in cells expressing WT PRPF8 tagged at the C-terminus. Additionally, WT PRPF8-LAP fully complemented depletion of endogenous PRPF8 (see below: Results, chapter 4) showing that the tag at the C-terminus did not affect the function of the protein.

2 RP mutations affect PRPF8 localization and stability

First of all, we determined basic characteristics of the prepared cell lines. Neither WT nor RP mutants noticeably altered cell proliferation (personal observation, data not shown) and both WT and mutated proteins localized to the cell nucleus. However, most mutated proteins were also partially present in the cytoplasm, with the S2118F mutant exhibiting the strongest cytoplasmic accumulation (Fig. 11A and B).

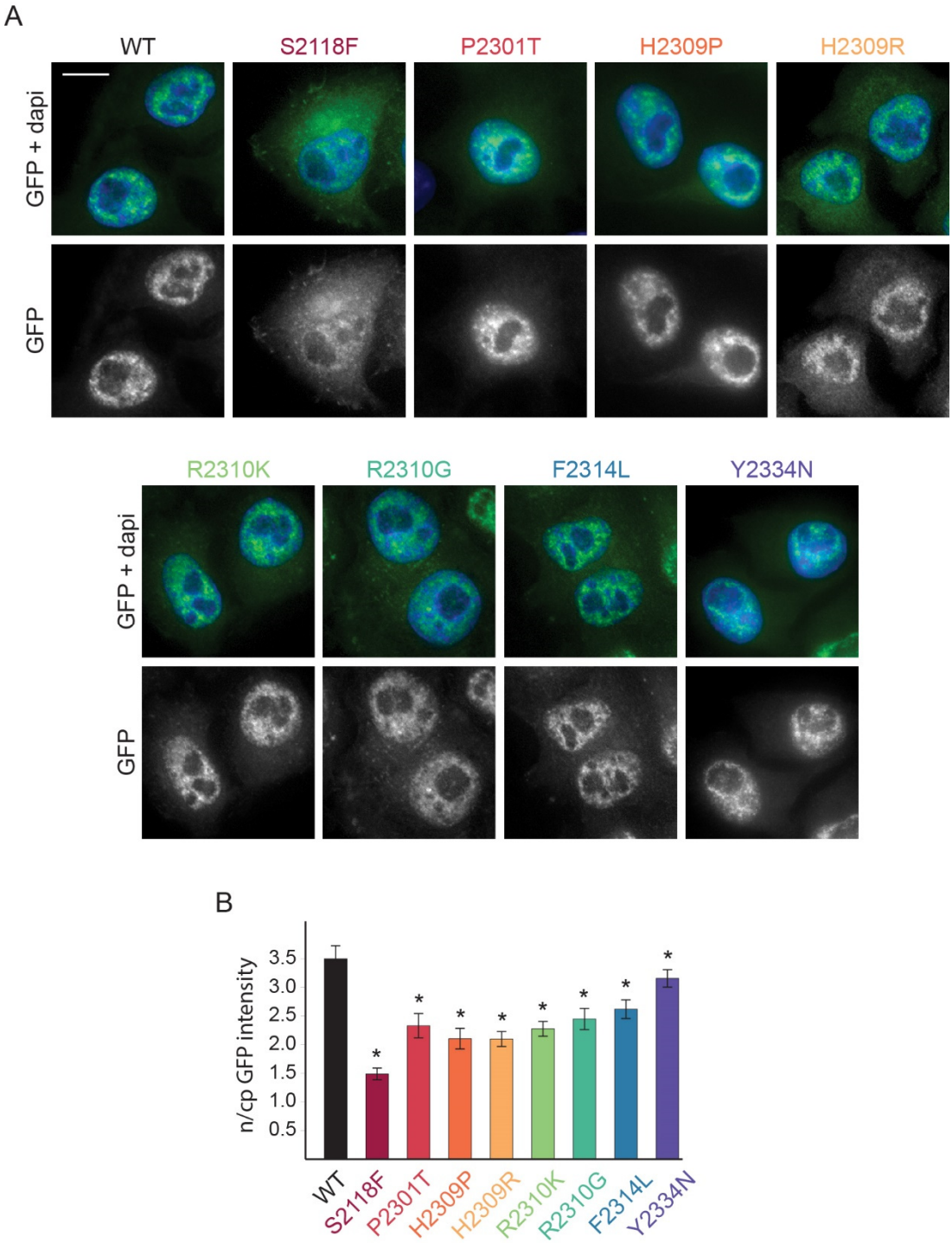

Figure 11: Cell lines expressing PRPF8-LAP variants

(A) The localization of PRPF8 proteins tagged with LAP tag containing GFP and stably expressed in HeLa cells is shown. GFP (green); DAPI (blue); scale bar - 10 µm

(B) The ratio of nuclear and cytoplasmic GFP signal intensity in cell lines expressing PRPF8-LAP variants was quantified using ImageJ software. The average of 50-125 cells together with the standard deviation is shown. The significance was assayed by t-test against the GFP signal ratio in cells expressing WT protein; * indicates $p \leq 0.05$.

The expression of all RP mutants, with the exception of F2314L, was lower than that of WT PRPF8-LAP (Fig. 12A). The decrease in protein levels may be caused by reduced expression or faster degradation. Since the promoter and cis regulatory elements are identical for all PRPF8 variants, we examined the protein degradation rate. In order to do that, we blocked protein synthesis using cycloheximide and measured the decrease of GFP fluorescence in time by time-lapse microscopy. The GFP fluorescence intensity was measured at 15-min intervals over an eight-hour period (Fig. 12B). We observed that the stability of the mutated proteins correlated with their expression levels. Only the F2314L mutant exhibited the degradation rate similar to the WT protein while the other mutated proteins were degraded faster. Of the mutants analyzed, S2118F and H2309P/R were found to be the least stable.

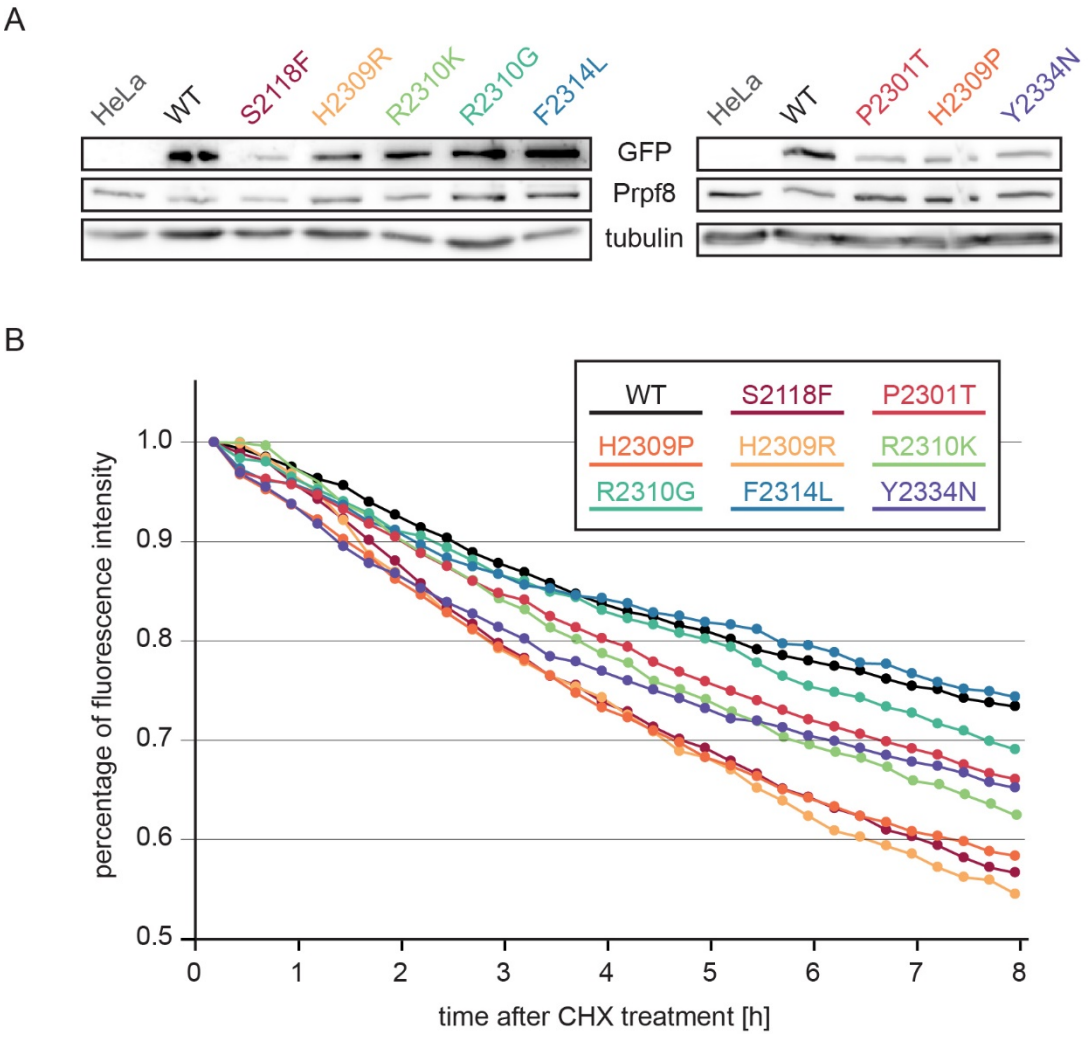

Figure 12: PRPF8-LAP proteins with RP mutations are less stable
(A) Levels of endogenous PRPF8 (anti-PRPF8 antibody line) and PRPF8-LAP (anti-GFP antibody line) were assesed by Western blot. Tubulin was used as a loading control.
(B) Protein degradation rate was determined using time-lapse microscopy. Proteosynthesis was inhibited by cycloheximide (CHX) and GFP fluorescence intensity was measured in 15 min intervals over 8 hours.

3 PRPF8-LAP gets stabilized after depletion of the endogenous protein

An important question we further wanted to address was, how the RP mutations in PRPF8 affect the efficiency of splicing in the cells. Therefore, we tested whether the mutants were able to complement the splicing defects caused by the depletion of the endogenous PRPF8. To knock down specifically the endogenous PRPF8, we utilized siRNA that was designed over the stop codon, and thus did not target the exogenous protein which had the LAP tag in that region (Fig. 13A). We knocked down endogenous PRPF8 in parental HeLa cells and in cells stably expressing WT or RP mutants. We frequently observed an increase in the expression of PRPF8-LAP proteins upon the knockdown of the endogenous protein (Fig. 13A and data not shown), which might reflect that the cells compensate for reduced levels of the endogenous protein or that the proteins are stabilized. Interestingly, the localization of PRPF8-LAP variants substantially changed after the depletion (Fig. 13B). All the mutants, even those that have exhibited increased cytoplasmic signal (Fig. 11), translocated to the nucleus. This suggest that the mutated proteins are able to get to the nucleus, but under normal conditions are outcompeted by more efficient endogenous proteins and are either left or retained in the cytoplasm.

A

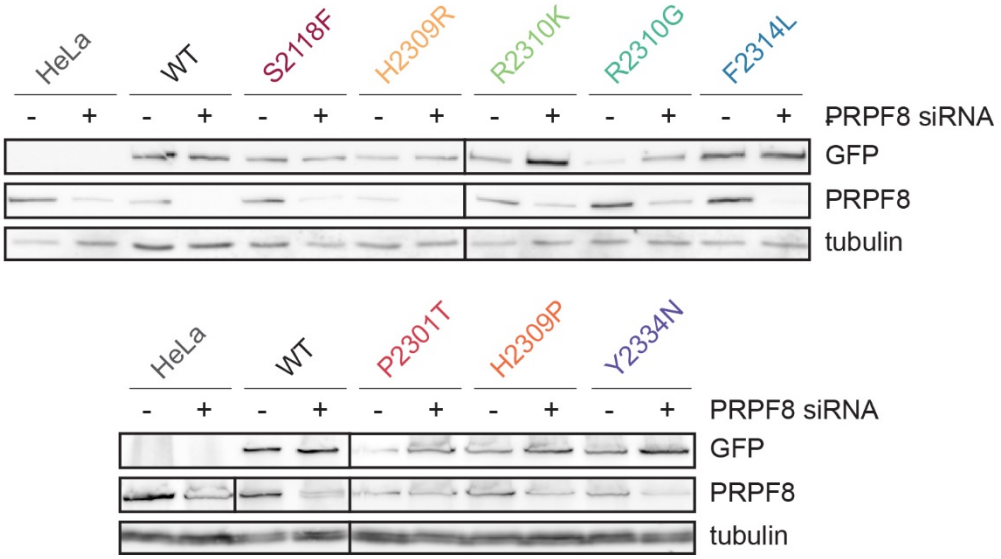

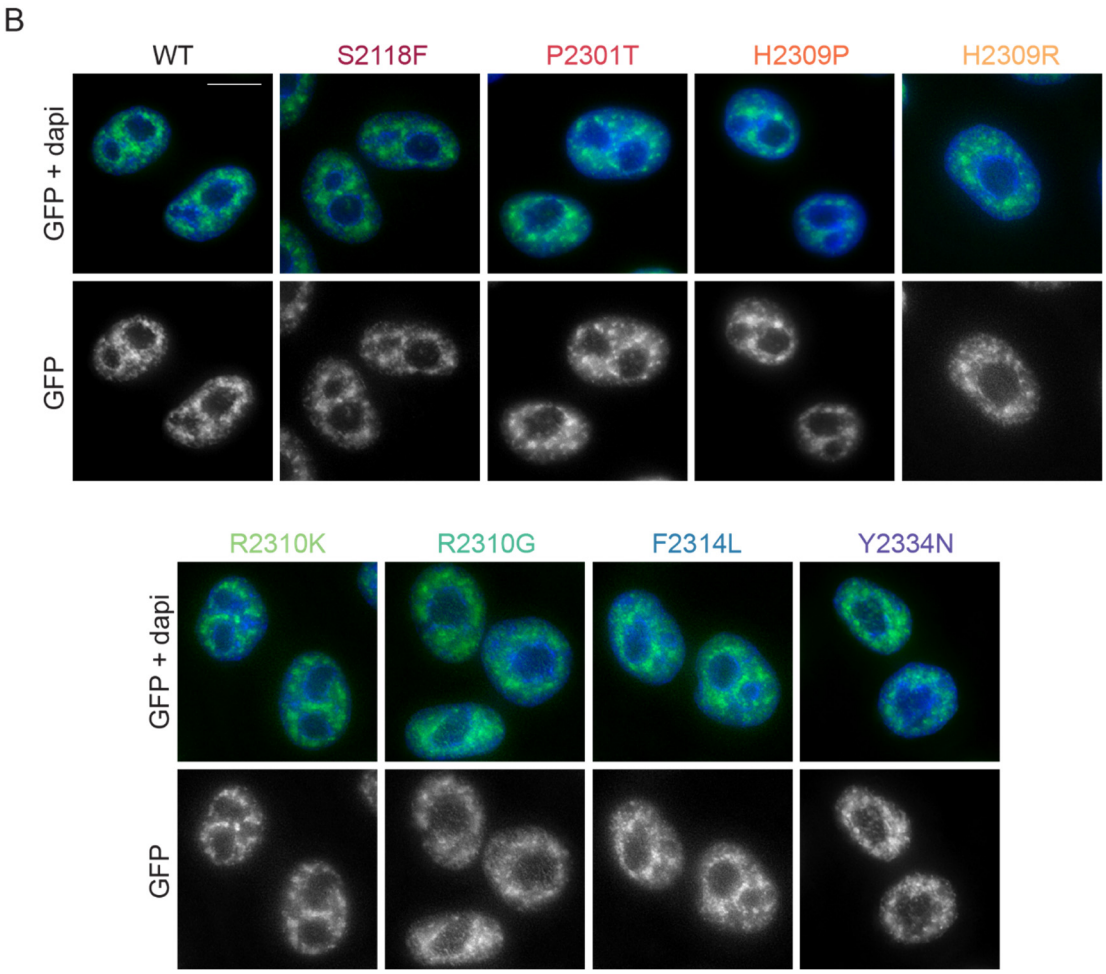

Figure 13: Relocalization of PRPF8-LAP variants after endogenous PRPF8 KD
(A) Endogenous PRPF8 was knocked down by siRNA directed against sequence around the stop codon. The siRNA specifically target endogenous Prpf8 (anti-Prpf8 antibody line), while BAC expressed proteins were not reduced (anti-GFP antibody line). Tubulin was used as a loading control.
(B) The localization of PRPF8-LAP proteins (GFP) stably expressed in HeLa cells changed after the knockdown of the endogenous PRPF8 protein. GFP (green); DAPI (blue); scale bar - 10 µm

4 RP mutations reduce the efficiency of splicing

After the endogenous PRPF8 knockdown, either RT-qPCR or RT-PCR were performed to assay the splicing efficiency of different genes. First, we analyzed the splicing efficiency of endogenous *LDHA* gene. Knockdown of PRPF8 in parental HeLa cells reduced splicing efficiency by 50% (Fig. 14A). Expression of WT PRPF8-LAP rescued splicing efficiency to a level that was fully comparable to the control cells. However, none of the mutants was able to completely rescue splicing of *LDHA* gene and P2301T and Y2334N mutants did not complement endogenous PRPF8 at all (Fig. 14A).

Next, we determined the splicing efficiency of a β-globin-derived gene that was ectopically expressed from a reporter. Again, WT PRPF8-LAP fully complemented endogenous protein in splicing of the β-globin reporter gene. Four mutants (R2310K, R2310G, F2314L and Y2334N) partially rescued reporter splicing, while S2118F, P2301T, H2309P and H2309R mutants were unable to substitute endogenous PRPF8 (Fig. 14B and C).

Finally, we investigated the influence of RP mutations on splicing of genes specifically expressed in retina. We employed three reporters derived from retina-specific genes: rhodopsin (*RHO*), which plays a crucial role during phototransduction, and two genes that code for photoreceptor structural proteins: fascin actin-bundling protein 2 (*FSCN2*) and retinal outer segment membrane protein 1 (*ROM1*) (Mordes *et al.*, 2007; Yuan *et al.*, 2005). Similarly to our results observed with *LDHA* and β-globin genes, knockdown of endogenous PRPF8 significantly reduced the splicing efficiency of retina splicing reporters and it was rescued by the expression of WT PRPF8 -LAP (Fig. 14D-I). The Y2334N mutant completely substituted endogenous PRPF8 in case of *RHO* and *ROM1* splicing, however, we observed only partial complementation in the case of *FSCN2* splicing. None of the other mutants was able to fully complement endogenous PRPF8 and mutations S2118F, H2309P, H2309R and R2310K exhibited the strongest negative effect (Fig. 14D-I).

Taken together, these data show that all RP mutations affect the splicing activity of PRPF8 to some extent but the splicing defects vary among different genes and mutants. The strongest defects were observed for S2118F and H2309R mutants, which correlated with their strong effect on protein levels and stability. On the other hand, Y2334N mutant exhibited a rather gene specific effect and significantly reduced splicing of only *LDHA*, which was in direct contrast to the other mutants which generally displayed lower effects for the *LDHA* gene.

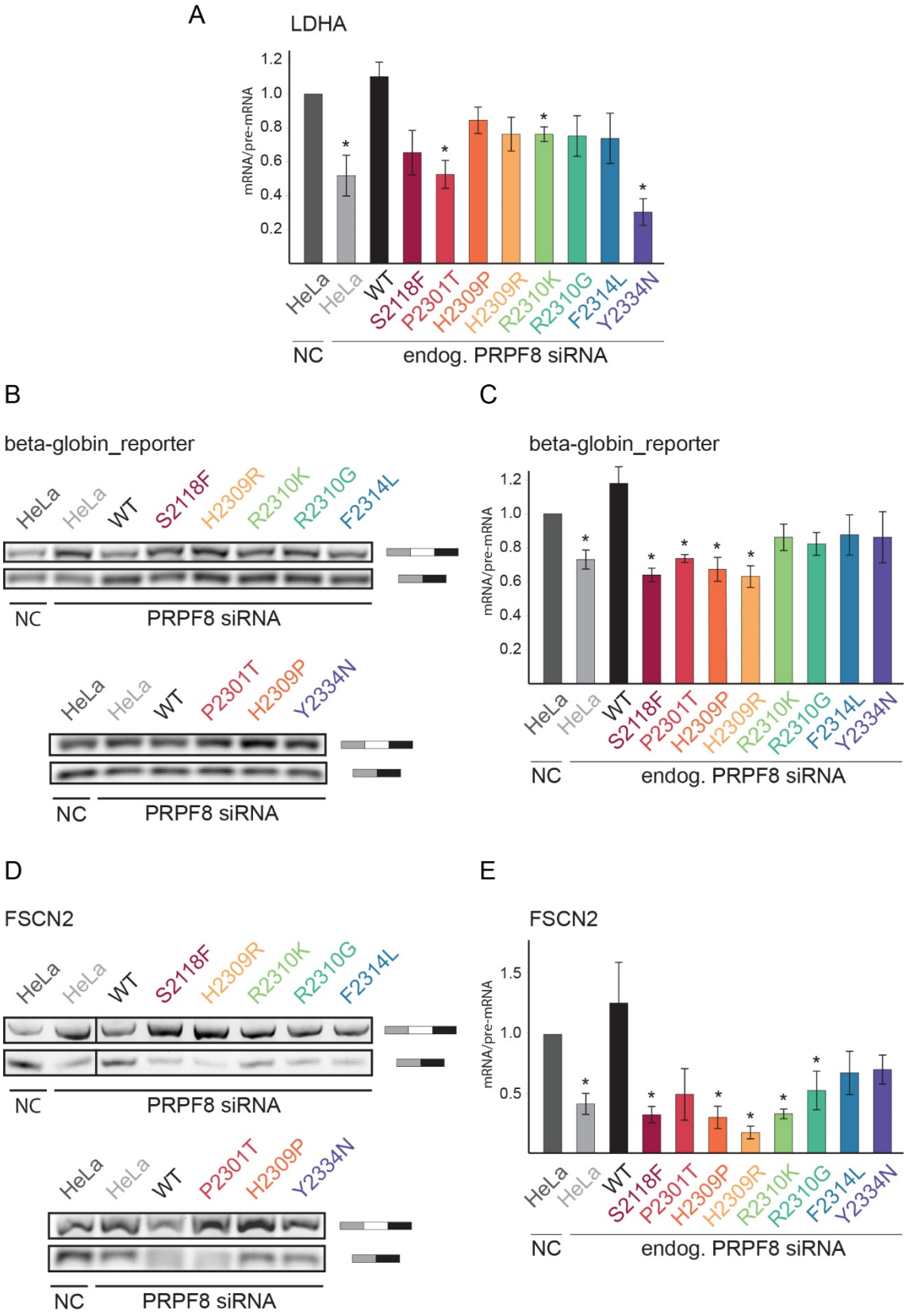
A
LDHA
mRNA/pre-mRNA
1.2
1.0
0.8
0.6
0.4
0.2
HeLa
HeLa
WT
S2118F
P2301T
H2309P
H2309R
R2310K
R2310G
F2314L
Y2334N
NC
endog. PRPF8 siRNA
B
beta-globin_reporter
HeLa
HeLa
WT
S2118F
H2309R
R2310K
R2310G
F2314L
NC
PRPF8 siRNA
HeLa
HeLa
WT
P2301T
H2309P
Y2334N
NC
PRPF8 siRNA
C
beta-globin_reporter
mRNA/pre-mRNA
1.2
1.0
0.8
0.6
0.4
0.2
HeLa
HeLa
WT
S2118F
P2301T
H2309P
H2309R
R2310K
R2310G
F2314L
Y2334N
NC
endog. PRPF8 siRNA
D
FSCN2
HeLa
HeLa
WT
S2118F
H2309R
R2310K
R2310G
F2314L
NC
PRPF8 siRNA
HeLa
HeLa
WT
P2301T
H2309P
Y2334N
NC
PRPF8 siRNA
E
FSCN2
mRNA/pre-mRNA
1.5
1.0
0.5
HeLa
HeLa
WT
S2118F
P2301T
H2309P
H2309R
R2310K
R2310G
F2314L
Y2334N
NC
endog. PRPF8 siRNA

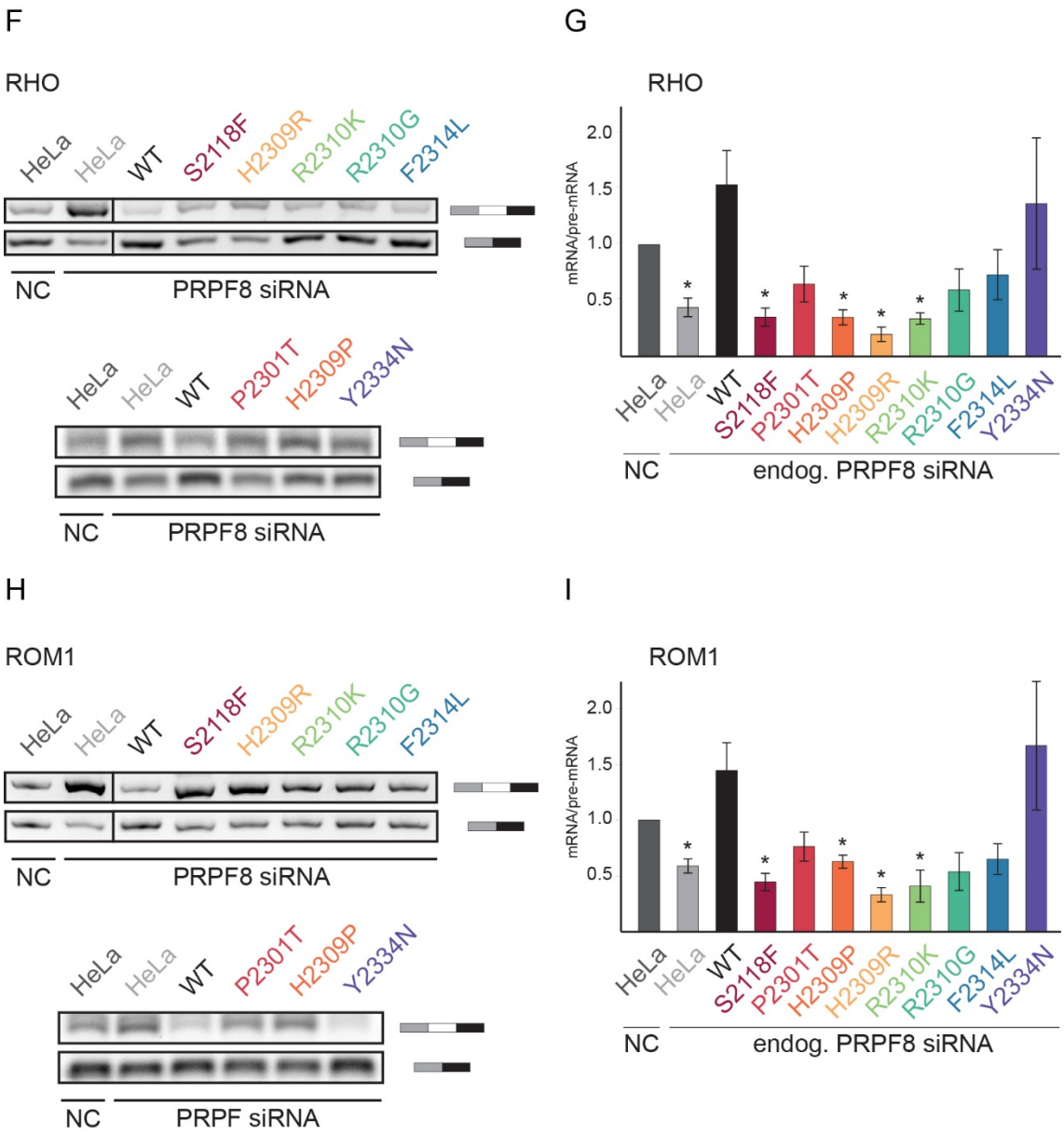

Figure 14: RP mutations affect the splicing efficiency of different genes

(A) The graph shows the average splicing efficiencies of endogenous LDHA gene in parental HeLa cells and in cell lines expressing PRPF8-LAP upon knockdown of the endogenous protein. Values were determined from the ratio of mRNA/pre-mRNA measured by quantitative RT-PCR and are an average of 3-8 experiments. All values were normalized to the LDHA mRNA/pre-mRNA ratio in parental HeLa cells treated with control siRNA (NC). The standard error of the mean is shown; the significance was assayed by t-test against parental cells treated with negative control siRNA; * indicates $p \leq 0.05$.

(B, D, F, H) The gels show products of RT-PCR reactions with gene-specific primers. As a PCR template, cDNA from parental HeLa cells and from PRPF8-LAP cell lines upon knockdown of the endogenous protein, was used. The upper bands represent pre-mRNA; the lower bands represent mRNA of the specific gene.

(C, E, G, I) The graphs showe average splicing efficiencies of β-globin gene reporter (C) and retina-specific gene reporters (E, F, G) quantified from the agarose gels using ImageJ software. For each gene reporter, values are an average of 3-8 experiments and were normalized to the mRNA/pre-mRNA ratio in parental HeLa cells treated with control siRNA (NC). The standard error of the mean is shown; the significance was assayed by t-test against parental cells treated with negative control siRNA; * indicates $p \leq 0.05$.

5 RP mutations compromise U5 snRNP and tri-snRNP formation

It was previously reported that several RP mutations in snRNP proteins, including yeast Prp8, inhibit the formation of mature snRNPs (Boon *et al.*, 2007; Pena *et al.*, 2007; Gonzalez-Santos *et al.*, 2008; Huranová *et al.*, 2009; Maeder *et al.*, 2009; Tanackovic *et al.*, 2011; Mozaffari-Jovin *et al.*, 2013). To test whether the observed splicing defects in the human cell lines are caused by reduced formation of snRNPs, we mapped the association of PRPF8 carrying RP mutations with snRNP-specific proteins. We immunoprecipitated PRPF8-LAP using anti-GFP antibodies and detected co-precipitated proteins specific for individual snRNPs on Western blot (Fig. 15A and B).

WT PRPF8-LAP was properly incorporated into U5 and tri-snRNP as documented by the co-precipitation of U5-specific proteins - SNRNP200, EFTUD2 and PRPF6, and U4/U6 di-snRNP-specific protein - PRPF31 (Fig. 15A). For easier comparison, the amount of co-precipitated proteins was quantified and normalized to the signal of co-precipitated GFP (Fig. 15B). Only the Y2334N mutant co-precipitated all the tested U5 and U4/U6 di-snRNP proteins to a similar extent as the WT PRPF8 did. The F2314L mutation did not affect the interaction of PRPF8 with EFTUD2, PRPF6 and PRPF31, but it reduced the binding of SNRNP200. The remaining mutants presumably disrupted the snRNP formation as they co-purified significantly lower amount of U5 and U4/U6 specific proteins when compared to WT. The only protein that was bound well by both WT and all mutated PRPF8 variants was the U5-specific EFTUD2. Interestingly, several RP mutants even enhanced pull-down of EFTUD2, which suggests an accumulation of the proteins in this complex (Fig. 15A and B).

In summary, our data demonstrate that most RP mutations in the *PRPF8* gene reduce the formation of fully-functional snRNPs in human cells. On the top of it, the results suggest an existence of PRPF8/EFTUD2 intermediate complex.

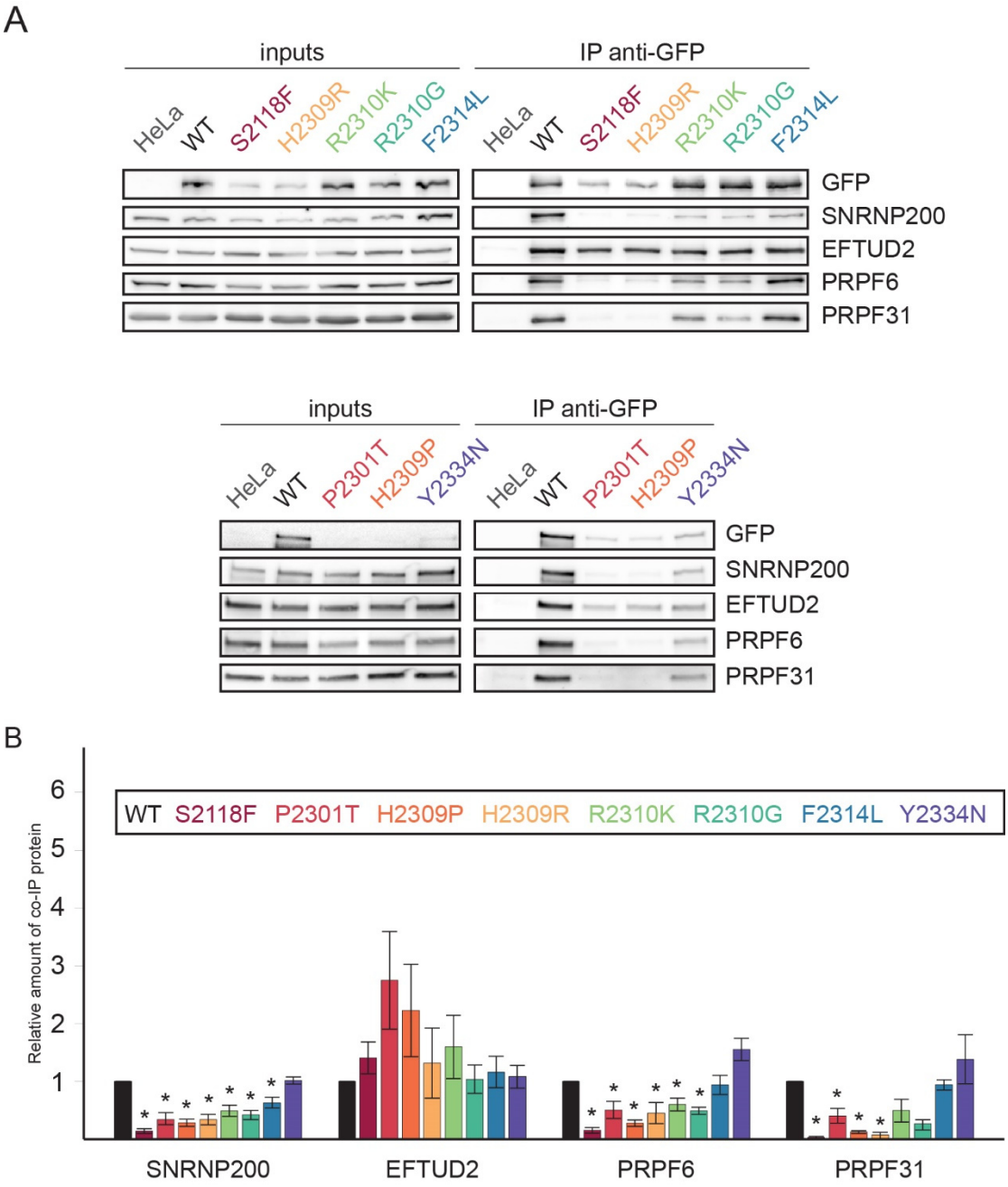

Figure 15: RP mutations inhibit U5 snRNP assembly

(A) Incorporation of PRPF8-LAP variants (indicated at the top) into spliceosome was tested by immunoprecipitation using anti-GFP antibodies. The image represents a Western blot and the detected proteins are indicated on the right side.

(B) The immunoprecipitation results were quantified using ImageJ software and normalized to the GFP intensity in the IP and to the WT. The average of 3-11 experiments together with the standard error of the mean is shown. The significance was assayed by t-test against WT; * indicates $p \leq 0.05$.

We know from our previous experiments that upon depletion of the endogenous PRPF8, the LAP-tagged mutant variants get stabilized and increase their nuclear localization to a level comparable with WT PRPF8-LAP (Fig. 13). We wondered if the interacting properties of mutant proteins also change after endogenous PRPF8 KD. To test it, we selected the S2118F mutant, which was exhibiting the strongest effect on U5 snRNP and tri-snRNP formation, and we compared proteins immunoprecipitated from NC or PRPF8 siRNA-treated cell lysates using anti-GFP antibodies (Fig. 16). The depletion of the endogenous protein enhanced the S2118F PRPF8-LAP incorporation into U5 and tri-snRNP, as documented by pull down of SNRNP200, PRPF6 and PRPF31. This finding supports the hypothesis that RP mutants are outcompeted by endogenous proteins. When the concentration of the endogenous PRPF8 decreases, the mutants might get integrated into the U5 snRNP as well, although with much lower efficiency. The increased incorporation into complexes also explains the higher stability and nuclear localization of the mutants after the KD.

A

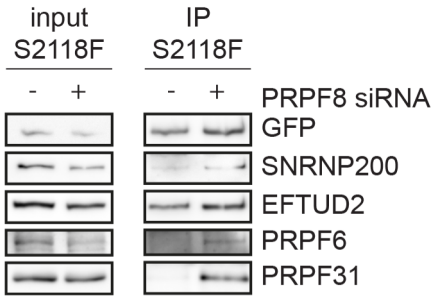

Fig. 16: S2118F PRPF8-LAP gets incorporated into tri-snRNP after endogenous PRPF8 KD
(A) Incorporation of S2118F PRPF8-LAP into spliceosome upon treatment with negative control (-) or PRPF8 (+) siRNA was tested by immunoprecipitation using anti-GFP antibodies. The image represents a Western blot and the detected proteins are indicated on the right side.

6 Incomplete snRNPs accumulate in Cajal bodies

PRPF8 is the biggest U5 snRNP protein that forms the heart of the particle. Our results show that single amino acid substitutions in PRPF8 are able to compromise U5 snRNP assembly and cause retinitis pigmentosa (Fig. 15). To get deeper insight into the mechanisms of the disease, it is crucial to understand the process of snRNP formation. In yeast, yPrp8 deficiency was shown to disrupt spliceosome assembly (Brown & Beggs, 1992). In order to better characterize the importance of PRPF8 within human U5 snRNP, we depleted PRPF8 in HeLa cells and immunoprecipitated snRNPs via Sm proteins. In our paper, Ivan Novotný performed experiments showing that the core U5 snRNP is formed even after PRPF8 downregulation (Novotný *et al.*, 2015). However, the amounts of U5 snRNP proteins (SNRNP200, EFTUD2 and PRPF31) co-precipitated by Sm proteins decreased after PRPF8 knockdown (Fig. 17). On the other hand, the composition of other snRNPs seemed unaffected as documented by pull down of U4-specific PRPF31. Altogether, these results indicate that PRPF8 is like a scaffold of U5 particle. Without it, only the core U5 snRNP is formed but the main U5-specific proteins do not associate properly.

A

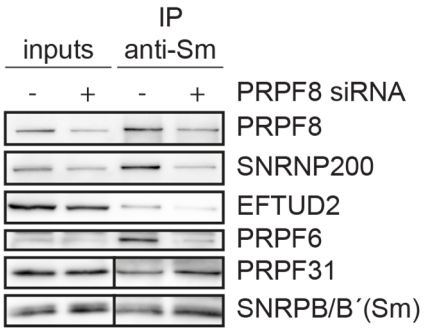

Figure 17: The composition of U5 snRNP after PRPF8 KD
(A) The image represents Western blot made with extracts of cells treated with NC siRNA (-) or anti-PRPF8 siRNA (+) before (input) and after immunoprecipitated with anti-Sm antibodies. U5-specific (SNRNP200, EFTUD2 and PRPF6) and U4-specific (PRPF31) proteins were detected, as well as pull-down control, SNRPB/B´.

The following question was, what happens with the unassembled U5 snRNP particles. Using HeLa cells, we downregulated PRPF8 and analyzed the localization of the U5 snRNA by fluorescence *in situ* hybridization (Fig. 18A). We observed a dramatic change in snRNA distribution. Whereas in cells treated with negative control siRNA (NC) the U5 snRNA was scattered throughout the nucleus (excluding nucleoli), in cells treated with siRNA against PRPF8 the snRNA was highly accumulated in nuclear dots. These dots were identified as CBs, which was confirmed by co-localization with marker protein

coilin. To control if the effect of the PRPF8 KD was specific, we performed a rescue experiment depleting PRPF8 in the cell line expressing WT PRPF8-LAP (Fig. 18A). The expression of exogenous siRNA-resistant PRPF8 fully rescued the knockdown phenotype and reduced the accumulation of U5 snRNA in CBs. Interestingly, the knockdown of U5-specific protein PRPF8 caused not only accumulation of U5 snRNA, but the U4 and U6 snRNAs were highly enriched in CBs as well (Fig. 18 B and C). The phenomenon was rescued in cell line expressing WT PRPF8-LAP.

To confirm our observations by unbiased quantitative date, we analyzed the nuclear distribution of individual snRNAs using automated high-content microscopy. The ScanR module for data analysis enables automatic detection of nuclei and CBs and calculates the ratio of the mean probe fluorescence intensity between these compartments. This approach confirmed our results showing up to 2.5-fold increase of the accumulation of snRNAs in CBs after PRPF8 KD (Fig. 18D).

These results suggest that although other snRNPs might be assembled correctly after PRPF8 KD (Fig. 17), the tri-snRNP cannot be formed and the U4 and U6 particles without their binding partner, U5, accumulate in Cajal bodies.

A

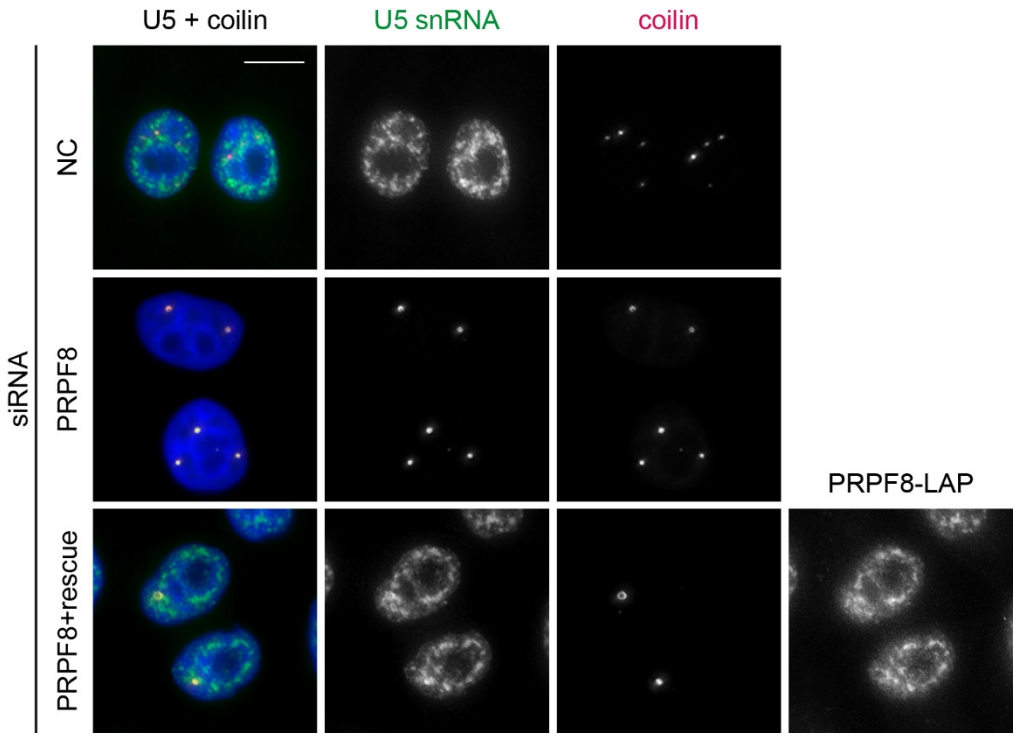

B

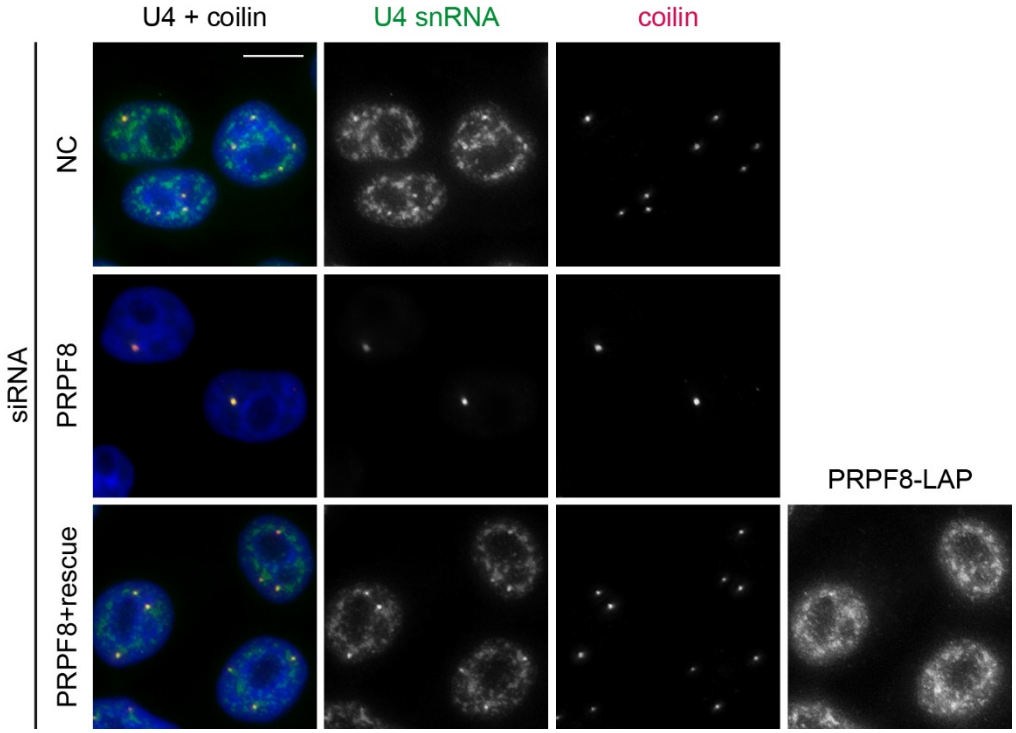
U4 + coilin
U4 snRNA
coilin
siRNA
NC
PRPF8
PRPF8+rescue
PRPF8-LAP

C

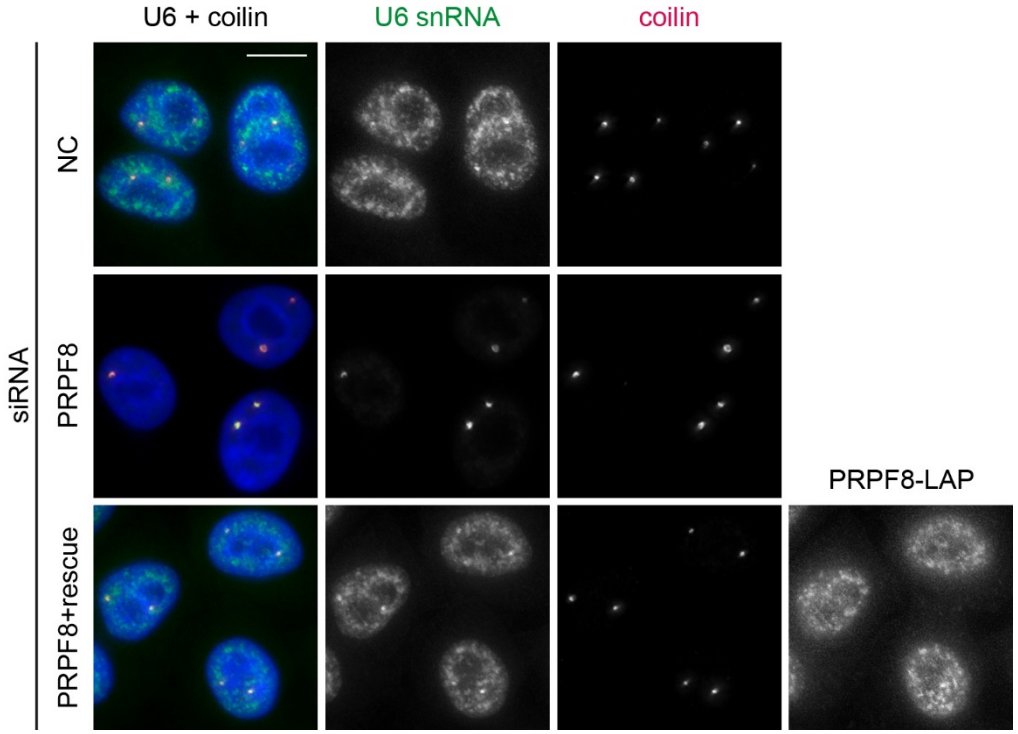
U6 + coilin
U6 snRNA
coilin
siRNA
NC
PRPF8
PRPF8+rescue
PRPF8-LAP

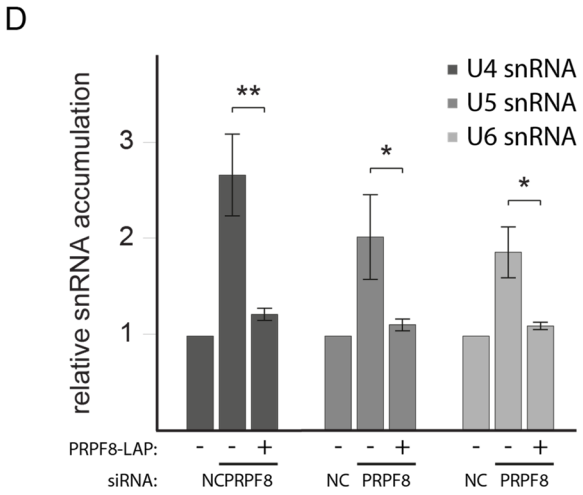

Figure 18: Accumulation of snRNAs in Cajal bodies after PRPF8 KD
(A,B,C) Parental HeLa cells (1st and 2nd raw) or HeLa cells stably expressing siRNA-resistant WT PRPF8-LAP (3rd raw) were treated with siRNA against PRPF8 or a negative control siRNA (siNC). U5 (A), U4 (B) or U6 (C) snRNAs were detected by fluorescence in situ hybridization (FISH) probe (green); coilin was used as a marker of Cajal bodies (red); dapi marks the nucelus (blue). scale bar - 10 µm
(D) The CB accumulation of snRNAs (CB/nuclear probe fluorescence intensity) was measured by high-content microscopy. An average of 3 experiments is shown together with the SEM; values were normalized to the NC treated cells. The significance was assayed by t-test; * indicates $p \leq 0.05$ and ** indicates $p \leq 0.01$.

7 RP mutants are stalled in a complex with AAR2

Up to now, we found that PRPF8 is fundamental for U5 snRNP formation and after its depletion, the core U5 snRNP is left solitary without its major protein components. The question remains, how are the U5-specific proteins assembled onto the core snRNP and if there are any factors involved in this process. In our human cell lines, we found RP PRPF8 mutants trapped in a complex with EFTUD2, human homologue of Snu114. In yeast, a complex containing the core U5 snRNP with Prp8, Snu114 and Aar2 was identified and proposed as the U5 snRNP assembly precursor (Boon *et al.*, 2007). Therefore, we inquired into the similarities between the yeast and human complexes and we tested whether the PRPF8-LAP mutants are associated also with AAR2. Indeed, mutations that reduced the assembly of functional snRNPs (S2118F, P2301T, H2309P/R and R2310K/G) enhanced the co-precipitation of AAR2 with respect to WT protein or mutants that did not inhibit snRNP assembly (F2314L and Y2334N) (Fig. 19A and B).

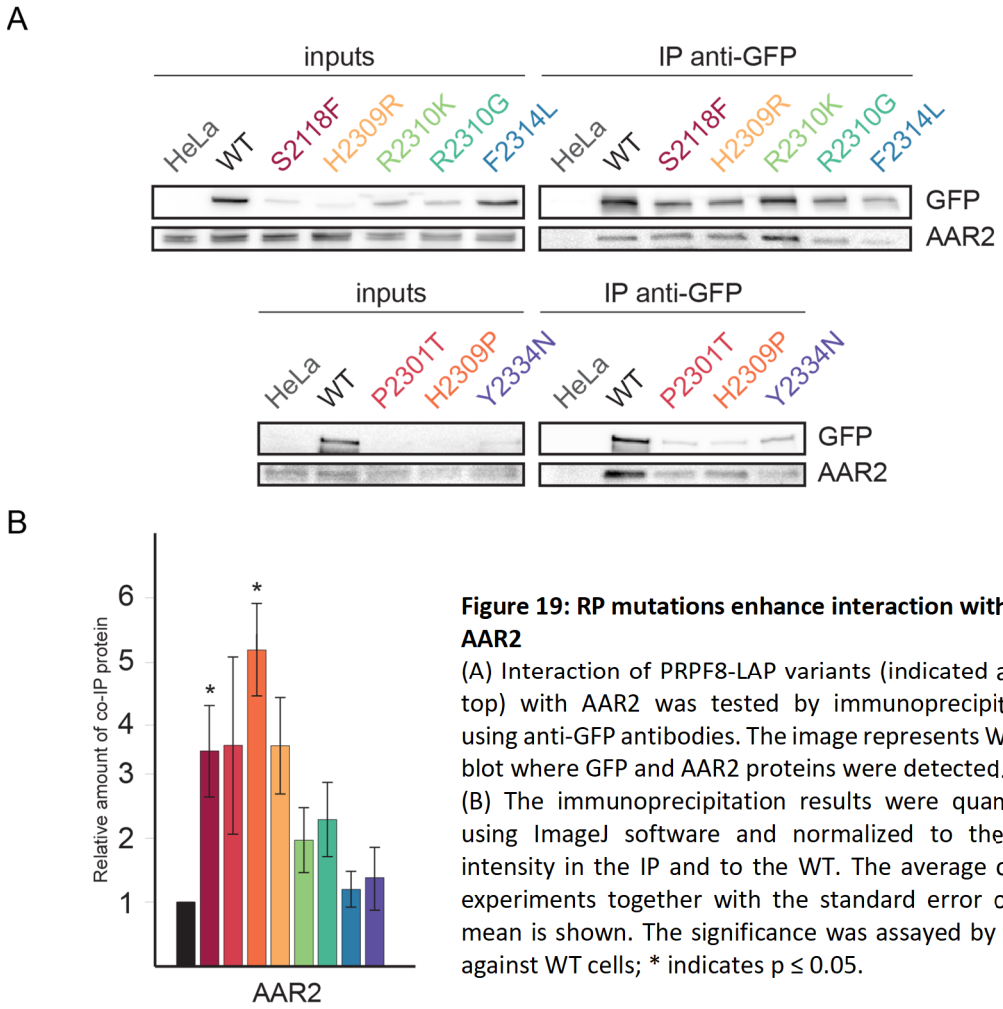

Figure 19: RP mutations enhance interaction with AAR2

(A) Interaction of PRPF8-LAP variants (indicated at the top) with AAR2 was tested by immunoprecipitation using anti-GFP antibodies. The image represents Wester blot where GFP and AAR2 proteins were detected.

(B) The immunoprecipitation results were quantified using ImageJ software and normalized to the GFP intensity in the IP and to the WT. The average of 3-6 experiments together with the standard error of the mean is shown. The significance was assayed by t-test against WT cells; * indicates $p \leq 0.05$.

In yeast, the Prp8/Snu114/Aar2 complex interacts with the core U5 snRNP (U5 snRNA + Sm proteins). To test whether the human complex is bound to the core snRNP, we performed immunoprecipitation with the anti-Sm antibody and detected co-precipitated PRPF8-LAP fusion proteins on a Western blot (Fig. 20A). WT and F2314L proteins, which are incorporated into tri-snRNP (see above Fig. 15), were co-purified with Sm proteins. However, two mutated proteins S2118F and H2309R, which are arrested in the complex with EFTUD2, showed only negligible interaction with Sm proteins (Fig. 20).

Thus, it seems that the RP mutants are stalled in the PRPF8/EFTUD2/AAR2 complex but in contrast to the yeast, this complex does not contain the core snRNP.

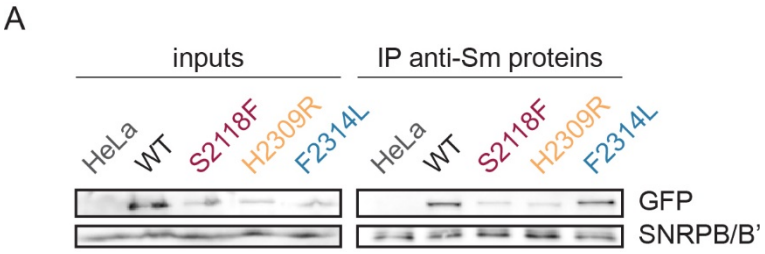

Figure 20: RP mutations decrease association with the core snRNP
(A) Interaction of several PRPF8-LAP variants (indicated at the top) with the core snRNP was tested by immunoprecipitation using anti-Sm antibodies. The image represents Western blot with GFP and SNRPB/B´ proteins were detected.

8 AAR2 is important for U5 snRNP assembly

After the identification of the PRPF8/EFTUD2/AAR2 complex as an early intermediate of U5 snRNP particle, we wanted to confirm the suggested role of AAR2 as an U5 snRNP assembly factor. To do that, we knocked down AAR2 and looked on the formation of the mature U5 via immunoprecipitation. After AAR2 depletion, WT PRPF8-LAP pulled down lower levels of SNRNP200 and EFTUD2, whereas the PRPF6 pulldown was not affected (Fig. 21A and B). These results suggest that without AAR2, the U5 particles are not formed properly, and thus confirm the importance of AAR2 in U5 snRNP assembly pathway.

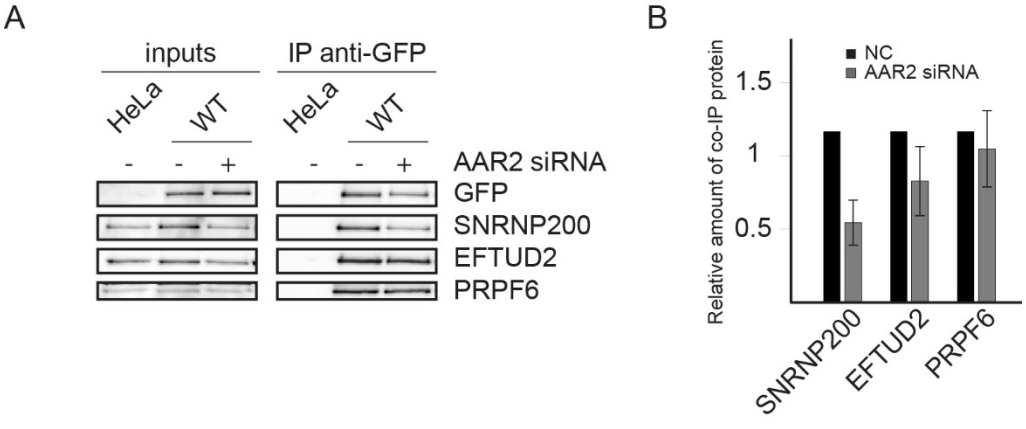

Figure 21: U5 snRNP formation after AAR2 KD
(A) U5 snRNP assembly after AAR2 knockdown was tested in cell line expressing WT PRPF8-LAP by immunoprecipitation with anti-GFP antibodies. The image represents a Western blot and the detected proteins are indicated on the right side.
(B) The immunoprecipitation results were quantified using ImageJ software and normalized to the NC. The average of 3 experiments together with the standard error of the mean is shown. The significance was assayed by t-test against parental cells treated with negative control siRNA; * indicates $p \leq 0.05$.

9 PRPF8 interacts with ZNHIT2 and ECD proteins and the R2TP complex

The previous findings brought up the question of U5 snRNP biogenesis, and thus we decided to identify other factors involved in the assembly process. In order to do that, we sent our WT PRPF8-LAP cell line to the collaborators from the laboratory of Edouard Bertrand in Montpellier (France) and they performed stable isotope labeling in cell culture (SILAC) (Ong *et al.*, 2002) followed by IP and quantitative mass spectrometry (MS) (Fig. 22A). SILAC experiments rely on incorporation of either light or heavy non-radioactive amino acid isoforms into proteins of two different cell lines, WT PRPF8-LAP and control HeLa cells. The isotopic labeling then enables differentiation between proteins from control HeLa cells immunoprecipitated with anti-GFP antibody non-specifically and proteins specifically binding PRPF8-LAP.

As anticipated, the PRPF8-LAP bait co-purified spliceosomal proteins, especially the components of the U5 snRNP (EFTUD2, SNRNP200, SNRNP40, PRPF6, Sm proteins – SNRP etc.) were highly enriched, as well as some tri-snRNP components (PRPF4, SART1 etc.) (Fig. 22A). This confirms that the PRPF8-LAP proteins were correctly incorporated into tri-snRNPs and it verifies the specificity of the method. In agreement with our previously conducted IP results and with *in vitro* studies (Santos *et al.*, 2015), we confirmed the interaction of PRPF8 with AAR2 in human cells.

Remarkably, a group of proteins revolving around chaperones HSP90 and HSP70 was enriched in the PRPF8 pull-down. Apart from the chaperones themselves, proteins of the R2TP complex (PIH1D1, RPAP3, RUVBL1 and RUVBL2) were identified in the MS too (Fig. 22A). As discussed above (Introduction, chapter 5.2), the HSP90/R2TP complex is known to be involved in the biogenesis of U4 snRNP (Bizarro *et al.*, 2015) but nothing is known about its role in the maturation of U5 snRNP.

Interestingly, the analysis also revealed the association of PRPF8 with a number of other proteins. Among these, especially ZNHIT2 and ECD are worth noticing (Fig. 22A). ZNHIT2 belongs to the family of Zinc-Finger HIT proteins together with several other assembly factors connected to the R2TP complex, which are known to be part of the assembly machinery of various RNP. The function of ZNHIT2 has not been described yet

but our data suggest that it might be involved in U5 snRNP maturation. ECD was proposed to function in the U5 snRNP biogenesis in flies (Claudius *et al.*, 2014) and our data further support that hypothesis. Finally, several regulators of HSP90 (e.g. PTGES3 and STIP1) were also enriched in the IPs, as well as a set of poorly characterized proteins including TTC27, TSSC4, EAPP and NCND (Fig. 22A). These proteins are not components of the mature U5 snRNP and so possibly belong among additional U5 snRNP assembly factors.

In summary, many different factors that might be involved in the biogenesis of the human U5 particle were identified using a MS-based approach.

A

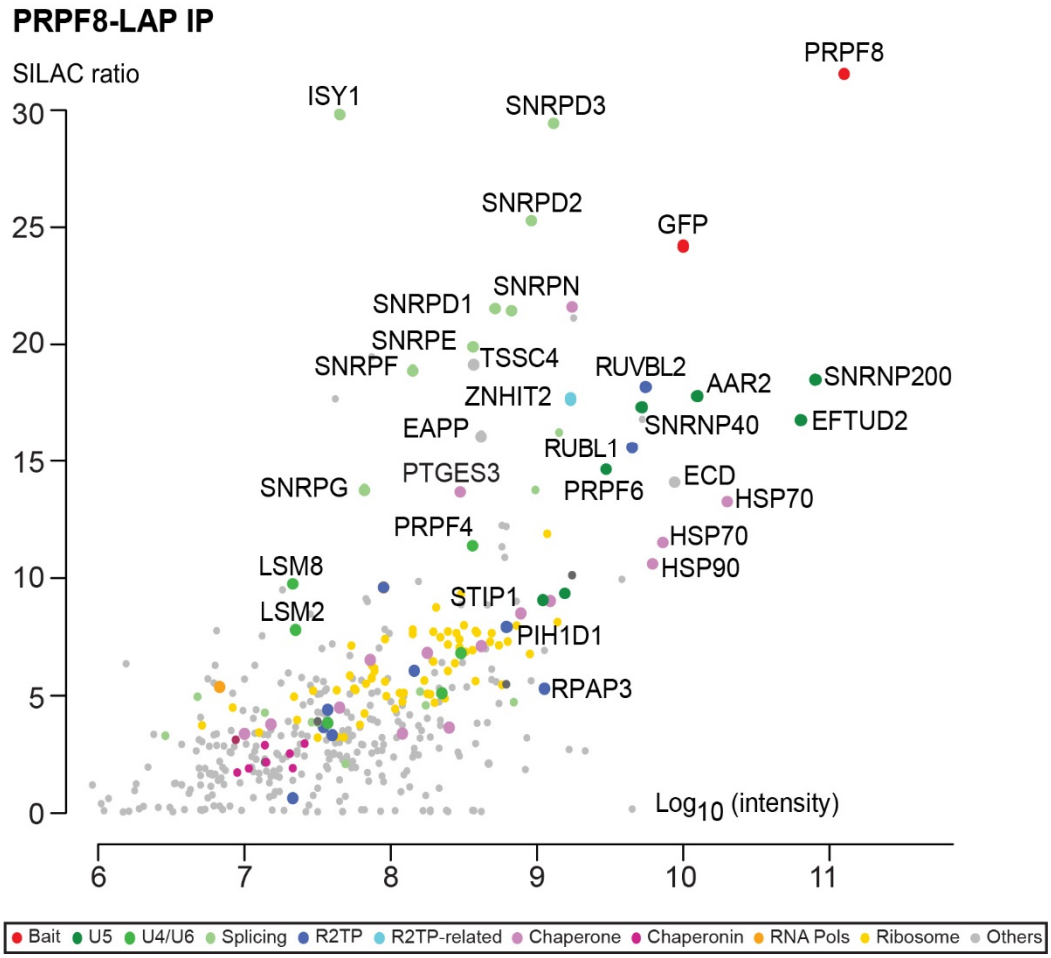

Figure 22: Quantitative proteomic analysis of PRPF8-LAP interactores
(A) SILAC of WT PRPF8-LAP cell line followed by anti-GFP IP and quantitative mass spectrometry was performed. The graph shows the SILAC ratio (y axis) over signal intensity (x axis). Each dot represents a protein and is color-coded according to the classification shown below the panel.

10 HSP90 is involved in maturation of U5 proteins

The HSP90 is a key chaperon involved in folding of many client proteins. In our SILAC experiments, it was identified to be associate with PRPF8-LAP. To test whether HSP90 is involved in the folding of U5-specific protein, we inhibited HSP90 activity by geldanamycin (GA), which locks HSP90 in a close state and usually results in client protein degradation (Whitesell *et al.*, 1994). HSP90 inhibition resulted in reduced levels of PRPF8 and SNRNP200 proteins. Interestingly, EFTUD2 was unaffected by the treatment (Fig. 23A and B). This result suggests that PRPF8 and SNRNP200, both over 200 kDa large proteins, are HSP90 clients and it further supports the hypothesis that the HSP90/R2TP machinery is involved in the early assembly steps of the U5 snRNP particles.

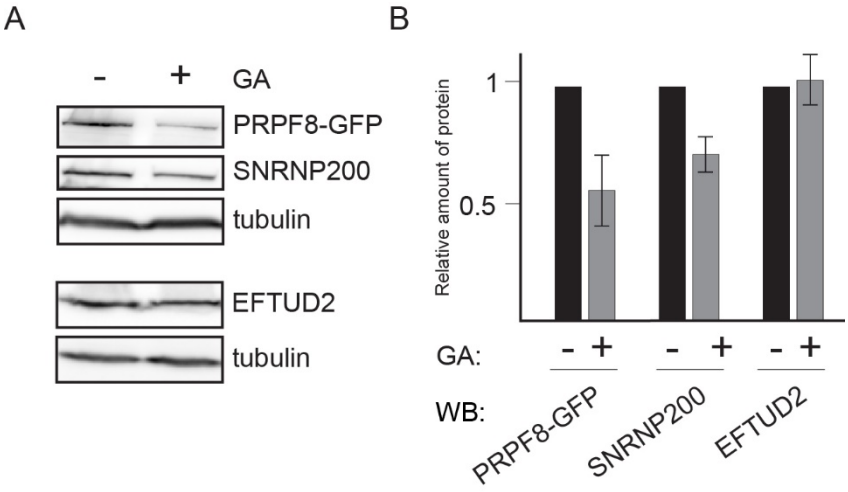

Figure 23: HSP90 is required for PRPF8 and SNRNP200 stability
(A) Cells expressing WT PRPF8-LAP were treated (+) or untreated (-) with HSP90 inhibitor, Geldanamycin. Western blots were run with the extracts from these cells and were probed with antibodies indicated at the right.
(B) The intensity of Western blot bands was quantified using ImageJ software and normalized to tubulin as a loading control and to the not treated cells. The average of 3 experiments together with the standard error of the mean is shown. The significance was assayed by t-test against the untreated cells; * indicates $p \leq 0.05$.

11 RUVBL proteins are required for proper U5 snRNP maturation

To get deeper insight into the role of the R2TP complex in the biogenesis of U5 snRNP, we knocked down individual R2TP proteins and analyzed (1) PRPF8 association with remaining R2TP components, AAR2 and U5-specific proteins and (2) changes in the behavior of the core U5 snRNPs.

First, we depleted PIH1D1, RUVBL1 and RUVBL2 in cell line expressing WT PRPF8-LAP and immunoprecipitated the tag protein with anti-GFP antibodies (Fig. 24). In contrast to AAR2 knockdown, PIH1D1 depletion increased PRPF8-LAP interaction with AAR2, remaining R2TP complex components (Fig. 24A and B), and U5 snRNP-specific proteins (Fig. 24C and D). The effect of RUVBL2 knockdown was not so pronounced but had a similar tendency as PIH1D1 depletion (Fig. 24E-H). In case of the RUVBL1 knockdown, RPAP3 or PIH1D1 were also enriched in the pulldowns (Fig. 24E and F) but the difference in PRPF8-LAP interactions with AAR2 and U5 proteins was just mild (Fig. 24G and H). These observations suggest that the R2TP complex is not absolutely necessary for recruitment of PRPF8 to its main interacting partners from the U5 particle. On the contrary, the increase of interactions indicate that PRPF8 is sequestered together with the remaining R2TP components and other U5 snRNP proteins, hence the R2TP complex might be involved in the assembly process by other means, for example it may control the quality of the U5 assembly.

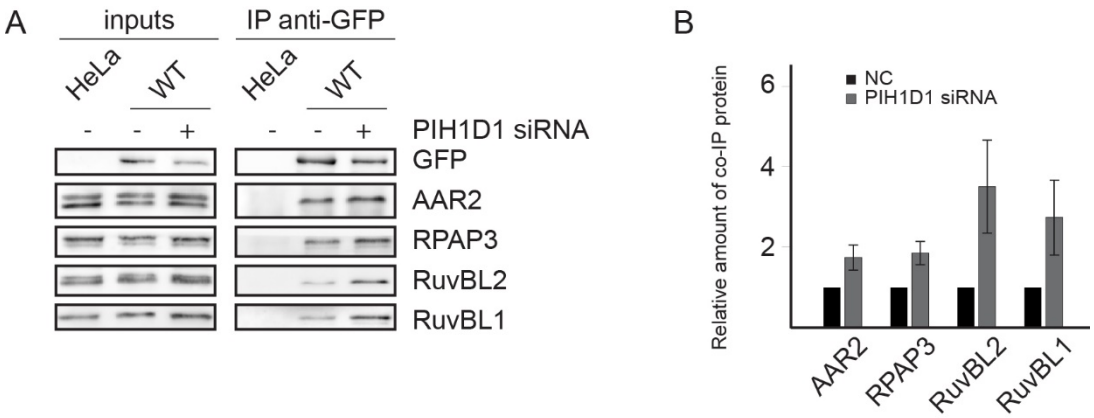

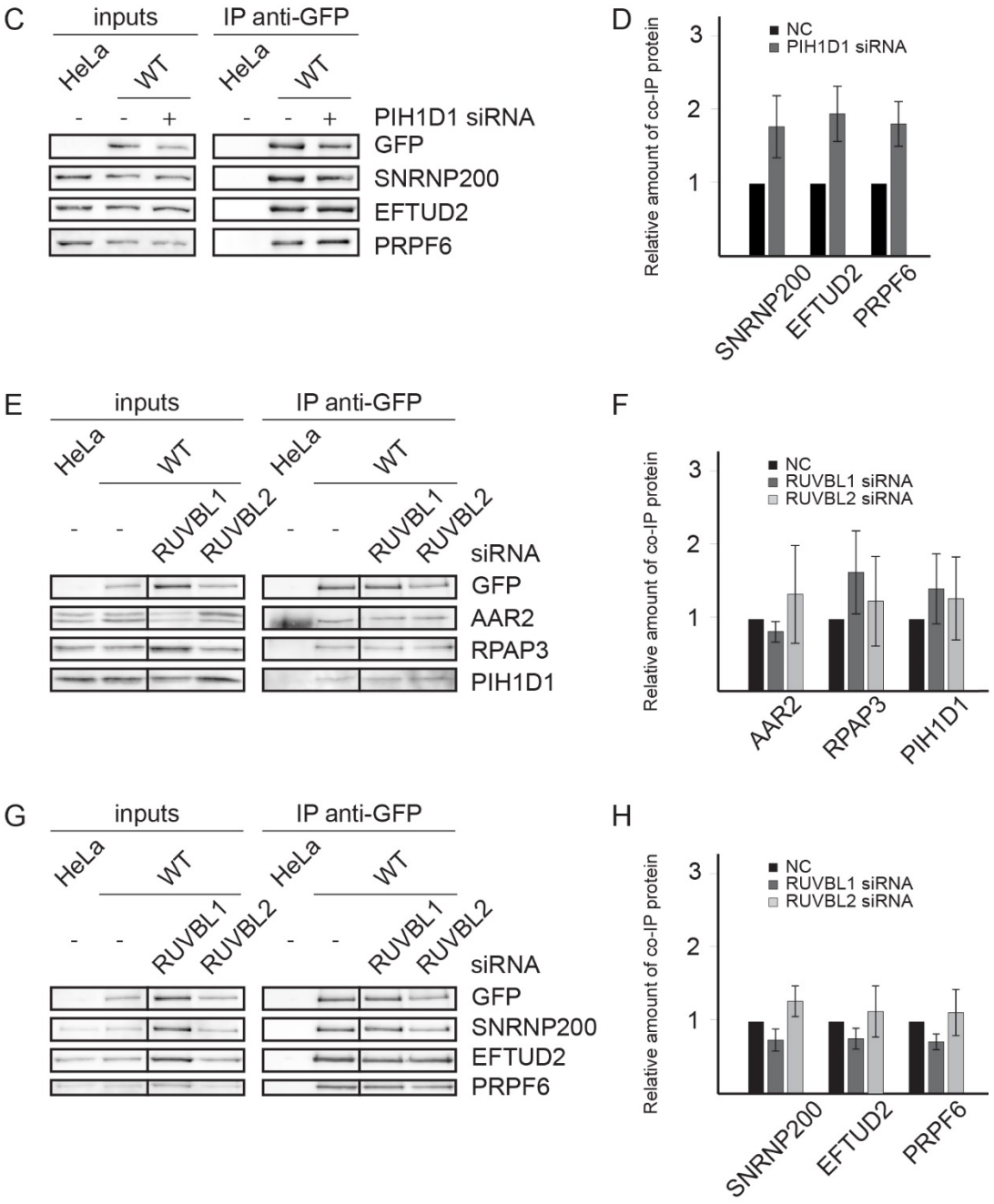

Figure 24: R2TP complex KDs do not prevent assembly of the U5 snRNP
(A,C,E,G) Interactions of WT PRPF8-LAP with R2TP complex components (A, E) and U5 snRNP proteins (C, G) after PIH1D1 (A, C) and RUVBL1/2 (E, G) knockdowns were tested by immunoprecipitation with anti-GFP antibodies. The images represent Western blots and the detected proteins are indicated on the right side.
(B,D,F,H) The immunoprecipitation results were quantified using ImageJ software and normalized to the NC. The average of 3 experiments together with the standard error of the mean is shown. The significance was assayed by t-test against WT cells treated with negative control siRNA; * indicates $p \leq 0.05$.

The previous immunoprecipitation experiments showed that PRPF8 is in complex with other U5 snRNP proteins even after the depletion of the R2TP components. To address the question whether functional snRNPs are formed, we took advantage of our

finding that defects in U5 snRNP maturation cause the accumulation of U5 snRNA in Cajal bodies (see above Fig. 18). We knocked down individual R2TP proteins (PIH1D1, RUVBL1 and RUVBL2) and looked on the localization of U5 snRNA using fluorescence *in situ* hybridization (FISH) probes (Fig. 25). We did not observe any noticeable difference in case of PIH1D1 depletion, but RUVBL1 and 2 depleted cells displayed an evident accumulation of U5 snRNA in Cajal bodies (Fig. 25; compare to Fig. 18). We can therefore conclude that at least the RUVBL proteins are required for proper maturation of U5 snRNPs particles.

A

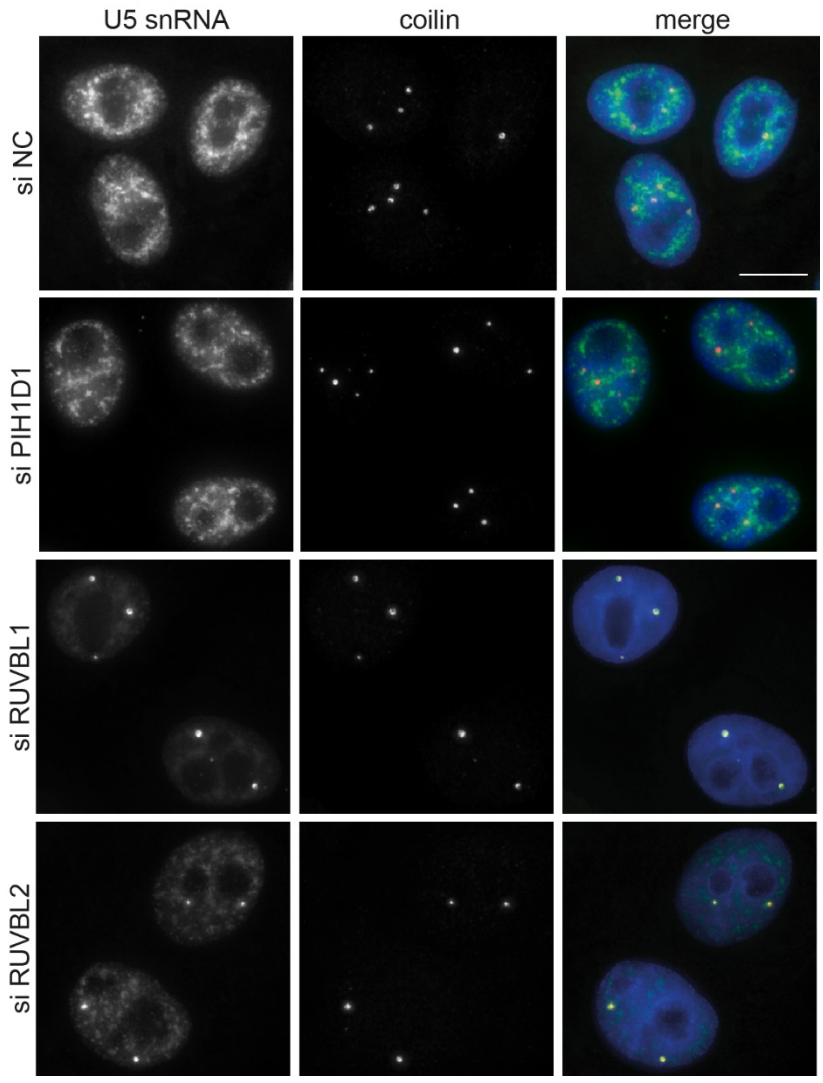

Figure 25: Accumulation of U5 snRNA in Cajal bodies after RUVBL1/2 KD
(A) HeLa cells were treated with siRNA against R2TP proteins (PIH1D1, RUVBL1 and RUVBL2) or a negative control siRNA (siNC). U5 snRNA was detected by fluorescence in situ hybridization (FISH) probe (green); coilin was used as a marker of Cajal bodies (red); dapi marks the nucelus (blue). scale bar - 10 µm

12 The HSP90/R2TP complex and ZNHIT2 associate preferentially with mutated PRPF8

So far, we have shown that majority of the tested RP mutations reduce the association of PRPF8 with U5 snRNP and that the mutated PRPF8 proteins are stalled in an intermediate complex with EFTUD2 and an assembly factor AAR2 (see above Fig. 15 and 18). Our results have also shown that the HSP90/R2TP complex participates on U5 snRNP maturation and together with ZNHIT2 and other proteins interacts with WT PRPF8-LAP (see above Fig. 22). We therefore decided to test whether the mutated PRPF8-LAP variants associate with HSP90/R2TP complex and ZNHIT2 similarly as they associate with AAR2.

We immunoprecipitated PRPF8-LAP variants with an anti-GFP antibodies and analyzed their interactions with HSP90, R2TP complex proteins and ZNHIT2 (Fig. 26). We focused only on mutations S2118F and H2309R, which exhibited the strongest assembly phenotype, and compare them with WT PRPF8-LAP and the PRPF8 with F2314L mutation that are incorporated into the tri-snRNP (see Fig. 15). Both S2118F and H2309R mutants increased the co-precipitation of HSP90 (Fig. 26A), R2TP complex proteins (Fig. 26B and D) and ZNHIT2 (Fig. 26C and E). These results are consistent with our previous findings and confirm that similarly to AAR2, the identified assembly factors associate predominantly with unassembled particles.

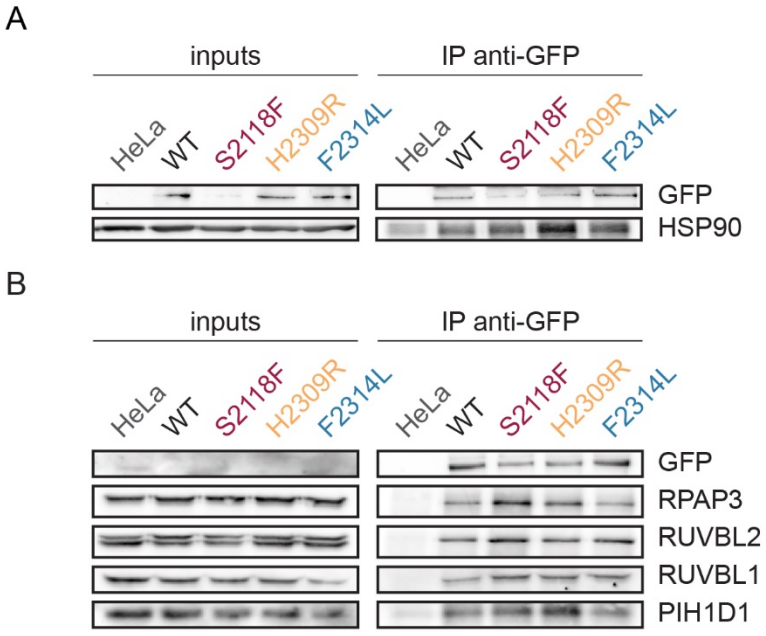

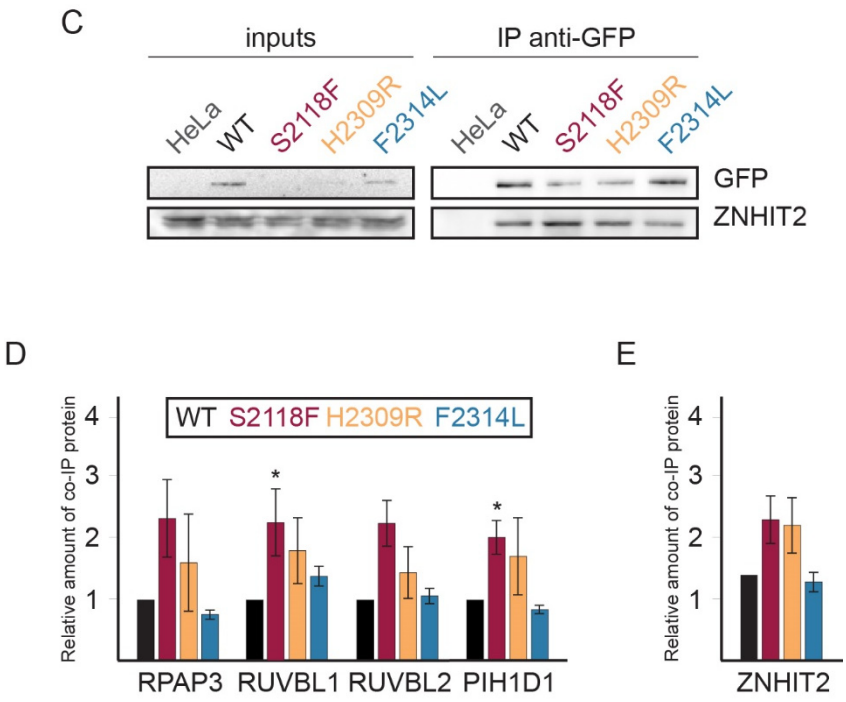

Figure 26: Identified assembly factors associate preferentially with mutated PRPF8
(A-C) Interactions of PRPF8-LAP variants (indicated at the top) with HSP90 (A), R2TP complex components (B) and ZNHIT2 (C) were tested by immunoprecipitation with anti-GFP antibodies. The images represent Western blots and the detected proteins are indicated on the right side.
(D-E) The immunoprecipitation results were quantified using ImageJ software and normalized to the GFP intensity in the IP and to the WT. The average of 3-4 experiments together with the standard error of the mean is shown. The significance was assayed by t-test against WT cells; * indicates $p \leq 0.05$.

13 The R2TP complex sequesters mutated PRPF8 in the cytoplasm

We observed that despite containing a putative nuclear localization signal at the N-terminus, PRPF8 proteins with RP mutations are not efficiently imported to the nucleus and display increased cytoplasmic localization (Fig. 11). We also know that R2TP complex preferentially binds these mutated proteins (Fig. 26) and that the PRPF8-R2TP interaction occurs in the cytoplasm (personal communication with Edouard Bertrand and Celine Verheggen). We therefore decided to test whether R2TP is involved in tethering mutated PRPF8 in the cytoplasm. We used siRNA against R2TP proteins (PIH1D1, RUVBL1 and RUVBL2) in the cell line expressing the PRPF8-LAP with the S2118F mutation, which exhibits the strongest accumulation in the cytoplasm (Fig. 11). Both RUVBL1 and 2 knockdowns resulted in higher nuclear localization of the S2118F protein (Fig. 27A and B). This finding suggest that the HSP90/R2TP complex sequesters assembly-defective PRPF8 mutants in the cytoplasm which is consistent with our hypothesis about a role of this chaperon complex in the quality control of the U5 snRNP assembly process.

A question remains concerning the fate of S2118F mutants after RUVBL1 and 2 KDs. We know that they are localized in what appears to be nuclear speckles (Fig. 26A) but we also know that the KDs result in the accumulation of the U5 snRNA in CBs, indicating a U5 snRNP assembly defects (Fig. 25). We therefore performed immunoprecipitations of S2118F PRPF8-LAP mutant after RUVBL1/ 2 depletion and analyzed the interactions with U5 proteins (Fig. 27C). We did not observe any increased interactions, which suggests that it does not get incorporated into U5 snRNPs even though it is in the speckles. Nothing is known about the targeting of spliceosomal components to nuclear speckles and so it is possible that PRPF8 contains an unknown targeting signal and can travel to the speckles independently of U5 snRNP.

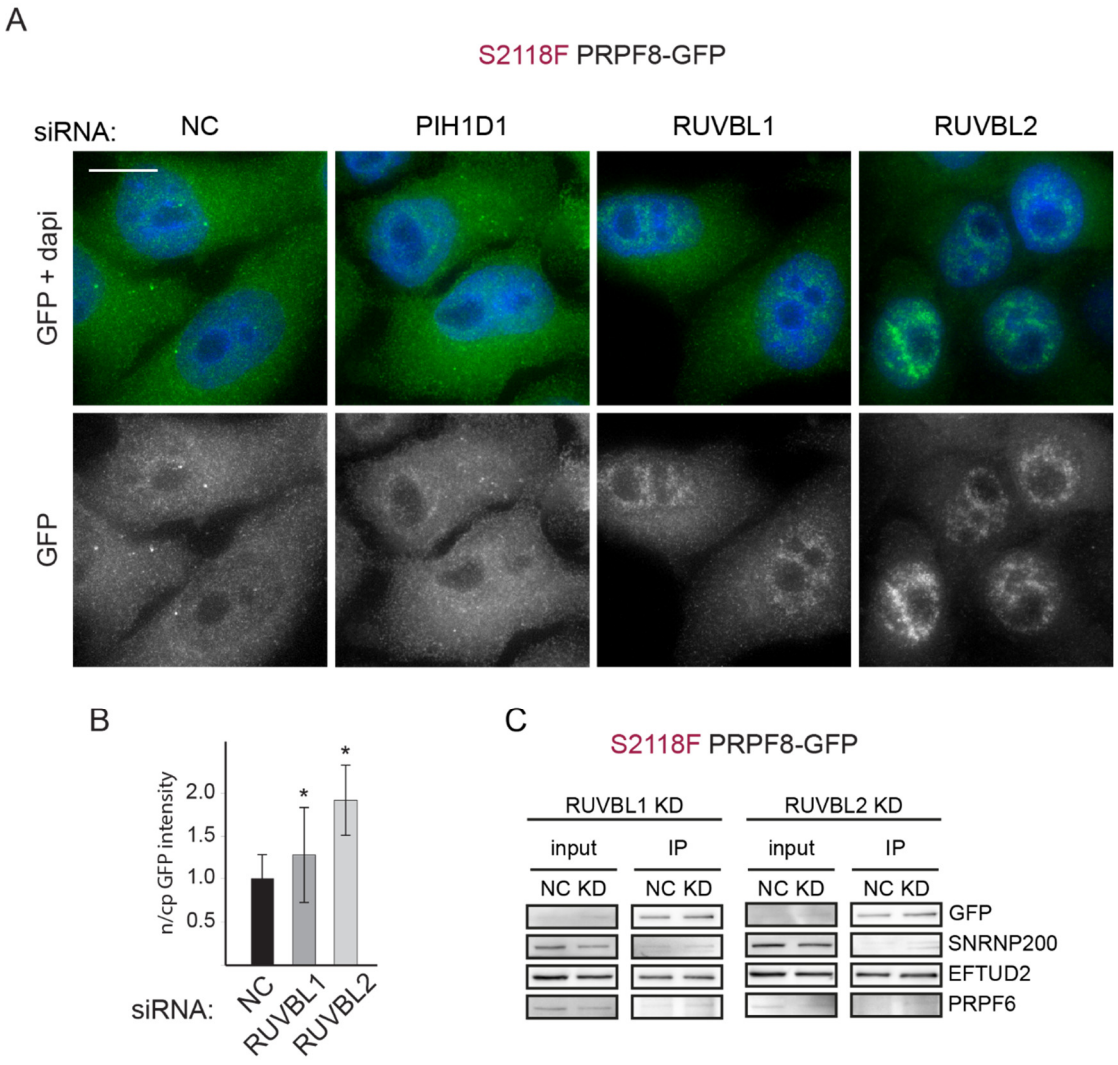

Fig. 27: S2118F PRPF8-LAP relocalizes to the nucleus after RUVBL KD

(A) HeLa cells expressing S2118F PRPF8-GFP were treated with siRNA against R2TP proteins ((PIH1D1, RUVBL1 and RUVBL2) or a negative control siRNA (siNC). GFP (green); DAPI (blue); scale bar - 10 µm.

(B) The ratio of nuclear and cytoplasmic GFP signal intensity was quantified using ImageJ software. The average of 100-150 cells together with the standard error of the mean is shown. The significance was assayed by t-test against the GFP signal ratio in cells treated with NC; * indicates $p \leq 0.05$.

DISCUSSION

1 RP-associated PRPF8 mutations disrupt splicing

RP is a hereditary eye disorder causing gradual damage of retinal cells and consequently severe vision impairments. RP is a monogenic disease and it has been associated with more than 80 genes, including those that encode pre-mRNA splicing factors. Here, we studied eight RP-associated missense mutations in the spliceosomal U5 snRNP-specific protein, PRPF8. We stably expressed LAP-tagged PRPF8 mutant variants in human cells and showed that none of the mutations is able to rescue the splicing defects caused by depletion of the endogenous protein (Fig. 14) and that all of them impair nuclear translocation of PRPF8-LAP (Fig. 11). That can be for most mutants explained by defects in spliceosome formation (Fig. 15). An overview that summarizes observed effects of the studied RP PRPF8 mutations on various aspects of PRPF8 and cellular functions is shown in Table 1.

Mozaffari-Jovin *et al.* (2013) studied RP mutations in yeast and divided Jab1 residues affected by RP into three groups. Residues within the globular region of Jab1 domain (group I - residues up to 2309) effect mainly the fold stability of the protein. Group II residues in the proximal part of the C-terminal tail of Jab1 domain (residues 2310 – 2314) influence interaction with SNRNP200. Group III residues at the distal part of the C-terminal tail of Jab1 domain (residues 2315 – 2336) regulate SNRNP200 activity. In line with that, the three mutations that lie within the globular region (S2118F, H2309P and H2309R) decrease the stability of PRPF8 the most (Fig. 12B). However, the stability of PRPF8 is affected in the majority of the tested RP-variants, so the situation appears to be more complex. We believe that the instability also reflects reduced incorporation of mutated PRPF8-LAP variants into spliceosome, because integration of proteins into bigger complexes is a general way to stabilize proteins. Indeed, PRPF8 mutations that belong to both groups I and II significantly decrease the ability of PRPF8 to interact with SNRNP200 and PRPF6 proteins and to get incorporated into the tri-snRNP (Fig. 15). Y2334N, the sole group III mutation, is the only tested RP mutation that does not affect the formation of mature snRNPs (Fig. 15).

The group I mutations exhibit the strongest assembly defects as well as more pronounced effects on splicing efficiency, faster degradation rate of the protein and increased cytoplasmic localization compared to other tested mutants. These consistent results imply that the lower protein stability even enhances the problems caused by misfolding of the Jab1 domain and/or by disruption of the protein interaction platform. The mutation S2118F manifests the strongest phenotype of all tested mutations which might be connected to the fact that it is the only mutation located further apart from the others, which are mainly on the border of the globular part of the Jab1 domain and its C-terminal tail (see scheme in Fig. 10B). Also the scarce clinical data that are available correlate with our observation and patients carrying group I mutations, H2309P or H2309R, have a more severe phenotype, reflected by earlier onset, progress and outcome of the disease, than patients carrying a group II mutation, R2310K (Towns *et al.*, 2010).

The F2314L mutation lies on the border of group II and group III mutations and its effect on the spliceosome assembly is therefore milder. It loosens the association with SNRNP200, the U5-specific RNA helicase, but it does not disrupt the PRPF8 interaction with PRPF6, core U5 snRNP and tri-snRNP (Fig. 15). Nevertheless, the mutation has a very similar global effect on splicing as other PRPF8 mutations (Fig. 14), which we explain by the fact that SNRNP200 helicase is essential for splicing activation.

The group III Y2334 residue is found at the very end of the C-terminal tail which can be inserted into the SNRNP200's RNA-binding tunnel and so it blocks the unwinding activity of the helicase. Yeast yPrp8 with equivalent mutation enhanced yBrr2's RNA affinity and repressed yBrr2 activity less eficiently compared to WT (Mozaffari-Jovin *et al.*, 2013). Consistently, our data indicate that Y2334N mutation does not prevent formation of snRNPs (Fig. 15) but it has a gene-specific effect on splicing efficiency (Fig. 14). Therefore, we speculate that similarly to yeast, the Y2334N mutation may affect proper regulation of SNRNP200 during spliceosome activation which might be critical for proper splicing outcomes. The observed gene-specific splicing defects might then be a consequence of different susceptibility of individual genes.

When we compare our data with available data of RP-associated PRPF8 mutations, the situation becomes less clear. The snRNP maturation defects and reduced SNRNP200/yBrr2 binding are unifying elements of various studies, however some details

differ. Pena *et al.* (2007) did not observed by yeast two-hybrid assay any effect of mutations H2309P/R on U5 snRNP formation but saw reduction of EFTUD2 and SNRNP200 interactions in case of mutations R2310K/R and F2314L. In contrast, the mutations H2309P/R have the biggest effects in our hands and the PRPF8/EFTUD2 association seems unaffected for all tested RP-mutants. Similarly, Tanackovic *et al.* (2011b) claimed that PRPF8 with R2310G and Y2334N mutations are normally incorporated into U5 snRNP and tri-snRNP but the association with other U5 proteins to spliceosome is reduced. We do not observe any problems with snRNPs formation in case of Y2334N mutation and according to our results, the R2310G mutant stays associated with EFTUD2 and does not join the spliceosome. So far, we do not know what lies behind the observed discrepancies. Nevertheless, our data are consistent with other studies done in yeast where most mutations reduce association with yBrr2 (except for Y2334N), do not disrupt the ySnu114 binding, and lower tri-snRNP levels (except for Y2334N and F2314L) (Boon *et al.*, 2007; Maeder *et al.*, 2009; Mozaffari-Jovin *et al.*, 2013).

Effect:	WT	S2118F	P2301T	H2309P	H2309R	R2310K	R2310G	F2314L	Y2334N
splicing efficiency	no	++	++	++	++	++	++	++	+
U5 snRNP assembly	no	+++	++	+++	+++	++	++	+	no
tri-snRNP assembly	no	+++	++	+++	+++	++	++	no	no
nuclear localization	no	++	+	+	+	+	+	+	+
stability	no	++	+	++	++	+	+	no	+

Table 1: The effects of RP-mutations
The table summarizes the observed effects of the studied RP PRPF8 mutations on various aspects of PRPF8 and cellular functions. The strength of the effects was assigned approximately based on our results and ranges from none (no), mild (+), medium (++) to strong (+++).

Why the genes coding ubiquitously expressed pre-mRNA splicing factors represent a common target of RP mutations still remains elusive. RP-associated mutations in 8 genes related to splicing have been identified so far, 6 genes encode tri-snRNP specific proteins and 2 non-snRNP spliceosomal components (summarized in Introduction, chapter 7.4.1). Mutations in snRNP genes are often associated with reduced assembly

of snRNP particles (Gonzalez-Santos *et al.*, 2008; Huranová *et al.*, 2009; Linder *et al.*, 2014; Tanackovic *et al.*, 2011b) and we observe a similar phenotype for most herein studied RP mutations in *PRPF8* gene. Thus the most plausible conclusion is that RP mutations reduce concentration of the splicing competent tri-snRNP via PRPF8 destabilization and/or disruption of PRPF8's interactions, which fits to the loss-of-function and haploinsufficiency model of RP. That is further supported by the fact that the cell lines expressing exogenous PRPF8-LAP RP variants do not display any noticeable cell proliferation defects (personal observation, data not shown) and so a dominant negative effect of these mutations is not likely. On the other hand, it might be surprising why despite deficiency of a crucial spliceosomal component, the symptoms are restricted to retina and the progress of the disease is rather slow. This can be partially answered by our experiments after knock down of the endogenous PRPF8. The KD efficiency is never 100% and there is always some endogenous protein left, so the situation roughly resembles the natural conditions where only one healthy allele of PRPF8 is present. The KD results in increased incorporation of the otherwise assembly-defective PRPF8 mutants into snRNPs (Fig. 16). It seems that the endogenous PRPF8 is able to outcompete the mutants but when its concentration is reduced, the RP mutants might get integrated into the U5 snRNP as well, although with lower efficiency. This would explain the relatively slow manifestation of the disease as the effect of the mutations is not as strict as anticipated. However, the mutants still have problems to rescue the efficiency of splicing after the depletion of the endogenous PRPF8 (Fig. 14). We therefore speculate that either small changes in the efficiency of incorporation into spliceosom are enough to cause problems with splicing, or the snRNPs assemble but due to the RP mutations are not fully functional.

However, some RP mutations in snRNP-specific proteins do not interfere with spliceosome assembly. This is the case of Y2334N mutation from our study and of two mutations in *SNRNP200* gene which were shown to affect the selection of 5' ss and reduce SNRNP200 unwinding activity (Zhao *et al.*, 2009; Cvačková *et al.*, 2014). This therefore suggests that the common mechanism of RP mutations in spliceosomal proteins is not the inhibition of a putative retina-specific function of the tri-snRNP but rather the defects in pre-mRNA splicing efficiency and fidelity. As our results suggest, these defects are rather general (Fig. 14) and retina cells might be specifically sensitive

to it due to their high demand for splicing. Alternatively, RP mutations in splicing factors could preferentially affect splicing of some retina-specific transcripts which are crucial for the function of the eye. In any case, enhancing the expression of healthy PRPF8 might help to prevent or slow down retina degeneration.

2 U5 snRNP step-wise assembly

RP mutations compromise U5 snRNP assembly but little is known about how the U5 snRNP biogenesis actually works in human cells. In yeasts, yPrp8 first interacts with yAar2 forming an assembly intermediate which contains the core U5 snRNP, yAar2, yPrp8 and Snu114 (EFTUD2 in human). According to the model proposed, the intermediate is formed in the cytoplasm and remaining U5 snRNP-specific proteins join the complex in the nucleus. The nuclear import of the whole intermediate is dependent on the NLS of yPrp8 (Boon *et al.*, 2007; Gottschalk *et al.*, 2001). Here, we have identified a human assembly intermediate containing PRPF8, EFTUD2 and AAR2 (Figs. 15 and 19). The RP mutations increase both the cytoplasmic localization of PRPF8 and its interactions with EFTUD2 and AAR2, and we therefore assume that similarly to yeast, the formation of this complex takes place in the cytoplasm. The NLS of PRPF8 should not be affected by RP mutations and the proteins are able to get to the nucleus. The increased cytoplasmic localization of PRPF8 mutants can be probably attributed to a retention by a quality control mechanism, as will be discussed later.

In contrast to yeast however, the PRPF8/EFTUD2/AAR2 complex does not interact with the core U5 snRNP. This conclusion is based mainly on the fact that the core U5 snRNPs are accumulated in nuclear Cajal bodies after PRPF8 depletion (Fig. 18) and thus are apparently able to translocate to the nucleus independently of PRPF8 and its NLS. This discrepancy suggests a differences between the nuclear transport system of core snRNPs in HeLa cells and in yeast. One such difference might be given by snurportin1, which is the TGM-cap binding adaptor for snRNP nuclear transport in vertebrates (see also Introduction, chapter 4.2). No orthologue of snurportin1 is known for *S. cerevisiae* (http://www.genecards.org) and that might be the reason why core snRNPs in yeast require PRPF8 for the translocation.

Where SNRNP200 joins the U5 snRNP remains unclear. The crystal structure of yeast yPrp8/yAar2 complex revealed that the binding of yAar2 to yPrp8 sterically interferes with binding of yBrr2 (SNRNP200 in human). The exchange of yAar2 for yBrr2 occurs in the nucleus after yAar2 phosphorylation (see also Introduction, chapter 5.1). Interestingly, in our recent article Malinová *et al.* (2017) our collaborators performed SILAC experiments followed by GFP-AAR2 IP and co-purified a lot of PRPF8, EFTUD2 and SNRNP200, considerable number of SNRNP40, but only negligible amounts of Sm proteins and PRPF6. That implies existence of an intermediate complex with both SNRNP200 and AAR2 bound to PRPF8 before the exchange occurs. Although the interactions should be mutually exclusive, yAar2 and yBrr2 do not bind the same surface of yPrp8 and it is the tightly packed conformation that blocks the binding. It is thereby possible that the human AAR2 slightly differs from the yeast protein or that the conformation of PRPF8 in the assembly intermediate is different from that observed in *in vitro* experiments, and it actually allows the binding. An alternative explanation could be that AAR2 may play an unanticipated role in SNRNP200 maturation independent of its role in PRPF8 biogenesis. The GFP-AAR2 SILAC experiment also gave as a hint at the order in which the proteins join the U5 particle. It seems that SNRNP200 and SNRNP40 bind PRPF8 first, and the final assembly with PRPF6 and the core snRNP takes place later.

When PRPF8, the central hub of U5 particle, is depleted, U5 snRNA without the main U5-specific proteins, as well as U4 and U6 snRNAs, are accumulated in Cajal bodies (Fig. 17 and 18)). Accumulation of U4 and U6 snRNAs in CBs was already reported by Schaffert *et al.* (2004), when the formation of tri-snRNP was inhibited by knockdown of the U5 and di-snRNP bridging proteins, PRPF6 and PRPF31. This strongly supports the hypothesis that final snRNP assembly steps take place in CBs (see also Introduction, chapter 4.5), at least loading of U5-specific proteins onto U5 snRNA and the tri-snRNP formation. Finally, CBs also seem to work as a final checkpoint and they retain the incomplete snRNPs until all the specific proteins are loaded and form the tri-snRNP. This might be a mechanism to prevent immature snRNPs escape to the nucleoplasm and interfere with the splicing reaction.

Taken together, we propose a model where several U5-specific proteins form an assembly intermediate and in contrast to yeast, they join the core U5 snRNP later on (Fig. 28). The assembly intermediate formation starts with PRPF8/EFTUD2/AAR2

complex in the cytoplasm. Subsequently, SNRNP200 and SNRNP40 associate to the complex which probably triggers conformational changes and leads to AAR2 release. In the end, the complex binds the core U5 snRNP in CBs. It is still not known in which step the remaining U5 proteins join the particle. It is likely that PRPF6 associate to the U5 snRNP also in CBs because it is essential for the tri-snRNP formation which ocures in these structures.

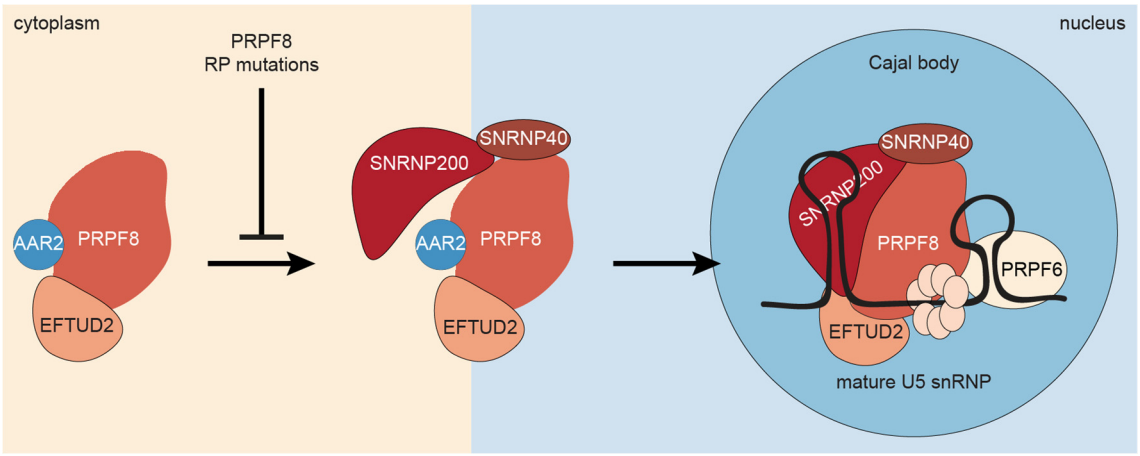

Fig. 28: Model of U5 snRNP biogenesis in human
According to the proposed model, the complex PRPF8/EFTUD2/AAR2 is formed in the cytoplasm first. SNRNP200 and SNRNP40 associate to the complex later, AAR2 is released and maturation of U5 snRNP is finished in Cajal bodies. Most studied RP mutations block the biogenesis in the first stage.

3 Factores involved in U5 snRNP assembly

Ribonucleoprotein particles, such as U5 snRNP, are huge complexes that undergo an intricate maturation. Therefore, assembly factors are often required to assist with folding of individual components and during assembly and remodeling of intermediate complexes. The HSP90/R2TP complex have been suggested to assist during the assembly of several multi-component particles (see Introduction, chapter 5.2). Our data strongly indicate that the HSP90/R2TP machinery functions during U5 snRNP biogenesis.

Heat shock protein 90 (HSP90) is an essential eukaryotic chaperon which instead of helping with maturation of nascent proteins, rather facilitates last steps of client proteins folding. These qualities make it convenient for controlling formation of large proteins which do not fold properly (see Introduction, chapter 5.2.1). Herein, we provide evidence that inhibition of HSP90 leads to decreased levels of U5 snRNP specific

proteins, namely PRPF8 and SNRNP200 (Fig. 23). The molecular weight of both proteins is over 200 kDa and they belong to the biggest proteins in the spliceosome, which makes them ideal targets of the HSP90 chaperon. Furthermore, Whitesell *et al.* (1994) reported that the inhibition of HSP90 activity usually results in client protein degradation. Our data thus strongly indicate that both PRPF8 and SNRNP200 are HSP90's clients.

HSP90 controls folding of proteins from several RNP complexes that are known to be connected with the R2TP complex (Boulon *et al.*, 2008; Boulon *et al.*, 2010). The fact that we identified R2TP complex components as novel PRPF8 interactors (Fig. 22, 24 and 26) is therefore consistent with the role of HSP90 in U5 snRNP maturation. The R2TP complex is a HSP90's co-chaperon and so its main role is to recruit specific client proteins and modulate HSP90 function. One of the possible connections of the R2TP complex with U5 snRNP might be mediated by the interaction of PIH1D1 with EFTUD2. Hořejší *et al.* (2014) proposed that R2TP complex substrates are recognized by PIH1D1 N-terminal domain through phosphorylation of a specific motif and their *in vitro* experiments showed that one such PIH1D1's substrate is EFTUD2. Nonetheless, in our recent work the N-terminus of PIH1D1 did not co-purified EFTUD2 or other U5 proteins in *in vivo* co-IP experiments (Malinová *et al.*, 2017). Besides, the interaction between PRPF8 and R2TP did not decrease after PIH1D1 depletion (Fig. 24A and B). Yet, the phosphorylation motif of EFTUD2 plays an important role during U5 snRNP biogenesis because mutation of the critical serine dramatically altered EFTUD2 interactions with U5 components (Malinová *et al.*, 2017). It seems that phosphorylation of EFTUD2 is important but not sufficient for interaction with PIH1D1 N-terminus. The interaction might be too weak to be detected *in vivo* and additional interactions and/or factors may be necessary to secure the U5-R2TP binding.

It is worth noticing that a situation similar to PIH1D1-EFTUD2 binding was described for ECD (ecdysoneless), a protein important for cell cycle progression. ECD was shown to interact *in vitro* with PIH1D1 in a phosphor-dependent manner (Hořejší *et al.*, 2014) and phosphorylation-deficient ECD mutants caused problems of the cell cycle, yet *in vivo* the ECD mutants remained bound to the R2TP complex ECD. Subsequently, an additional phosphorylation-independent interaction of ECD with the RUVBL1 was identified (Mir *et al.*, 2015). Remarkably, the orthologues of ECD and PRPF8 directly interact in *D. melanogaster* and ECD deficiency influences splicing outcome in flies

(Claudius *et al.*, 2014). In line with these findings, we identified ECD as a PRPF8 interactor in our SILAC co-IP experiments (Fig. 22) and propose that it might be the factor bridging R2TP complex with U5 snRNP particles. Since ECD was also shown to directly bind AAR2 orthologue in flies (Claudius *et al.*, 2014), it is tempting to speculate that it is involved in conformational re-arrangements during AAR2 dissociation.

ZNHIT2 is another factor identified in our proteomic analysis (Fig. 22) that has a potential to create a bridge between R2TP complex and U5 snRNP. The ZNHIT2 protein belongs to the Zinc-Finger HIT protein family that contains six members, ZNHIT1-6. ZNHIT1 and 4 are part of chromatin remodeling complexes INO90 and SCRAP; ZNHIT 3 and 6 function in snoRNP biogenesis (reviewed in Verheggen *et al.*, 2015). Recently, ZNHIT3 was also shown to be involved in U4 snRNP maturation (Bizarro *et al.*, 2014). In all these cases, RUVBL1 and 2 are key partners of ZNHIT proteins. Functions of ZNHIT2 and 5 has not been described so far, but our data strongly suggest a role of ZNHIT2 in the biogenesis of U5 snRNP. A yeast two hybrid assay performed by our French collaborators confirmed interaction of ZNHIT2 with both EFTUD2 and RUVBL1 (Malinová *et al.*, 2017), which supports the hypothesis about ZNHIT2 as additional factor interconnecting U5 and R2TP complex. From the perspective of this thesis it is interesting to note that the interaction with yeast ZNHIT3-homolog (yHit1) is disrupted by mutation in yPrp31 (from U4 snRNP), which in human PRPF31 causes retinitis pigmentosa (Bizarro *et al.*, 2015). Herein studied RP-mutations that compromise U5 snRNP assembly however increase the amount of ZNHIT2 pulled down by PRPF8 (Fig. 26C and E). Disrupted ZNHIT2 binding is thus not the mechanism behind studied PRPF8 mutations and ZNHIT2 is rather stalled with the unassembled protein-only U5 particles.

Remarkably, these mutated PRPF8 proteins also co-immunoprecipitate more HSP90/R2TP complex components (Fig. 26A, B and D). A similar observation was done previously in Boulon *et al.* (2010), where they noticed an increased interaction of R2TP complex protein, RPAP3, with a RNA polymerase II subunit, RPB1, when RNA polymerase II assembly was disrupted. These findings imply that similarly to ZNHIT2, the R2TP complex preferentially binds unassembled client complexes.

The preferential binding of unassembled U5 intermediates by the R2TP complex supports its potential role in U5 snRNP biogenesis. However, the knockdown of R2TP components (namely PIH1D1, RUVBL1 and RUVBL2) did not inhibit U5 maturation and

PIH1D1 knockdown even increased PRPF8-LAP interaction with the remaining R2TP complex components and U5 proteins (Fig. 24A-D). Likewise, in yeast strains devoid of PIH1D1 orthologue, both RUVBL1 and 2 orthologues were enriched with complexes they are helping to assemble (Zhao *et al.*, 2005; Lakshminarasimhan *et al.*, 2016). From the available data, PIH1D1 should hold together the R2TP complex as it interconnects both RPAP3 and the ring of RUVBL1/2 proteins, and it should recruit specific substrates (Pal *et al.*, 2014). However, our data suggest that RPAP3 stays with the RUVBL1/2 proteins even in the absence PIH1D1 (Fig. 24A and B). Moreover, the interaction between PIH1D1 and the R2TP substrate EFTUD2 is rather weak and EFTUD2 can interact also with other R2TP complex components, as discussed earlier in this chapter. We also know that PRPF6 should join the U5 snRNP after AAR2 leaves (see Discussion, chapter 2), but both AAR2 and PRPF6 are enriched in PRPF8 pull down after PIH1D1 depletion. That implies that it is not a mature U5 snRNP that is formed upon PIH1D1 KD. We conclude that the interaction network between R2TP complex components and its substrates is more complex than anticipated, and we suggest that the main role of PIH1D1 might be in regulation of RUVBL ATPases activity and/or modulation of the substrates rearrangements.

From the IP experiments it seems that the impact of RUVBL2 and partially also RUVBL1 knockdowns is milder but similar to that of PIH1D1. As an exception, after RUVBL1 knockdown the interactions of PRPF8 with AAR2 and U5-specific proteins went slightly down. The effect is not significant but could indicate that RUVBL1 is important for the assembly, possibly also due to the previously discussed interaction EFTUD2-ZNHIT2-RUVBL1. Nevertheless, when we look on the RUVBL1 and 2 knockdowns under a microscope, we see more striking effect. Firstly, we observed an accumulation of the U5 snRNA in CBs after RUVBL1/2 depletion. That indicates problems with U5 snRNP assembly, however the IP experiments do not show much effect on PRPF8's interactions (Fig. 24E-H). We speculate that RUVBL1 and 2 might be important for proper loading of the protein complexes onto the core U5 snRNP. Alternatively, the U5 specific proteins might be bound to the core snRNP but the assembly factors remain bound as well and block the release of the particle from CBs. Eitherway, we can conclude that RUVBL proteins are required for proper maturation of U5 snRNPs particles. The second microscopic observation comes from the RP cell lines. Under normal conditions, the

assembly-defective RP PRPF8 mutants are more in the cytoplasm compared to WT, with S2118F mutant exhibiting the most pronounced cytoplasmic localization (Fig. 11). Upon RUVBL1 and 2 depletions, we observed strong nuclear localization even in case of S2118F PRPF8 (Fig. 27A and B), which suggest that the RUVBL1/2 proteins participate in the cytoplasmic retention of defective PRPF8 complexes. We therefore propose a model in which R2TP complex associates with the U5 snRNP assembly intermediates in the cytoplasm and allows only the properly folded complexes to enter the nucleus. According to this model, an important role of R2TP complex is thus to provide a quality control of U5 snRNP assembly.

SUMMARY

In this PhD thesis, I'm taking a close look on the assembly process of human U5 snRNP particles and I'm paying special attention to the protein PRPF8, U5-specific protein which occupies a central position in the catalytic core of the spliceosome. Multiple biochemical and microscopic approaches were used to address the main questions.

We started by analysis of the retinitis pigmentosa-associated PRPF8 mutations in human cells. Similarly to RP mutations in other splicing factors, the splicing defects caused by most herein studied RP mutations in *PRPF8* gene can be explained by disrupted assembly of snRNP particles. However, this is not a general principle as the Y2334N mutation do not interfere with the spliceosome assembly while affecting splicing probably through misregulation of SNRNP200 activity. We therefore propose that defects in splicing efficiency and fidelity are the mechanism underlying RP phenotype.

The RP-associated PRPF8 mutants are stalled together with EFTUD2 and AAR2 in the cytoplasm and we believe that formation of the PRPF8/EFTUD2/AAR2 complex is the first step of the U5 snRNP assembly pathway. Subsequently, SNRNP200 and SNRNP40 associate to the complex which probably triggers conformational changes and leads to AAR2 release. It is not clear in which moment the remaining U5 proteins join the particle. At the end, the complex binds the core U5 snRNP in Cajal bodies. CBs likely work as a final checkpoint of the biogenesis since we observed accumulation of snRNPs when U5 snRNP formation was halted by PRPF8 knock down. It seems that CBs retain the incomplete snRNPs until all the specific proteins are loaded and tri-snRNP is formed, which might be a mechanism to prevent immature snRNPs escape and interfere with splicing.

Finally, we identified several factors involved in the assembly of human U5 snRNP. Apart from AAR2, which is already known from yeast, we showed that the HSP90/R2TP machinery plays an important role during U5 snRNP biogenesis. According to our data, HSP90 and the R2TP complex promote and control folding of U5 snRNP-specific proteins, help to form intermediate complexes by bridging their protein components (PRPF8, EFTUD2, AAR2 and SNRNP200) and facilitate the AAR2-SNRNP200 exchange on PRPF8.

Finally, our experiments suggest that the R2TP complex is involved in quality control, interacts with misassembled proteins, surveillances biogenesis of U5-specific proteins and inhibits nuclear translocation of improperly assembled complexes and/or proteins. Furthermore, the SILAC co-IP experiments revealed a plenty of other proteins interacting with PRPF8 that are not part of the mature U5 particle. We propose that ECD and ZNHIT2 serve as bridging factors between the R2TP complex and U5 proteins. The role of the other potential factors remains to be elucidated.

REFERENCES

Agafonov, D. E., Kastner, B., Dybkov, O., Hofele, R. V, Liu, W., Urlaub, H. (2016). Molecular architecture of the human U4/U6.U5 tri-snRNP. Science, 2085, 1–11.

Achsel, T., Ahrens, K., Brahms, H., Teigelkamp, S., Lührmann, R. (1998). The human U5-220kD protein (hPrp8) forms a stable RNA-free complex with several U5-specific proteins, including an RNA unwindase, a homologue of ribosomal elongation factor EF-2, and a novel WD-40 protein. Molecular and Cellular Biology, 18(11), 6756–6766.

Achsel, T., Brahms, H., Kastner, B., Bachi, A., Wilm, M., Lührmann, R. (1999). A doughnut-shaped heteromer of human Sm-like proteins binds to the 3'-end of U6 snRNA, thereby facilitating U4/U6 duplex formation *in vitro*. EMBO Journal, 18(20), 5789–5802.

Ajmal, M., Khan, M. I., Neveling, K., Khan, Y. M., Azam, M., Waheed, N. K., … Cremers, F. P. M. (2014). A missense mutation in the splicing factor gene DHX38 is associated with early-onset retinitis pigmentosa with macular coloboma. Journal of Medical Genetics, 1–5.

Andrade, L. E., Chan, E. K., Raska, I., Peebles, C. L., Roos, G., Tan, E. M. (1991). Human autoantibody to a novel protein of the nuclear coiled body: immunological characterization and cDNA cloning of p80-coilin. The Journal of Experimental Medicine, 173(6), 1407–19.

Andrade, L. E., Tan, E. M., Chan, E. K. (1993). Immunocytochemical analysis of the coiled body in the cell cycle and during cell proliferation. Proc. Natl. Acad. Sci. USA, 90(5), 1947–51.

Audo, I., Bujakowska, K. M., Léveillard, T., Mohand-Saïd, S., Lancelot, M.-E., Germain, A., … Zeitz, C. (2012). Development and application of a next-generation-sequencing (NGS) approach to detect known and novel gene defects underlying retinal diseases. Orphanet J. Rare Dis., 7, 8.

Audo, I., Bujakowska, K., Mohand-Saïd, S., Lancelot, M.-E., Moskova-Doumanova, V., Waseem, N. H., … Zeitz, C. (2010). Prevalence and novelty of PRPF31 mutations in French autosomal dominant rod-cone dystrophy patients and a review of published reports. BMC Medical Genetics, 11, 145.

Bach, M., Winkelmann, G., Lührmann, R. (1989). 20S small nuclear ribonucleoprotein U5 shows a surprisingly complex protein composition. Proc. Natl. Acad. Sci. USA, 86(16), 6038–42.

Baillat, D., Hakimi, M. A., Näär, A. M., Shilatifard, A., Cooch, N., Shiekhattar, R. (2005). Integrator, a multiprotein mediator of small nuclear RNA processing, associates with the C-terminal repeat of RNA polymerase II. Cell, 123(2), 265–276.

Bäumer, D., Lee, S., Nicholson, G., Davies, J. L., Parkinson, N. J., Murray, L. M., … Talbot, K. (2009). Alternative splicing events are a late feature of pathology in a mouse model of spinal muscular atrophy. PLoS Genetics, 5(12), e100077.

Benaglio, P., San Jose, P. F., Avila-Fernandez, A., Ascari, G., Harper, S., Manes, G., … Rivolta, C. (2014). Mutational screening of splicing factor genes in cases with autosomal dominant retinitis pigmentosa. Molecular Vision, 20, 843–51.

Bentley, D. L. (2014). Coupling mRNA processing with transcription in time and space. Nature Reviews. Genetics, 15, 163–175.

Bernier, F. P., Caluseriu, O., Ng, S., Schwartzentruber, J., Buckingham, K. J., Innes, A. M., … Parboosingh, J. S. (2012). Haploinsufficiency of SF3B4, a component of the pre-mRNA spliceosomal complex, causes nager syndrome. American Journal of Human Genetics, 90(5), 925–933.

Berson, E. L., Rosner, B., Sandberg, M. A., Hayes, K. C., Nicholson, B. W., Weigel-DiFranco, C., Willett, W. (1993). A randomized trial of vitamin a and vitamin e supplementation for retinitis pigmentosa. Arch. Ophthalmol., 111(6), 761–772.

Berson, E. L., Rosner, B., Sandberg, M. A., Weigel-DiFranco, C., Brockhurst, R. J., Al., E. (2010). Clinical Trial of Lutein in Patients with Retinitis Pigmentosa Receiving Vitamin A. Arch. Ophthalmol., 122(9), 1306-1314.

Berson, E. L., Rosner, B., Sandberg, M. A., Weigel-DiFranco, C., Moser, A., Brockhurst, R. J., … Schaefer, E. J. (2004). Clinical trial of docosahexaenoic acid in patients with retinitis pigmentosa receiving vitamin A treatment. Arch. Ophthalmo., 122(9), 1297–1305.

Bertram, K., Agafonov, D. E., Liu, W.-T., Dybkov, O., Will, C. L., Hartmuth, K., … Lu Hrmann, R. (2017). Cryo-EM structure of a human spliceosome activated for step 2 of splicing. Nature, 542, 1–22.

Bier, K., Kunz, W., Ribbert, D. (1967). Struktur und Funktion der Oocytenchromosomen und Nukleolen sowie der Extra-DNS während der Oogenese panoistischer und meroistischer Insekten. Chromosoma, 23(2), 214–254.

Bizarro, J., Dodré, M., Huttin, A., Charpentier, B., Schlotter, F., Branlant, C., … Bertrand, E. (2015). NUFIP and the HSP90/R2TP chaperone bind the SMN complex and facilitate assembly of U4-specific proteins. Nucleic Acids Research, 43(18), 8973–89.

Bizarro, J., Charron, C., Boulon, S., Westman, B., Pradet-Balade, B., Vandermoere, F., … Bertrand, E. (2014). Proteomic and 3D structure analyses highlight the C/D box snoRNP assembly mechanism and its control. Journal of Cell Biology, 207(4), 463–480.

Boon, K.L., Grainger, R. J., Ehsani, P., Barrass, J. D., Auchynnikava, T., Inglehearn, C. F., Beggs, J. D. (2007). prp8 mutations that cause human retinitis pigmentosa lead to a U5 snRNP maturation defect in yeast. Nature Structural & Molecular Biology, 14(11), 1077–1083.

Boulon, S., Bertrand, E., Pradet-Balade, B. (2012). HSP90 and the R2TP co-chaperone complex: Building multi-protein machineries essential for cell growth and gene expression. RNA Biology, 9, 148–155.

Boulon, S., Marmier-Gourrier, N., Pradet-Balade, B., Wurth, L., Verheggen, C., Jády, B. E., … Charpentier, B. (2008). The Hsp90 chaperone controls the biogenesis of L7Ae RNPs through conserved machinery. Journal of Cell Biology, 180(3), 579–595.

Boulon, S., Pradet-Balade, B., Verheggen, C., Molle, D., Boireau, S., Georgieva, M., … Bertrand, E. (2010). HSP90 and its R2TP/Prefoldin-like cochaperone are involved in the cytoplasmic assembly of RNA polymerase II. Molecular Cell, 39(6), 912–924.

Bowne, S. J., Sullivan, L. S., Avery, C. E., Sasser, E. M., Roorda, A., Duncan, J. L., … Daiger, S. P. (2013). Mutations in the small nuclear riboprotein 200 kDa gene (SNRNP200) cause 1.6% of autosomal dominant retinitis pigmentosa. Mol. Vis., 19, 2407–2417.

Brahms, H., Raymackers, J., Union, A., De Keyser, F., Meheus, L., Lührmann, R. (2000). The C-terminal RG dipeptide repeats of the spliceosomal Sm proteins D1 and D3 contain symmetrical dimethylarginines, which form a major B-cell epitope for anti-Sm autoantibodies. Journal of Biological Chemistry, 275(22), 17122–17129.

Brenner, T. J., Guthrie, C. (2006). Assembly of Snu114 into U5 snRNP requires Prp8 and a functional GTPase domain. RNA, 12, 862–87.

Brown, J. D., Beggs, J. D. (1992). Roles of PRP8 protein in the assembly of splicing complexes. The EMBO Journal, 11(10), 3721–3729.

Cajal, S. R. (1903). Un sencillo metodo de coloracion seletiva del reticulo protoplasmatico y sus efectos en los diversos organos nerviosos de vertebrados e invertebrados. Trab. Lab. Invest. Biol. (Madrid), 2, 129–221.

Cioce, M., Lamond, A. I. (2005). Cajal Bodies : A Long History of Discovery. Annu. Rev. Cell Dev. Biol., 21, 105–131.

Claudius, A. K., Romani, P., Lamkemeyer, T., Jindra, M., Uhlirova, M. (2014). Unexpected Role of the Steroid-Deficiency Protein Ecdysoneless in Pre-mRNA Splicing. PLoS Genetics, 10(4), e1004287.

Coady, T. H., Lorson, C. L. (2011). SMN in spinal muscular atrophy and snRNP biogenesis. RNA, 2(4), 546–564.

Collier, S., Pendle, A., Boudonck, K., van Rij, T., Dolan, L., Shaw, P. (2006). A Distant Coilin Homologue Is Required for the Formation of Cajal Bodies in Arabidopsis. MBC, 17, 2942–2951.

Comitato, A., Spampanato, C., Chakarova, C., Sanges, D., Bhattacharya, S. S., Marigo, V. (2007). Mutations in splicing factor PRPF3, causing retinal degeneration, form detrimental aggregates in photoreceptor cells. Human Molecular Genetics, 16(14), 1699–1707.

Cordin, O., Hahn, D., Beggs, J. D. (2012). Structure, function and regulation of spliceosomal RNA helicases. Current Opinion in Cell Biology, 24(3), 431–438.

Cvačková, Z., Matějů, D., Staněk, D. (2014). Retinitis pigmentosa mutations of SNRNP200 enhance cryptic splice-site Recognition. Human Mutation, 35(3), 308–317.

Dahlberg, J. E., Lund, E. (1988). The Genes and Transcription of the Major Small Nuclear RNAs. Structure and Function of Major and Minor Small Nuclear Ribonucleoprotein Particles. Berlin, Heidelberg: Springer, 38-70.

Dahlberg, J., Yang, H., Neuman de Vegvar, H., Lund, E. (1990). Formation of the 3 end of U1 snRNA. Mol. Biol. Rep., 14(2–3), 161–2.

Daiger, S., Sullivan, L., Bowne, S. (2013). Genes and mutations causing retinitis pigmentosa. Clin Genet., 84(2), 132–141.

Darzacq, X., Jady, B. E., Verheggen, C., Kiss, a M., Bertrand, E., Kiss, T. (2002). Cajal body-specific small nuclear RNAs: a novel class of 2 0 -O-methylation and pseudouridylation guide RNAs. Embo J., 21(11), 2746–2756.

Darzacq, X., Kittur, N., Roy, S., Shav-Tal, Y., Singer, R. H., Meier, U. T. (2006). Stepwise RNP assembly at the site of H/ACA RNA transcription in human cells. Journal of Cell Biology, 173(2), 207–218.

David, C. J., Manley, J. L. (2010). Alternative pre-mRNA splicing regulation in cancer: Pathways and programs unhinged. Genes and Development, 24(21), 2343–2364.

De Erkenez, A., Dryja, E., Berson, T. (2002). Novel Mutations in the PRPC8 Gene, Encoding a Pre-mRNA Splicing Factor in Patients with Autosomal Dominant Retinitis Pigmentosa. Invest. Ophthalmol. Visual. Sci., 43(13), 791.

Dix, I., Russell, C. S., O'Keefe, R. T., Newman, a J., Beggs, J. D. (1998). Protein-RNA interactions in the U5 snRNP of *Saccharomyces cerevisiae*. RNA (New York, N.Y.), 4, 1239–1250.

Dundr, M., Hebert, M. D., Karpova, T. S., Stanek, D., Xu, H., Shpargel, K. B., … Misteli, T. (2004). *In vivo* kinetics of Cajal body components. Journal of Cell Biology, 164(6), 831–842.

Edery, P., Marcaillou, C., Sahbatou, M., Labalme, A., Chastang, J., Touraine, R., … Pessa, H. K. (2011). Association of TALS developmental disorder with defect in minor splicing component U4atac snRNA. Science (New York, N.Y.), 332(6026), 240–3.

Egloff, S., O'Reilly, D., Murphy, S. (2008). Expression of human snRNA genes from beginning to end. Biochemical Society Transactions, 36(4), 590–4.

Fabrizio, P., Laggerbauer, B., Lauber, J., Lane, W. S., Lührmann, R. (1997). An evolutionarily conserved U5 snRNP-specific protein is a GTP-binding factor closely related to the ribosomal translocase EF-2. EMBO J., 16(13), 4092–4106.

Fallini, C., Bassell, G. J., Rossoll, W. (2012). Spinal muscular atrophy: The role of SMN in axonal mRNA regulation. Brain Research, 1462, 81–92.

Ferrari, S., DiIorio, E., Barbaro, V., Ponzin, D., Sorrentino, F. S., Parmeggiani, F. (2011). Retinitis pigmentosa: genes and disease mechanisms. Current Genomics, 12(4), 238–49.

Fischer, U., Sumpter, V., Sekine, M., Satoh, T., Lührmann, R. (1993). Nucleo-cytoplasmic transport of U snRNPs: definition of a nuclear location signal in the Sm core domain that binds a transport receptor independently of the m3G cap. Embo J., 12(2), 573–583.

Fornerod, M., Ohno, M., Yoshida, M., Mattaj, I. W. (1997). CRM1 is an export receptor for leucine-rich nuclear export signals. Cell, 90(6), 1051–1060.

Frey, M. R., Matera, A. G. (1995). Coiled bodies contain U7 small nuclear RNA and associate with specific DNA sequences in interphase human cells. Proc. Natl. Acad. Sci. USA, 92(13), 5915–5919.

Frey, M. R., Matera, A. G. (2001). RNA-mediated interaction of Cajal bodies and U2 snRNA genes. Journal of Cell Biology, 154(3), 499–509.

Friesen, W. J., Massenet, S., Paushkin, S., Wyce, A., Dreyfuss, G. (2001). SMN, the product of the spinal muscular atrophy gene, binds preferentially to dimethylarginine-containing protein targets. Molecular Cell, 7(5), 1111–1117.

Gabanella, F., Butchbach, M. E. R., Saieva, L., Carissimi, C., Burghes, A. H. M., Pellizzoni, L. (2007). Ribonucleoprotein assembly defects correlate with spinal muscular atrophy severity and preferentially affect a subset of spliceosomal snRNPs. PLoS ONE, 2(9), 1–12.

Galej, W. P., Oubridge, C., Newman, A. J., Nagai, K. (2013). Crystal structure of Prp8 reveals active site cavity of the spliceosome. Nature, 493(7434), 638–43.

Gall, J. G. (2003). The centennial of the Cajal body. Nature Reviews. Molecular Cell Biology, 4(12), 975–80.

Gall, J. G., Bellini, M., Wu, Z., Murphy, C. (1999). Assembly of the nuclear transcription and processing machinery: Cajal bodies (coiled bodies) and transcriptosomes. Molecular Biology of the Cell, 10(12), 4385–402.

Gamundi, M. J., Hernan, I., Muntanyola, M., Maseras, M., López-Romero, P., Álvarez, R., … Carballo, M. (2008). Transcriptional expression of cis-acting and trans-acting splicing mutations cause autosomal dominant retinitis pigmentosa. Human Mutation, 29(6), 869–878.

Ganot, P., Jady, B. E., Bortolin, M. L., Darzacq, X., Kiss, T. (1999). Nucleolar factors direct the 2'-O-ribose methylation and pseudouridylation of U6 spliceosomal RNA. Molecular and Cellular Biology, 19(10), 6906–6917.

Garcia, E. L., Lu, Z., Meers, M. P., Praveen, K., Matera, A. G. (2013). Developmental arrest of Drosophila survival motor neuron (Smn) mutants accounts for differences in expression of minor intron-containing genes. RNA (New York, N.Y.), 19 (11), 1510–1516.

Gonzalez-Cordero, A., West, E. L., Pearson, R. A., Duran, Y., Carvalho, L. S., Chu, C. J., … Ali, R. R. (2013). Photoreceptor precursors derived from three-dimensional embryonic stem cell cultures integrate and mature within adult degenerate retina. Nat. Biotechnol., 31(8), 741–747.

Gonzalez-Santos, J. M., Cao, H., Duan, R. C., Hu, J. (2008). Mutation in the splicing factor Hprp3p linked to retinitis pigmentosa impairs interactions within the U4/U6 snRNP complex. Human Molecular Genetics, 17(2), 225–239.

Gottschalk, A., Kastner, B., Lührmann, R., Fabrizio, P. (2001). The yeast U5 snRNP coisolated with the U1 snRNP has an unexpected protein composition and includes the splicing factor Aar2p. RNA (New York, N.Y.), 7(11), 1554–1565.

Grainger, R. J., Beggs, J. D. (2005). Prp8 protein: At the heart of the spliceosome. RNA, 11(5), 533–557.

Graziotto, J. J., Farkas, M. H., Bujakowska, K., Deramaudt, B. M., Zhang, Q., Nandrot, E. F., … Pierce, E. A. (2011). Three gene-targeted mouse models of RNA splicing factor RP show late-onset RPE and retinal degeneration. Investigative Ophthalmology and Visual Science, 52(1), 190–198.

Graziotto, J. J., Inglehearn, C. F., Pack, M. A., Pierce, E. A. (2008). Decreased levels of the RNA splicing factor Prpf3 in mice and zebrafish do not cause photoreceptor degeneration. Investigative Ophthalmology and Visual Science, 49(9), 3830–3838.

Hahn, D., Kudla, G., Tollervey, D., Beggs, J. D. (2012). Brr2p-mediated conformational rearrangements in the spliceosome during activation and substrate repositioning. Genes and Development, 26(21), 2408–2421.

Hamel, C. (2006). Retinitis pigmentosa. Orphanet Journal of Rare Diseases, 1, 40.

Hartong, D. T., Berson, E. L., Dryja, T. P. (2006). Retinitis pigmentosa. Lancet, 368(9549), 1795–1809.

He, H., Liyanarachchi, S., Akagi, K., Nagy, R., Li, J., Dietrich, R. C., … Padgett, R. A. (2011). Mutations in U4atac snRNA, a Component of the Minor Spliceosome, in the Developmental Disorder MOPD I. Science, 332(6026), 238–240.

Hebert, M. D., Matera, A. G. (2000). Self-association of coilin reveals a common theme in nuclear body localization. Molecular Biology of the Cell, 11(12), 4159–4171.

Hebert, M. D., Szymczyk, P. W., Shpargel, K. B., Matera, G. A. (2001). Coilin forms the bridge between Cajal bodies and SMN, the spinal muscular atrophy protein. Genes and Development, 15(20), 2720–2729.

Hermann, H., Fabrizio, P., Raker, V. A., Foulaki, K., Hornig, H., Brahms, H., Lührmann, R. (1995). snRNP Sm proteins share two evolutionarily conserved sequence motifs which are involved in Sm protein-protein interactions. The EMBO J., 14(9), 2076–88.

Hoddges, P. E., Jackson, S. P., Brown, J. D., Beggs, J. D. (1995). Extraordinary sequence conservation of the PRP8 splicing factor. Yeast, 11(4), 337–342.

Hogg, R., De Almeida, R. A., Ruckshanthi, J. P. D., O'Keefe, R. T. (2014). Remodeling of U2-U6 snRNA helix i during pre-mRNA splicing by Prp16 and the nineteen complex protein Cwc2. Nucleic Acids Research, 42(12), 8008–8023.

Hořejší, Z., Stach, L., Flower, T. G., Joshi, D., Flynn, H., Skehel, J. M., … Boulton, S. J. (2014). Phosphorylation-Dependent PIH1D1 Interactions Define Substrate Specificity of the R2TP cochaperone complex. Cell Reports, 7(1), 19–26.

Hořejší, Z., Takai, H., Adelman, C. A., Collis, S. J., Flynn, H., Maslen, S., … Boulton, S. J. (2010). CK2 phospho-dependent binding of R2TP complex to TEL2 is essential for mTOR and SMG1 stability. Molecular Cell, 39(6), 839–850.

Huber, J., Cronshagen, U., Kadokura, M., Wada, T., Sekine, M., Lu, R. (1998). Snurportin1, an m 3 G-cap-specific nuclear import receptor with a novel domain structure, 17(14), 4114–4126.

Humayun, M. S., Dorn, J. D., Da Cruz, L., Dagnelie, G., Sahel, J. A., Stanga, P. E., … Greenberg, R. J. (2012). Interim results from the international trial of second sight's visual prosthesis. Ophthalmology, 119(4), 779–788.

Huranová, M., Hnilicová, J., Fleischer, B., Cvačková, Z., Staněk, D. (2009). A mutation linked to retinitis pigmentosa in HPRP31 causes protein instability and impairs its interactions with spliceosomal snRNPs. Human Molecular Genetics, 18(11), 2014–2023.

Chakarova, C. F., Hims, M. M., Bolz, H., Abu-Safieh, L., Patel, R. J., Papaioannou, M. G., … Bhattacharya, S. S. (2002). Mutations in HPRP3, a third member of pre-mRNA splicing factor genes, implicated in autosomal dominant retinitis pigmentosa. Human Molecular Genetics, 11(1), 87–92.

Chandrasekharappa, S., Smith, J., Eliceiri, G. (1983). Biosynthesis of small nuclear RNAs in human cells. J Cell Physiol., 117(2), 169–74.

Chen, X., Liu, Y., Sheng, X., Tam, P. O. S., Zhao, K., Chen, X., … Zhao, C. (2014). PRPF4 mutations cause autosomal dominant retinitis pigmentosa. Human Molecular Genetics, 23(11), 2926–2939.

Izaurralde, E., Lewis, J., Gamberi, C., Jarmolowski, A., McGuigan, C., Mattaj, I. W. (1995). A cap-binding protein complex mediating U snRNA export. Nature, 376, 709–712.

Jakob, U., Lilie, H., Meyer, I., Buchner, J. (1995). Transient interaction of Hsp90 with early unfolding intermediates of citrate synthase: Implications for heat shock *in vivo*. Journal of Biological Chemistry. 270(13), 7288-7294.

Jeronimo, C., Forget, D., Bouchard, A., Li, Q., Chua, G., Poitras, C., … Coulombe, B. (2007). Systematic Analysis of the Protein Interaction Network for the Human Transcription Machinery Reveals the Identity of the 7SK Capping Enzyme. Molecular Cell, 27(2), 262–274.

Kambach, C., Mattaj, I. W. (1994). Nuclear transport of the U2 snRNP-specific U2B'' protein is mediated by both direct and indirect signalling mechanisms. J. Cell Sci., 107 (7), 1807–1816.

Keen, T. J., Hims, M. M., McKie, A. B., Moore, A. T., Doran, R. M., Mackey, D. a, … Inglehearn, C. F. (2002). Mutations in a protein target of the Pim-1 kinase associated with the RP9 form of autosomal dominant retinitis pigmentosa. European Journal of Human Genetics, 10(4), 245–9.

Kitao, S., Segref, A., Kast, J., Wilm, M., Mattaj, I. W., Ohno, M. (2008). A compartmentalized phosphorylation/dephosphorylation system that regulates U snRNA export from the nucleus. Molecular and Cellular Biology, 28(1), 487–497.

Kondo, H., Tahira, T., Mizota, A., Adachi-Usami, E., Oshima, K., Hayashi, K. (2003). Diagnosis of autosomal dominant retinitis pigmentosa by linkage-based exclusion screening with multiple locus-specific microsatellite markers. Investigative Ophthalmology and Visual Science, 44(3), 1275–1281.

Kornblihtt, A. R., Schor, I. E., Alló, M., Dujardin, G., Petrillo, E., Muñoz, M. J. (2013). Alternative splicing: a pivotal step between eukaryotic transcription and translation. Nature Reviews. Molecular Cell Biology, 14(3), 153–65.

Laggerbauer, B., Achsel, T., Lührmann, R. (1998). The human U5-200kD DEXH-box protein unwinds U4/U6 RNA duplices *in vitro*. Proc. Natl. Acad. Sci. USA, 95(8), 4188–92.

Laggerbauer, B., Liu, S., Makarov, E., Vornlocher, H.-P., Makarova, O., Ingelfinger, D., … Lührmann, R. (2005). The human U5 snRNP 52K protein (CD2BP2) interacts with U5-102K (hPrp6), a U4/U6.U5 tri-snRNP bridging protein, but dissociates upon tri-snRNP formation. RNA (New York, N.Y.), 11(5), 598–608.

Lakshminarasimhan, M., Boanca, G., Banks, C. A. S., Hattem, G. L., Gabriel, A. E., Groppe, B. D., … Washburn, M. P. (2016). Proteomic and genomic analyses of the Rvb1 and Rvb2 interaction network upon deletion of R2TP complex components. Molecular & Cellular Proteomics, 15.3, 960-974.

Lander, E. S., *et al.* (2001). Initial sequencing and analysis of the human genome. Nature, 409, 860–921.

Ledoux, S., Guthrie, C. (2016). Retinitis Pigmentosa Mutations in Bad Response to Refrigeration 2 (Brr2) Impair ATPase and Helicase Activity. Journal of Biological Chemistry, 2, 1-24.

Lefebvre, S., Bürglen, L., Reboullet, S., Clermont, O., Burlet, P., Viollet, L., … Melki, J. (1995). Identification and characterization of a spinal muscular atrophy-determining gene. Cell, 80(1), 155–165.

Li, J., Buchner, J. (2013). Structure, Function and Regulation of the Hsp90 Machinery. Biomedical Journal, 36(3), 106–117.

Li, N., Mei, H., MacDonald, I. M., Jiao, X., Fielding Hejtmancik, J. (2010). Mutations in ASCC3L1 on 2q11.2 are associated with autosomal dominant retinitis pigmentosa in a chinese family. Investigative Ophthalmology and Visual Science, 51(2), 1036–1043.

Li, Z. Y., Possin, D. E., Milam, A. H. (1995). Histopathology of bone spicule pigmentation in retinitis pigmentosa. Ophthalmology, 102, 805–816.

Linder, B., Hirmer, A., Gal, A., Rother, K., Bolz, H. J., Winkler, C., … Fischer, U. (2014). Identification of a PRPF4 loss-of-function variant that abrogates U4/U6.U5 Tri-snRNP integration and is associated with retinitis pigmentosa. PLoS ONE, 9(11), 1–8.

Lines, M. A., Huang, L., Schwartzentruber, J., Douglas, S. L., Lynch, D. C., Beaulieu, C., … Boycott, K. M. (2012). Haploinsufficiency of a spliceosomal GTPase encoded by EFTUD2 causes mandibulofacial dysostosis with microcephaly. American Journal of Human Genetics, 90(2), 369–377.

Liu, J. L., Wu, Z., Nizami, Z., Deryusheva, S., Rajendra, T. K., Beumer, K. J., … Gall, J. G. (2009). Coilin Is Essential for Cajal Body Organization in *Drosophila melanogaster*. Molecular Biology of the Cell, 20(5), 1661–1670.

Liu, Q., Dreyfuss, G. (1996). A novel nuclear structure containing the survival of motor neurons protein. The EMBO Journal, 15(14), 3555–65.

Liu, S., Rauhut, R., Vornlocher, H., Lührmann, R. (2006). The network of protein–protein interactions within the human U4/U6. U5 tri-snRNP. RNA, 12, 1418–1430.

Liu, T., Jin, X., Zhang, X., Yuan, H., Cheng, J., Lee, J., … Wang, W. (2012). A Novel Missense SNRNP200 Mutation Associated with Autosomal Dominant Retinitis Pigmentosa in a Chinese Family. PLoS ONE, 7(9), 3–10.

López-Bigas, N., Audit, B., Ouzounis, C., Parra, G., Guigó, R. (2005). Are splicing mutations the most frequent cause of hereditary disease? FEBS Letters, 579(9), 1900–1903.

López-Perrote, A., Muñoz-Hernández, H., Gil, D., Llorca, O. (2012). Conformational transitions regulate the exposure of a DNA-binding domain in the RuvBL1-RuvBL2 complex. Nucleic Acids Research, 40(21), 11086–11099.

Lorson, C. L., Hahnen, E., Androphy, E. J., Wirth, B. (1999). A single nucleotide in the SMN gene regulates splicing and is responsible for spinal muscular atrophy. Proc. Natl. Acad. Sci. USA, 96(11), 6307–11.

Lund, E., Dahlberg, J. E. (1992). Cyclic 2’,3’-phosphates and nontemplated nucleotides at the 3’ end of spliceosomal U6 small nuclear RNA’s. Science, 255(5042), 327–330.

Lynch, D. C., Revil, T., Schwartzentruber, J., Bhoj, E. J., Innes, A. M., Lamont, R. E., … Bernier, F. P. (2014). Disrupted auto-regulation of the spliceosomal gene SNRPB causes cerebro-costo-mandibular syndrome. Nature Communications, 5, 4483.

MacLaren, R. E., Pearson, R. A., MacNeil, A., Douglas, R. H., Salt, T. E., Akimoto, M., … Ali, R. R. (2006). Retinal repair by transplantation of photoreceptor precursors. Nature, 444(7116), 203–7.

MacMillan, A. M., Query, C. C., Allerson, C. R., Chen, S., Verdine, G. L., Sharp, P. A. (1994). Dynamic association of proteins with the pre-mRNA branch region. Genes and Development, 8(24), 3008–3020.

Maeder, C., Kutach, A. K., Guthrie, C. (2009). ATP-dependent unwinding of U4/U6 snRNAs by the Brr2 helicase requires the C terminus of Prp8. Nat. Struct. Mol. Biol., 16(1), 42–48.

Machyna, M., Kehr, S., Straube, K., Kappei, D., Buchholz, F., Butter, F., … Neugebauer, K. M. (2014). The coilin interactome identifies hundreds of small noncoding RNAs that traffic through cajal bodies. Molecular Cell, 56(3), 389–399.

Machyna, M., Neugebauer, K. M., Staněk, D. (2015). Coilin : The first 25 years. RNA biology, 12(6), 590--596.

Maita, H., Kitaura, H., Keen, T. J., Inglehearn, C. F., Ariga, H., Iguchi-Ariga, S. M. M. (2004). PAP-1, the mutated gene underlying the RP9 form of dominant retinitis pigmentosa, is a splicing factor. Experimental Cell Research, 300(2), 283–296.

Makarov, E. M., Makarova, O. V, Achsel, T., Lührmann, R. (2000). The human homologue of the yeast splicing factor Prp6p contains multiple TPR elements and is stably associated with the U5 snRNP via protein-protein interactions. Journal of Molecular Biology, 298(4), 567–75.

Makarov, E. M., Makarova, O. V, Urlaub, H., Gentzel, M., Will, C. L., Wilm, M., Lührmann, R. (2002). Small nuclear ribonucleoprotein remodeling during catalytic activation of the spliceosome. Science (New York, N.Y.), 298(5601), 2205–2208.

Makarova, O. V., Makarov, E. M., Liu, S., Vornlocher, H. P., Lührmann, R. (2002). Protein 61K, encoded by a gene (PRPF31) linked to autosomal dominant retinitis pigmentosa, is required for U4/U6·U5 tri-snRNP formation and pre-mRNA splicing. EMBO J., 21(5), 1148–1157.

Malinová A., Cvačková Z., Matějů D., Hořejší Z., Abéza C., Vandermoere F., Bertrand E., Staněk D., Verheggen C. (2017). Assembly of the U5 snRNP component PRPF8 is controlled by the HSP90/R2TP chaperones. J. Cell Biol., 216(5).

Mao, Y., Zhang, B., Spector, D. (2011). Biogenesis and function of nuclear bodies. Trends in Genetics, 27(8), 295–306.

Markowitz, J. A., Singh, P., Darras, B. T. (2012). Spinal muscular atrophy: A clinical and research update. Pediatric Neurology, 46(1), 1–12.

Martin, C. L., Duvall, J. A., Ilkin, Y., Simon, J. S., Arreaza, M. G., Wilkes, K., … Geschwind, D. H. (2007). Cytogenetic and molecular characterization of A2BP1/FOX1 as a candidate gene for autism. American Journal of Medical Genetics, 144(7), 869–876.

Martinez-Gimeno, M., Jose Gamundi, M., Hernan, I., Maseras, M., Milli, E., Ayuso, C., … Carballo, M. (2003). Mutations in the pre-mRNA splicing-factor genes PRPF3, PRPF8, and PRPF31 in Spanish families with autosomal dominant retinitis pigmentosa. Investigative Ophthalmology and Visual Science, 44(5), 2171–2177.

Matera, A. G., Terns, R. M., & Terns, M. P. (2007). Non-coding RNAs: lessons from the small nuclear and small nucleolar RNAs. Nat. Rev. Mol. Cell Biol., 8(3), 209–220.

Matera, A. G., Wang, Z. (2014). A day in the life of the spliceosome. Nature Reviews. Molecular Cell Biology, 15(2), 108–21.

Mattaj, I. W. (1986). Cap trimethylation of U snRNA is cytoplasmic and dependent on U snRNP protein binding. Cell, 46(6), 905–911.

McKie, A. B., McHale, J. C., Keen, T. J., Tarttelin, E. E., Goliath, R., van Lith-Verhoeven, J. J., … Inglehearn, C. F. (2001). Mutations in the pre-mRNA splicing factor gene PRPC8 in autosomal dominant retinitis pigmentosa (RP13). Human Molecular Genetics, 10(15), 1555–1562.

Mir, R. A., Bele, A., Mirza, S., Srivastava, S., Olou, A., Ammons, S. A., … Band, V. (2015). A novel interaction of ECD protein with R2TP complex component RUVBL1 is required for the functional role of ECD in cell cycle progression. Molecular and Cellular Biology, 36(6), 886-899.

Monneron, A., Bernhard, W. (1969). Fine structural organization of the interphase nucleus in some mammalian cells. Journal of Ultrastructure Research, 27(3), 266–288.

Mordes, D., Luo, X., Kar, A., Kuo, D., Xu, L., Fushimi, K., … Wu, J. Y. (2006). Pre-mRNA splicing and retinitis pigmentosa. Molecular Vision, 12(312), 1259–71.

Mordes, D., Yuan, L., Xu, L., Kawada, M., Molday, R. S., Wu, J. Y. (2007). Identification of photoreceptor genes affected by PRPF31 mutations associated with autosomal dominant retinitis pigmentosa. Neurobiology of Disease, 26(2), 291–300.

Mouaikel, J., Narayanan, U., Verheggen, C., Matera, A. G., Bertrand, E., Tazi, J., Bordonné, R. (2003). Interaction between the small-nuclear-RNA cap hypermethylase and the spinal muscular atrophy protein, survival of motor neuron. EMBO Reports, 4(6), 616–622.

Mozaffari-Jovin, S., Santos, K. F., Hsiao, H. H., Will, C. L., Urlaub, H., Wahl, M. C., Lührmann, R. (2012). The Prp8 RNase H-like domain inhibits Brr2-mediated U4/U6 snRNA unwinding by blocking Brr2 loading onto the U4 snRNA. Genes and Development, 26(21), 2422–2434.

Mozaffari-Jovin, S., Wandersleben, T., Santos, K. F., Will, C. L., Lührmann, R., Wahl, M. C. (2013). Inhibition of RNA Helicase Brr2 by the C-Terminal Tail of the Spliceosomal Protein Prp8. Science, 341, 80–84.

Mozaffari-Jovin, S., Wandersleben, T., Santos, K. F., Will, C. L., Lührmann, R., Wahl, M. C. (2014). Novel regulatory principles of the spliceosomal Brr2 RNA helicase and links to retinal disease in humans. RNA Biology, 11(4), 298–312.

Nakazawa, N., Harashima, S., Oshima, Y. (1991). AAR2, a Gene for Splicing Pre-mRNA of the MATal Cistron in Cell Type Control of *Saccharomyces cerevisiae*. Molecular and Cellular Biology, 11(11), 5693–5700.

Nano, N., Houry, W. A. (2013). Chaperone-like activity of the AAA+ proteins Rvb1 and Rvb2 in the assembly of various complexes. Philosophical Transactions of the Royal Society of London. Biological Sciences, 368(1617), 1-12.

Narayanan, A., Speckmann, W., Terns, R., Terns, M. P. (1999). Role of the box C/D motif in localization of small nucleolar RNAs to coiled bodies and nucleoli. Molecular Biology of the Cell, 10(7), 2131–2147.

Nathan, D. F., Vos, M. H., Lindquist, S. (1997). *In vivo* functions of the *Saccharomyces cerevisiae* Hsp90 chaperone. Proc. Natl. Acad. Sci. USA, 94(24), 12949–56.

Nemoto, T., Ohara-Nemoto, Y., Ota, M., Takagi, T., Yokoyama, K. (1995). Mechanism of dimer formation of the 90-kDa heat-shock protein. European Journal of Biochemistry, 233(1), 1–8.

Nesic, D., Tanackovic, G., Kramer, A. (2004). A role for Cajal bodies in the final steps of U2 snRNP biogenesis. J. Cell Sci., 117(19), 4423–4433.

Nguyen, T. H. D., Li, J., Galej, W. P., Oshikane, H., Newman, A. J., Nagai, K. (2013). Structural basis of Brr2-Prp8 interactions and implications for U5 snRNP biogenesis and the spliceosome active site. Structure, 21(6), 910–919.

Noble, S. M., Guthrie, C. (1996). Identification of novel genes required for yeast pre-mRNA splicing by means of cold-sensitive mutations. Genetics, 143(1), 67–80.

Nottrott, S., Urlaub, H., Lührmann, R. (2002). Hierarchical, clustered protein interactions with U4/U6 snRNA: A biochemical role for U4/U6 proteins. EMBO Journal, 21(20), 5527–5538.

Novotný, I., Blažíková, M., Staněk, D., Herman, P., Malinsky, J. (2011). *In vivo* kinetics of U4/U6·U5 tri-snRNP formation in Cajal bodies. Molecular Biology of the Cell, 22, 513–523.

Novotný, I., Malinová, A., Stejskalová, E., Matějů, D., Klimešová, K., Roithová, A., … Staněk, D. (2015). SART3-Dependent Accumulation of Incomplete Spliceosomal snRNPs in Cajal Bodies. Cell Reports, 10(3), 429–440.

Obermann, W. M. J., Sondermann, H., Russo, A. A., Pavletich, N. P., Hartl, F. U. (1998). *In vivo* function of Hsp90 is dependent on ATP binding and ATP hydrolysis. Journal of Cell Biology, 143(4), 901–910.

Ohno, M., Segref, A., Bachi, A., Wilm, M., Mattaj, I. W. (2000). PHAX, a mediator of U snRNA nuclear export whose activity is regulated by phosphorylation. Cell, 101(2), 187–198.

Ong, S.E., Blagoev, B., Kratchmarova, I., Kristensen, D. B., Steen, H., Pandey, A., Mann, M. (2002). Stable Isotope Labeling by Amino Acids in Cell Culture, SILAC, as a Simple and Accurate Approach to Expression Proteomics. Molecular & Cellular Proteomics, 1(5), 376–386.

Paci, A., Liu, X. H., Zhang, L., Zhao, R. (2016). The Proteasome Subunit Rpn8 Interacts with the snoRNP Assembly Protein Pih1 and Mediates its Ubiquitin-Independent Degradation in *Saccharomyces cerevisiae*. Journal of Biological Chemistry, 1-28.

Pagenstecher, C., Wehner, M., Friedl, W., Rahner, N., Aretz, S., Friedrichs, N., … Mangold, E. (2006). Aberrant splicing in MLH1 and MSH2 due to exonic and intronic variants. Human Genetics, 119(1), 9–22.

Pal, M., Morgan, M., Phelps, S. E. L., Roe, S. M., Parry-Morris, S., Downs, J. A., … Prodromou, C. (2014). Structural basis for phosphorylation-dependent recruitment of Tel2 to Hsp90 by Pih1. Structure, 22(6), 805–818.

Palacios, I., Hetzer, M., Adam, S. A., Mattaj, I. W. (1997). Nuclear import of U snRNPs requires importin beta. The EMBO Journal, 16(22), 6783–92.

Panaretou, B., Prodromou, C., Roe, S. M., O'Brien, R., Ladbury, J. E., Piper, P. W., … Yahara, I. (1998). ATP binding and hydrolysis are essential to the function of the Hsp90 molecular chaperone *in vivo*. The EMBO J., 17(16), 4829–4836.

Patel, A., Steitz, J. (2003). Splicing double: insights from the second spliceosome. Nature Reviews. Molecular Cell Biology, 4, 960–970.

Pena, V., Liu, S., Bujnicki, J. M., Lührmann, R., Wahl, M. C. (2007). Structure of a Multipartite Protein-Protein Interaction Domain in Splicing Factor Prp8 and Its Link to Retinitis Pigmentosa. Molecular Cell, 25(4), 615–624.

Petrs-Silva, H., & Linden, R. (2013). Advances in gene therapy technologies to treat retinitis pigmentosa. Clinical Ophthalmology, 8, 127–136.

Picard, D. (2002). Heat-shock protein 90, a chaperone for folding and regulation. Cellular and Molecular Life Sciences, 59, 1640–1648.

Poser, I., Sarov, M., Hutchins, J. R., Hériché, J.-K., Toyoda, Y., Pozniakovsky, A., … Hyman, A. a. (2008). BAC TransgeneOmics: a high-throughput method for exploration of protein function in mammals. Nature Methods, 5(5), 409–415.

Praveen K, Wen Y, Matera AG (2012) A Drosophila Model of Spinal Muscular Atrophy Uncouples snRNP Biogenesis Functions of Survival Motor Neuron from Locomotion and Viability Defects. Cell Rep., 1, 624–631

Prodromou, C., Roe, S. M., O'Brien, R., Ladbury, J. E., Piper, P. W., Pearl, L. H. (1997). Identification and structural characterization of the ATP/ADP-binding site in the Hsp90 molecular chaperone. Cell, 90(1), 65–75.

Puri, T., Wendler, P., Sigala, B., Saibil, H., Tsaneva, I. R. (2007). Dodecameric Structure and ATPase Activity of the Human TIP48/TIP49 Complex. Journal of Molecular Biology, 366(1), 179–192.

Radtke, N. D., Aramant, R. B., Petry, H. M., Green, P. T., Pidwell, D. J., Seiler, M. J. (2008). Vision Improvement in Retinal Degeneration Patients by Implantation of Retina Together with Retinal Pigment Epithelium. American Journal of Ophthalmology, 146(2), 172-182.

Raghunathan, P. L., Guthrie, C. (1998). RNA unwinding in U4/U6 snRNPs requires ATP hydrolysis and the DEIH-box splicing factor Brr2. Current Biology, 8(15), 847–55.

Raimer, A. C., Gray, K. M., Matera, A. G. (2016). SMN - A chaperone for nuclear RNP social occasions? RNA Biology, 919, 1–11.

Ranum, L. P. W., Cooper, T. A. (2006). Rna-Mediated Neuromuscular Disorders. Annual Review of Neuroscience, 29(1), 259–277.

Raška, I., Andrade, L. E. C., Ochs, R. L., Chan, E. K. L., Chang, C.-M., Roos, G., Tan, E. M. (1991). Immunological and ultrastructural studies of the nuclear coiled body with autoimmune antibodies. Experimental Cell Research, 195(1), 27–37.

Reddy, R., Henning, D., Das, G., Harless, M., Wright, D. (1987). The capped U6 small nuclear RNA is transcribed by RNA polymerase III. Journal of Biological Chemistry, 262(1), 75–81.

Romac, J. M., Graff, D. H., Keene, J. D. (1994). The U1 small nuclear ribonucleoprotein (snRNP) 70K protein is transported independently of U1 snRNP particles via a nuclear localization signal in the RNA-binding domain. Molecular and Cellular Biology, 14(7), 4662–4670.

Rose, A. M., Bhattacharya, S. S. (2016). Variant haploinsufficiency and phenotypic non-penetrance in PRPF31-associated retinitis pigmentosa. Clinical Genetics, 90(2), 118–126.

Růžičková, Š., Staněk, D. (2016). Mutations in spliceosomal proteins and retina degeneration. RNA Biology, Jun 14, 1-9.

Sahel, J. A., Marazova, K., Audo, I. (2015). Clinical characteristics and current therapies for inherited retinal degenerations. Cold Spring Harbor Perspectives in Medicine, 5(2), 1–26.

Santos, K. F., Jovin, S. M., Weber, G., Pena, V., Lührmann, R., Wahl, M. C. (2012). Structural basis for functional cooperation between tandem helicase cassettes in Brr2-mediated remodeling of the spliceosome. Proc. Natl. Acad. Sci. USA, 109(43), 17418–23.

Santos, K., Preussner, M., Heroven, A. C., Weber, G. (2015). Crystallization and biochemical characterization of the human spliceosomal Aar2-Prp8RNaseH complex. Structural Biology Communications, 71, 1421–28.

Scotti, M. M., Swanson, M. S. (2015). RNA mis-splicing in disease. Nature Reviews Genetics, 17(1), 19–32.

Shanbhag, R., Kurabi, A., Kwan, J. J., Donaldson, L. W. (2010). Solution structure of the carboxy-terminal Tudor domain from human coilin. FEBS Letters, 584(20), 4351–4356.

Shpargel, K. B., Ospina, J. K., Tucker, K. E., Matera, G., Hebert, M. D. (2003). Control of Cajal body number is mediated by the coilin C-terminus. Journal of Cell Science, 116(2), 303–312.

Schaffert, N., Hossbach, M., Heintzmann, R., Achsel, T., Lührmann, R. (2004). RNAi knockdown of hPrp31 leads to an accumulation of U4/U6 di-snRNPs in Cajal bodies. The EMBO Journal, 23(15), 3000–3009.

Schrank, B., Götz, R., Gunnersen, J. M., Ure, J. M., Toyka, K. V, Smith, A. G., Sendtner, M. (1997). Inactivation of the survival motor neuron gene, a candidate gene for human spinal muscular atrophy, leads to massive cell death in early mouse embryos. Proc. Natl. Acad. Sci. USA, 94(18), 9920–5.

Schul, W., van Driel, R., de Jong, L. (1998). Coiled bodies and U2 snRNA genes adjacent to coiled bodies are enriched in factors required for snRNA transcription. Molecular Biology of the Cell, 9(5), 1025–36.

Schwer, B., Guthrie, C. (1991). PRP16 is an RNA-dependent ATPase that interacts transiently with the spliceosome. Nature, 349, 494–499.

Singh, R. K., Cooper, T. A. (2012). Pre-mRNA splicing in disease and therapeutics. Trends in Molecular Medicine, 18(8), 472–482.

Singh, R., Reddy, R. (1989). Gamma-monomethyl phosphate: a cap structure in spliceosomal U6 small nuclear RNA. Proc. Natl. Acad. Sci. USA, 86(21), 8280–3.

Sleeman, J. E., Ajuh, P., Lamond, A. I. (2001). snRNP protein expression enhances the formation of Cajal bodies containing p80-coilin and SMN. Journal of Cell Science, 114(24), 4407–4419.

Sleeman, J. E., Lamond, A. I. (1999). Newly assembled snRNPs associate with coiled bodies before speckles, suggesting a nuclear snRNP maturation pathway. Current Biology, 9(19), 1065–1074.

Sleeman, J. E., Trinkle-Mulcahy, L. (2014). Nuclear bodies: New insights into assembly/dynamics and disease relevance. Current Opinion in Cell Biology, 28(1), 76–83.

Sleeman, J. E., Trinkle-Mulcahy, L., Prescott, A. R., Ogg, S. C., Lamond, A. I. (2003). Cajal body proteins SMN and Coilin show differential dynamic behaviour *in vivo*. Journal of Cell Science, 116, 2039–2050.

Small, E. C., Leggett, S. R., Winans, A. A., Staley, J. P. (2006). The EF-G-like GTPase Snu114p Regulates Spliceosome Dynamics Mediated by Brr2p, a DExD/H Box ATPase. Molecular Cell, 23(3), 389–399.

Smith, K. P., Lawrence, J. B. (2000). Interactions of U2 gene loci and their nuclear transcripts with Cajal (coiled) bodies: evidence for PreU2 within Cajal bodies. Molecular Biology of the Cell, 11, 2987–2998.

Sontheimer, E. J., Steitz, J. A. (1992). Three Novel Functional Variants of Human U5 Small Nuclear RNA. Mollecular and Cellular Biology, 12(2), 734–746.

Spector, D. L., Lamond, A. I. (2011). Nuclear speckles. Cold Spring Harbor Perspectives in Biology, 3(2), e000646.

Staněk, D., Neugebauer, K. M. (2004). Detection of snRNP assembly intermediates in Cajal bodies by fluorescence resonance energy transfer. Journal of Cell Biology, 166(7), 1015–1025.

Staněk, D., Neugebauer, K. M. (2006). The Cajal body: A meeting place for spliceosomal snRNPs in the nuclear maze. Chromosoma, 115(5), 343–354.

Staněk, D., Přidalová-Hnilicová, J., Novotný, I., Huranová, M., Blažíková, M., Wen, X., … Neugebauer, K. M. (2008). Spliceosomal Small Nuclear Ribonucleoprotein Particles Repeatedly Cycle through Cajal Bodies. Molecular Biology of the Cell, 19, 2534–2543.

Staněk, D., Rader, S. D., Klingauf, M., Neugebauer, K. M. (2003). Targeting of U4/U6 small nuclear RNP assembly factor SART3/p110 to Cajal bodies. Journal of Cell Biology, 160(4), 505–516.

Stejskalová, E., Staněk, D. (2014). Splicing factor U1-70K interacts with the SMN complex and is required for nuclear Gem integrity. Journal of Cell Science, 127, 3909–3915.

Strzelecka, M., Trowitzsch, S., Weber, G., Lührmann, R., Oates, A. C., Neugebauer, K. M. (2010). Coilin-dependent snRNP assembly is essential for zebrafish embryogenesis. Nature Structural & Molecular Biology, 17 (4), 403–409.

Sullivan, L. S., Bowne, S. J., Birch, D. G., Hughbanks-Wheaton, D., Heckenlively, J. R., Lewis, R. A., … Daiger, S. P. (2006). Prevalence of disease-causing mutations in families with autosomal dominant retinitis pigmentosa: A screen of known genes in 200 families. Investigative Ophthalmology and Visual Science, 47(7), 3052–3064.

Suzuki, T., Izumi, H., Ohno, M. (2010). Cajal body surveillance of U snRNA export complex assembly. Journal of Cell Biology, 190(4), 603–612.

Tanackovic, G., Kramer, A. (2005). Human Splicing Factor SF3a, but Not SF1, Is Essential for Pre-mRNA Splicing *In Vivo*. Molecular Biology of the Cell, 16, 1366–1377.

Tanackovic, G., Ransijn, A., Ayuso, C., Harper, S., Berson, E. L., Rivolta, C. (2011a). A missense mutation in PRPF6 causes impairment of pre-mRNA splicing and autosomal-dominant retinitis pigmentosa. American Journal of Human Genetics, 88(5), 643–649.

Tanackovic, G., Ransijn, A., Thibault, P., Elela, S. A., Klinck, R., Berson, E. L., … Rivolta, C. (2011b). PRPF mutations are associated with generalized defects in spliceosome formation and pre-mRNA splicing in patients with retinitis pigmentosa. Human Molecular Genetics, 20(11), 2116–2130.

Te, J., Jia, L., Rogers, J., Miller, A., Hartson, S. D. (2007). Novel subunits of the mammalian Hsp90 signal transduction chaperone. Journal of Proteome Research, 6(5), 1963–1973.

Teigelkamp, S., Newman, A. J., Beggs, J. D. (1995). Extensive interactions of PRP8 protein with the 5’ and 3’ splice sites during splicing suggest a role in stabilization of exon alignment by U5 snRNA. The EMBO Journal, 14(11), 2602–12.

Terns, M. P., Lund, E., Dahlberg, J. E. (1992). 3’-End-Dependent Formation of U6 Small Nuclear Ribonucleoprotein-Particles in Xenopus-Laevis Oocyte Nuclei. Molecular and Cellular Biology, 12(7), 3032–3040.

Tilgner, H., Knowles, D. G., Johnson, R., Davis, C. A., Chakrabortty, S., Djebali, S., … Guigó, R. (2012). Deep sequencing of subcellular RNA fractions shows splicing to be predominantly co-transcriptional in the human genome but inefficient for lncRNAs. Genome Research, 22(9), 1616–1625.

Towns, K. V., Kipioti, A., Long, V., McKibbin, M., Maubaret, C., Vaclavik, V., … Inglehearn, C. F. (2010). Prognosis for splicing factor PRPF8 retinitis pigmentosa, novel mutations and correlation between human and yeast phenotypes. Human Mutation, 31(5), 1361–1376.

Travis, G. H. (1998). Mechanisms of cell death in the inherited retinal degenerations. American Journal of Human Genetics, 62(3), 503–8.

Tseng, C. K., Liu, H. L., Cheng, S. C. (2011). DEAH-box ATPase Prp16 has dual roles in remodeling of the spliceosome in catalytic steps. RNA (New York, N.Y.), 17(1), 145–54.

Tycowski, K. T., Shu, M. D., Kukoyi, A., Steitz, J. A. (2009). A Conserved WD40 Protein Binds the Cajal Body Localization Signal of scaRNP Particles. Molecular Cell, 34(1), 47–57.

Verheggen, C., Pradet-balade, B., Bertrand, E. (2015). SnoRNPs , ZNHIT proteins and the R2TP pathway. Oncotarget, 6(39), 1–2.

Vidal, V. P. I., Verdone, L., Mayes, A. E., Beggs, J. D. (1999). Characterization of U6 snRNA – protein interactions. RNA, 5, 1470–1481.

Vithana, E. N., Abu-Safieh, L., Allen, M. J., Carey, A., Papaioannou, M., Chakarova, C., … Bhattacharya, S. S. (2001). A human homolog of yeast pre-mRNA splicing gene, PRP31, underlies autosomal dominant retinitis pigmentosa on chromosome 19q13.4 (RP11). Molecular Cell, 8(2), 375–381.

Wahl, M. C., Will, C. L., Lührmann, R. (2009). The Spliceosome: Design Principles of a Dynamic RNP Machine. Cell, 136(4), 701–718.

Walker, M. P., Tian, L., Matera, G. A. (2009). Reduced viability, fertility and fecundity in mice lacking the Cajal body marker protein, coilin. PLoS ONE, 4(7), e6171.

Wang, Q., Sawyer, I. A., Sung, M.H., Sturgill, D., Shevtsov, S. P., Pegoraro, G., … Dundr, M. (2016). Cajal bodies are linked to genome conformation. Nature Communications, 7, e10966.

Weber, G., Cristao, V. F., Alves, F. de L., Santos, K. F., Holton, N., Rappsilber, J., … Wahl, M. C. (2011). Mechanism for Aar2p function as a U5 snRNP assembly factor. Genes and Development, 25(15), 1601–1612.

Weber, G., Cristo, V. F., Santos, K. F., Jovin, S. M., Heroven, A. C., Holton, N., … Wahl, M. C. (2013). Structural basis for dual roles of Aar2p in U5 snRNP assembly. Genes and Development, 27(5), 525–540.

Weinberg, R. A., Penman, S. (1968). Small molecular weight monodisperse nuclear RNA. J. Mol. Biol., 38(3), 289–304.

Whitesell, L., Mimnaugh, E. G., De Costa, B., Myers, C. E., Neckers, L. M. (1994). Inhibition of heat shock protein HSP90-pp60v-src heteroprotein complex formation by benzoquinone ansamycins: essential role for stress proteins in oncogenic transformation. Proc. Natl. Acad. Sci. USA, 91(18), 8324–8.

Whittom, A. A., Xu, H., Hebert, M. D. (2008). Coilin levels and modifications influence artificial reporter splicing. Cellular and Molecular Life Sciences, 65(7–8), 1256–1271.

Wieczorek, D., Newman, W. G., Wieland, T., Berulava, T., Kaffe, M., Falkenstein, D., … Strom, T. M. (2014). Compound Heterozygosity of Low-Frequency Promoter Deletions and Rare Loss-of-Function Mutations in TXNL4A Causes Burn-McKeown Syndrome. American Journal of Human Genetics, 95(6), 698–707.

Will, C. L., Lührmann, R. (2011). Spliceosome structure and function. Cold Spring Harbor Perspectives in Biology, 3(7), 1–2.

Wright, A. F., Chakarova, C. F., Abd El-Aziz, M. M., Bhattacharya, S. S. (2010). Photoreceptor degeneration: genetic and mechanistic dissection of a complex trait. Nature Reviews. Genetics, 11(4), 273–84.

Wu, Q., Krainer, A. R. (1999). AT-AC pre-mRNA splicing mechanisms and conservation of minor introns in voltage-gated ion channel genes. Molecular and Cellular Biology, 19(5), 3225–3236.

Wyatt, J. R., Sontheimer, E. J., Steitz, J. A. (1992). Site-Specific Cross-Linking of Mammalian U5 Snrnp to the 5' Splice Site before the 1st Step of Premessenger RNA Splicing. Gene. Dev, 6(12B), 2542–2553.

Xu, H., Pillai, R. S., Azzouz, T. N., Shpargel, K. B., Kambach, C., Hebert, M. D., … Matera, A. G. (2005). The C-terminal domain of coilin interacts with Sm proteins and U snRNPs. Chromosoma, 114(3), 155–166.

Xu, Y., Guan, L., Shen, T., Zhang, J., Xiao, X., Jiang, H., … Zhang, Q. (2014). Mutations of 60 known causative genes in 157 families with retinitis pigmentosa based on exome sequencing. Human Genetics, 133(10), 1255–1271.

Yan, C., Hang, J., Wan, R., Huang, M., Wong, C. C. L., Shi, Y. (2015). Structure of a yeast spliceosome at 3.6-angstrom resolution. Science (New York, N.Y.), 349(6253), 1182-91.

Yuan, L., Kawada, M., Havlioglu, N., Tang, H., Wu, J. Y. (2005). Mutations in PRPF31 Inhibit Pre-mRNA Splicing of Rhodopsin Gene and Cause Apoptosis of Retinal Cells. Journal of Neuroscience, 25(3), 748–757.

Zhao, C., Bellur, D. L., Lu, S., Zhao, F., Grassi, M. A., Bowne, S. J., … Larsson, C. (2009). Autosomal-Dominant Retinitis Pigmentosa Caused by a Mutation in SNRNP200, a Gene Required for Unwinding of U4/U6 snRNAs. American Journal of Human Genetics, 85(5), 617–627.

Zhao, R., Davey, M., Hsu, Y. C., Kaplanek, P., Tong, A., Parsons, A. B., … Houry, W. A. (2005). Navigating the chaperone network: An integrative map of physical and genetic interactions mediated by the hsp90 chaperone. Cell, 120(5), 715–727.

Zhao, R., Kakihara, Y., Gribun, A., Huen, J., Yang, G., Khanna, M., … Houry, W. A. (2008). Molecular chaperone Hsp90 stabilizes Pih1/Nop17 to maintain R2TP complex activity that regulates snoRNA accumulation. Journal of Cell Biology, 180(3), 563–578.

Zhong, Z., Yan, M., Sun, W., Wu, Z., Han, L., Zhou, Z., … Chen, J. (2016). Two novel mutations in PRPF3 causing autosomal dominant retinitis pigmentosa. Scientific Reports, 6, e37840.

Zhu, Y., Tomlinson, R. L., Lukowiak, A. A., Terns, R. M., Terns, M. P. (2004). Telomerase RNA Accumulates in Cajal Bodies in Human Cancer Cells. Molecular Biology of the Cell, 15, 81–90.

Ziviello, C., Simonelli, F., Testa, F., Anastasi, M., Marzoli, S. B., Falsini, B., … Banfi, S. (2005). Molecular genetics of autosomal dominant retinitis pigmentosa (ADRP): a comprehensive study of 43 Italian families. Journal of Medical Genetics, 42(7), e47.